

23568

PREDICTION OF BEARING CAPACITY OF DRIVEN PILES IN AN ALLUVIAL  
DEPOSIT

A Master's Thesis  
Presented by  
Aylin KÖSEOĞLU

to

the Graduate School of Natural and Applied Sciences  
of Middle East Technical University  
in Partial Fulfillment for the Degree of

MASTER OF SCIENCE

in

CIVIL ENGINEERING

MIDDLE EAST TECHNICAL UNIVERSITY

ANKARA

SEPTEMBER, 1992

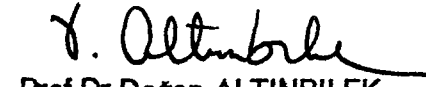
**Y.C. YÜKSEKÖĞRETİM KURULU  
DOKÜMANTASYON MERKEZİ**

Approval of the Graduate School of Natural and Applied Sciences

  
Prof. Dr. Alpay ANKARA

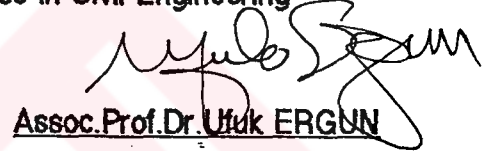
Director

I Certify that this thesis satisfies all the requirements as a thesis for the Master of Science

  
Prof. Dr. Doğan ALTINBILEK

Chairman of the Department

I certify that I have read this thesis and that in my opinion it is fully adequate, in scope and quality, for the degree of Master of Science in Civil Engineering

  
Assoc. Prof. Dr. Ufuk ERGUN

Supervisor

Examining Committee in Charge :

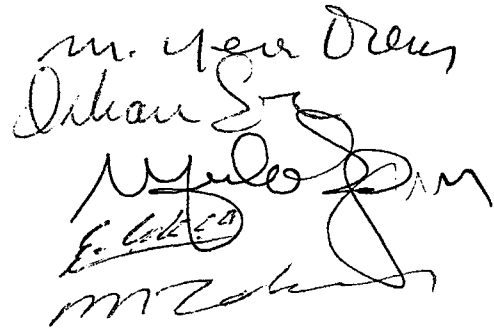
Prof. Dr. Yener ÖZKAN

Assoc. Prof. Dr. Orhan EROL

Assoc. Prof. Dr. Ufuk ERGUN

Dr. Erdal ÇOKÇA

Mustafa TOKER C.E M.S



## ABSTRACT

### PREDICTION OF BEARING CAPACITY OF DRIVEN PILES IN ALLUVIAL DEPOSIT

KÖSEOĞLU, Aylin

M.S. in Civil Engineering

Supervisor: Assoc.Prof.Dr.Ufuk ERGUN

September 1992, 129 pages

In this study, it was intended to prepare a complete document to provide a comprehensive review of the experiences of a case history of driven pile and soil investigation at Izmir Port Silo Project . The seven main sections of this study provide actual case history for prediction of bearing capacities of driven piles in alluvial deposits with sand bands occasionally and give an idea about the bearing capacity and settlement behaviour of further piles which may be driven around this construction site.

Ultimate axial capacity of driven piles was analysed using both conventional static and dynamic analyses, utilizing the compression load tests applied to both working and trial piles. The predictions are also based on Static Cone Penetrometer Test (CPT) data, using empirical correlations between CPT

results and pile shaft and tip resistance values. In the dynamic analysis, extensive amount of driving data of driven piles were also used to predict the soil profiling.

Agreement between predicted capacities, obtained from dynamic, static and CPT analysis and measured capacities in pile load test were remarkably good.

Keywords: Driven Pile, Ultimate Bearing Capacity, Ground Displacement,

CPT, Pile Load Test ,Driving Record.

Science Code : 624.01.01



## ÖZ

### KOHEZYONLU ZEMİNLERDE ÇAKMA KAZIKLARIN TAŞIMA KAPASİTESİ

KÖSEOĞLU , Aylin

Yüksek Lisans Tezi , İnşaat Mühendisliği Anabilim Dalı

Tez Yöneticisi : Doç.Dr. Ufuk Ergun

Eylül 1992, 132 sayfa

Bu çalışmada İzmir Liman Silo projesi kapsamındaki kazık çakma tecrübeleri ve zemin araştırmalarının komple dökümanlarıyla bir özeti verilmiştir. Yedi ana bölümde hesaplanan , yer yer kum bandlarının olduğu kohezyonlu zeminlerdeki çakma kazıkların taşıma kapasiteleri sahadaki veya yakın çevredeki kazıklı temellerin taşıma kapasiteleri ve oturmaları hakkında fikir verecektir.

Çakma kazıkların taşıma kapasitelerinin analizinde konvensiyonel statik ve dynamic analizlerle birlikte saha içinde çalışan kazıklarla, saha dışındaki test kazıklarına uygulanan yükleme deneyleri kullanılmıştır. Kapasite tahminleri ayrıca CPT sonuçlarıyla kazık taşıma kapasitelerinin ampirik korelasyonu ile bulunmuştur Dynamic analizde fazla sayıdaki kazık çakım dataları aynı zamanda zemin profilinin belirlenmesinde de kullanılmıştır. Dinamik, statik ve CPT analizlerinden elde edilen kazık taşıma kapasiteleri yükleme deneylerinden elde edilen kapasitelerle uyum içerisindedir.

Anahtar Kelimeler : akma Kazık, Taşıma gücü, Zemin Deplasmanı,CPT,  
Kazık Yükleme Deneyi , akım Datası.

Bilim Dalı Sayısal Kodu : 624.01.01



## ACKNOWLEDGEMENT

The author expresses her gratitude and thanks to her supervisor Assoc. Prof. Dr. Ufuk ERGUN for his guidance, directing opinions , in performing all stages of this study.

The author also takes the opportunity to express his gratitudes to the " Yüksel Proje A.ş. " staff for their help during the research work.

Special thanks are extended to Rüştü KÖSEOĞLU for his valuable suggestions.

## TABLE OF CONTENTS

	Page
ABSTRACT .....	iii
ÖZ .....	iii
ACKNOWLEDGEMENTS .....	vii
LIST OF TABLES.....	xii
LIST OF FIGURES .....	x
NOMENCLATURE .....	xx
CHAPTER I : INTRODUCTION AND PROPERTIES AND SOIL PROFILE	
1.1 Introduction.....	1
1.2 Outline of the Study.....	2
1.3 Soil Data.....	3
CHAPTER II: PILE DRIVING.....	9
2.1 Introduction.....	9
2.2 Function of Dynamic Formula.....	9
2.3 Prediction of Pile Capacity From Pile Driving Data.....	11
2.3.1 Analysis and Results.....	11
2.3.2 Calculation of Energy Losses.....	32

## 2.4 Correlation Between Dynamic and Static

Behavior of a Pile.....	40
-------------------------	----

## CHAPTER III. GROUND DISPLACEMENT DUE TO PILE DRIVING

3.1 Introduction.....	41
3.2 Action of Soil Around a Driven Pile.....	41
3.3 Action of Soil Around a Pile in Group.....	42
3.4 Difference in Bearing Capacity Behaviour Between Single Pile and Pile in Group.....	45
3.5 Prediction of the Amount of Compaction.....	47
3.5.1 Evaluation of the Relative Density.....	56

## CHAPTER IV. PREDICTION OF AXIAL PILE CAPACITY

BY STATIC FORMULA .....	60
4.1 Axial Capacity of Pile.....	60
4.2 Capacity of a Driven Pile in Cohesionless Soils.....	61
4.2.1 Skin Friction.....	61
4.2.2 End Bearing.....	62
4.3 Capacity of a Driven Pile in Cohesive Soils.....	63
4.3.1 Skin Friction.....	63
4.3.2 End Bearing.....	64

4.4 Capacity of Pile Groups.....	64
4.5 Pile Groups in Clay.....	65
4.6 Pile Groups in Sand.....	66
4.7 Bearing capacity calculation for single pile .....	66

## CHAPTER V. THE PRACTICAL USE OF CPT IN SOIL

### PROFILING AND IN PREDICTION OF AXIAL

PILE CAPACITY.....	79
--------------------	----

5.1 Introduction.....	79
-----------------------	----

#### 5.2 Difference in Behaviour Between Cone

Penetrometer Results and Test Piles.....	80
--	----

5.3 Review of Existing Methods.....	81
-------------------------------------	----

#### 5.3.1 Ultimate End Bearing From Cone

Resistance in Granular Soils.....	81
-----------------------------------	----

#### 5.3.2 Ultimate Shaft Resistance From Local Side

Friction in Cohesive Soils.....	84
---------------------------------	----

#### 5.4 Limit Values for Ultimate End Bearing and

Ultimate Shaft Resistance of a Pile.....	90
--	----

## CHAPTER VI. COMPRESSION LOAD TESTS ON DRIVEN

PILES IN ALLUVIAL DEPOSIT.....	96
--------------------------------	----

6.1 Introduction.....	96
6.2 Method of Testing.....	97
6.3 Pile Load Test Procedures.....	99
6.3.1 Maintained Load Test (ML).....	99
6.3.2 Constant Rate of Penetration Test (CRP).....	99
6.4. Pile Load Tests and Results.....	101
6.5 Estimation of Ultimate Load.....	115
6.6. Empirical Methods for Working Load.....	116
CHAPTER VII. CONCLUSION.....	124

## LIST OF TABLES

	<b>Page</b>
Table 1.1 Idealized Soil Profiling and Soil Properties .....	7
Table 1.2 Outline Of Study.....	
Table 2.1 Method of Separation of End Bearing Piles From Frictional Piles.....	15
Table 2.2 Ultimate Dynamic Capacity of Test Pile G2 and E10 in Block No 4.....	31
Table 3.1 Horizontal Stress on Pile Driven in Sand.....	43
Table 3.2 Relation Between Cone Resistance and Relative Density .....	52
Table 3.3 Angle of Wall Friction Between Pile and Soil .....	58
Table 4.1 Prediction of Ultimate Bearing Capacity of Test Piles	

	From Static Formula .....	67
<b>Table 5.1</b>	<b>Correlation of Cone Resistance and Relative Density .....</b>	<b>85</b>
<b>Table 5.2</b>	<b>Ultimate End Bearing of G2 Test Pile From Cone Resistance in Granular Soil .....</b>	<b>86</b>
<b>Table 5.3</b>	<b>Ultimate Shaft Resistance of B30 Test Pile From Local Side Friction in Cohesive Soils .....</b>	<b>86</b>
<b>Table 5.4</b>	<b>Prediction of Ultimate Bearing Capacity of the Test Piles from CPT Data .....</b>	<b>94</b>
<b>Table 6.1</b>	<b>Suggested Load Increments and Holding Times (ICE piling Model Procedures And Specification.) .....</b>	<b>102</b>

## LIST OF FIGURES

	Page
Figure 1.1 Location of Boreholes .....	5
Figure 1.2 Typical Soil Profiling Under Silo Block Along the Line Between SK 4 and SK2 .....	6
Figure 1.3 Location Of Test Piles.....	
Figure 2.1 Stop Blow Count of Piles in Whole Area .....	13
Figure 2.2 Toe Elevations of Piles In Whole Area .....	14
Figure 2.3 Plan View of Different Categories of Pile Groups According to Their Stop Blow Counts .....	18
Figure 2.4 Percent Distribution of Piles in Each Silo Block According to Stop Blow Counts.....	19
Figure 2.5 Distribution of Piles in All Blocks According to Stop Count.....	20
Figure 2.6 Pile Driving Records of Working Piles Around Test Pile B50 .....	21

Figure 2.8	Pile Driving Records of Working Piles Around Test Pile B30.....	23
Figure 2.9	Pile Driving Records of Working Piles Around Test Pile K39.....	24
Figure 2.10	Pile Driving Records of Working Piles Around Test Pile G2.....	25
Figure 2.11	Pile Driving Records of Working Piles Around Test Pile E10.....	26
Figure 2.12	Bearing Capacities Obtained From Driving Data in Block No 4.....	29
Figure 2.13	Distribution of Ultimate Capacities of Piles in Block No 4.....	30
Figure 2.14	Bearing Capacities of Piles in Relation to the Penetration . Length.....	33
Figure 2.15	Variation of Toe Elevation of Piles in Block No 4.....	34
Figure 2.16	Variation of Stop Blow Count of Piles in Block No 4.....	36
Figure 2.17	Influence of Ratio $W_p/W$ on Driving Coefficient $C_d$ in Janbu Driving formula (After Sarensen and Hansen , 1957).....	38
Figure 2.18	Diagram for the Determination of $k_u$ in Janbu Driving Formula ( After Flaate, 1964).....	39

<b>Figure 3.1</b>	<b>A comparison of N Values Before and After Driving Piles (Philcox,1962).....</b>	<b>44</b>
<b>Figure 3.2</b>	<b>Load-Settlement Behaviour of Two Test Piles.....</b>	<b>46</b>
<b>Figure 3.3</b>	<b>Relationship Between Angle of Shearing Resistance and Cone Resistance (After Durgunoğlu and Mitchell,1975).....</b>	<b>49</b>
<b>Figure 3.4</b>	<b>Correlation Between Effective Overburden Pressure <math>q_c</math> and <math>\phi</math> Trofimenzov,1974).....</b>	<b>50</b>
<b>Figure 3.5</b>	<b>Static Cone Resistance <math>q_c</math> Versus <math>D_R</math> (Schmertman, 1977).....</b>	<b>51</b>
<b>Figure 3.6</b>	<b>Relationship Between Peak Angle of Shearing Resistance and Relative Density (Schmertman, 1978).....</b>	<b>51</b>
<b>Figure 3.7</b>	<b>Correlation of SPT Value With Relative Density (Thorburn, 1963)..</b>	<b>53</b>
<b>Figure 3.8</b>	<b>Correlation Between Relative Density and Standard Penetration Resistance in Accordance With Gibbs and Holtz.....</b>	<b>54</b>
<b>Figure 3.9</b>	<b>Method for Estimating <math>\phi'</math> From SPT (DeMello's, 1971).....</b>	<b>54</b>
<b>Figure 3.10</b>	<b>Relative Density Obtained From Standard Penetration Test N-Values (After Gibbs and Holtz).....</b>	<b>55</b>

Figure 3.11	Average Unit Skin Friction on Driven Piles in Cohesionless Soils Related to Relative Density.....	57
Figure 3.12	Phase Diagram of the Fully Saturated Soil.....	58
Figure 4.1	Variation of $N_q$ With $\phi'$ (Berezantzev et al. , 1961).....	67
Figure 4.2	Location of Test Piles .....	68
Figure 4.3	Static Bearing Capacity Of Test Pile B50.....	69
Figure 4.4	Static Bearing Capacity Of Test Pile E54.....	70
Figure 4.5	Static Bearing Capacity Of Test Pile B30.....	71
Figure 4.6	Static Bearing Capacity Of Test Pile K39.....	72
Figure 4.7	Static Bearing Capacity Of Test Pile G2.....	73
Figure 4.8	Static Bearing Capacity Of Test Pile E10.....	74
Figure 4.9	Static Bearing Capacity Of Test Pile No 1.....	75
Figure 4.10	Static Bearing Capacity Of Test Pile No 3.....	76

Figure 4.11	Static Bearing Capacity Of Test Pile No 4.....	77
Figure 4.12	Static Bearing Capacity Of Test Pile No 6.....	78
Figure 5.1	Correction Factor, $k_c$ In Clay Layers, $k_s$ In Sand Layers.....	88
Figure 5.2	Prediction Of Ultimate Bearing Capacity Of a Pile From CPT 2 Data .....	91
Figure 5.3	Prediction Of Ultimate Bearing Capacity Of a Pile From CPT 3A Data .....	92
Figure 5.4	Prediction Of Ultimate Bearing Capacity Of a Pile From CPT 4 Data .....	93
Figure 6.1	Location of Test Piles .....	100
Figure 6.2	Maintaned Load Test On Pile No 1 and Pile No 2 .....	104
Figure 6.3	Maintaned Load Test On Pile No 3 .....	105
Figure 6.4	Maintaned Load Test On Pile No 4 and Pile No 6.....	106
Figure 6.5	Constant Rate Of Penetration Test Results Of SingleTest Piles.....	108
Figure 6.6	Constant Rate Of Penetration Test Results Of SingleTest	

Piles .....	109
Figure 6.7 Maintaned Load Test On Working Piles.....	114
Figure 6.8 Maintaned Load Test On Working Piles.....	115
Figure 6.9 Chin Failure Method For Calculation Of Ultimate Bearing Capacities Of Trial Test Piles.....	120
Figure 6.10 Chin Failure Method For Calculation Of Ultimate Bearing Capacities Of Trial Test Piles.....	121
Figure 6.11 Chin Failure Method For Calculation Of Ultimate Bearing Capacities Of Working Test Piles.....	122
Figure 6.12 Chin Failure Method For Calculation Of Ultimate Bearing Capacities Of Working Test Piles.....	123
Figure 7.1 Ultimate Bearing Capacity Test Piles.....	

## NOMENCLATURE

- $A_p$  : Point area of pile
- $A_s$  : Skin area of pile
- $\alpha$  : Empirical adhesion factor
- $B$  : Width of pile
- $C$  : Cohesion of the soil
- $C_d$  : Driving coefficient  $C_d$
- $C_u$  : Mean undrained shear strength
- $D$  : Diameter of pile
- $D_R$  : Relative density
- $\Delta$  : Elastic shortening
- $\Delta L$  : Increment in pile length
- $\Delta K_s$  : Difference in the ratio of horizontal to vertical effective stress
- $\Delta Z$  : Difference in angle of wall frictions between pile and soil
- $f_s$  : Unit frictional resistance for piles
- $q_c$  : Unit cone resistance for piles.
- $f_{s2}$  : Ultimate shaft resistance of the pile in group
- $f_{s1}$  : Ultimate shaft resistance of the single pile

- $e_i$  : Initial void ratio  
 $e_f$  : Final void ratio  
 $F_t$  : Total friction at depth L  
 $\phi$  : Angle of shearing resistance or internal friction  
 $\phi'$  : Effective angle of shearing resistance  
 $\gamma$  : Unit weight of soil  
  
 $E$  : Energy of hammer for one blow  
 $E_p$  : Young's modulus of the pile  
 $K_o$  : Coefficient of earth pressure at rest  
 $L$  : Length of pile  
 $\lambda_c$  : Pile friction correction factor  
 $m$  : Adherence coefficient  
 $N$  : Standard penetration number  
 $N_c$  : Bearing capacity factor for cohesion  
 $N_q$  : Bearing capacity factor for pressure  
 $N_\gamma$  : Bearing capacity factor for soil weight  
  
 $NC$  : Normally consolidated  
  
 $OCR$  : Overconsolidation ratio  
  
 $p_o$  : Average effective overburden pressure along shaft

- $Q_p$  : Point bearing capacity of pile
- $Q_s$  : Skin resistance of pile
- $Q_{ut}$  : Ultimate bearing capacity of the pile
- $q_p$  : Unit point resistance of pile
- $q_c$  : Cone tip resistance
- $q_{c1}$  : Average cone resistance over 2 diameters below the pile base
- $q_{c2}$  : Minimum cone resistance over 2 diameters below pile base
- $q_{c3}$  : Average of minimum values lower than  $q_{c2}$  over 8 diameter above pile base
- $q_1$  : Average of the cone resistance over a depth of 8 diameters base of the pile
- $q_2$  : Average of the cone resistance below the point of the pile tip for a depth of 3.5 diameter
- $q_1$  : Cone resistance just above the bearing stratum
- $q_{11}$  : Cone penetration resistance at a depth of 10 diameters measured from the surface of the bearing stratum
- $S$  : Penetration for one blow
- $\sigma'_v$  : Vertical effective stress at any given depth

$\sigma'_h$  : Horizontal effective stress at any given depth

$\sigma'_m$  : Mean effective overburden pressure

$V_w$  : Volume of water

$V_s$  : Volume of solid

$W_p$  : Weight of the pile

$W$  : Weight of the hammer



## CHAPTER I

### INTRODUCTION AND SOIL PROPERTIES AND SOIL PROFILE

#### 1.1 Introduction

Pile foundation behaviour has been studied for decades, but there are several gaps in the proper and quantitative understanding of the response of piles, both under static and dynamic loads. Field tests are the best methods of the study of their response, but these are expensive. Therefore, study of case histories are important.

The discrepancies observed between real and theoretical bearing capacities of piles are explained by the fact that estimation of pile capacity is still largely based on empirical methods, derived from correlations of measured pile capacity with soil data of variable quality. There is generally a wide scatter in the correlations and different approaches suit different soil types better than others.

On the other hand, although the result of pile tests are of considerable engineering significance and tests themselves are relatively costly exercises, the standard of recording of the results of pile load tests is generally low, sometimes

because of lack of attention by the Engineer and partly as a result of a tendency by contractors to provide no more than is asked. Large number of test results, many of the reports lacked details which were essential if meaningful evaluations of the test results were to be made.

Some of the best presented results were provided by piling contractors who had taken them up themselves , thus providing valuable reference documents.

## 1.2. Outline of the Study

A large reinforced concrete grain silo has been recently constructed on reclaimed land from the sea at the Izmir Bay. Soils are deep alluvial deposits and consist of bands of clay, sand and gravel. 400x400 precast concrete piles have been driven to carry the foundation loads. Approximately 800 piles were driven to 22-28 m depth. Before the final design stage, 500x500 and 400x400 precast trial piles, six in number, were driven outside the silo block and test loaded. Six more tests on project piles were performed before the raft was completed.

In Chapter 2, soil profiling was investigated initially by using driving data to eliminate the uncertainties about soil stratification obtained from limited number of boreholes in whole construction site. Ultimate capacities of 196 No driven piles were also estimated by using Janbu dynamic formula and softwares.

Amount of compaction in other words increase in relative density caused by the driving of groups within the fill has been predicted in Chapter 3.

Evaluation of bearing capacities of driven piles were presented in Chapter 4 by using conventional soil mechanics approach -that is static formulas. For this evaluation soil properties were taken from Chapter 5 in which standard penetration and cone penetration tests results correlate with pile capacity by using empirical correlations.

In Chapter 5, effective angle of friction,  $\phi'$ , before the pile driving was estimated in addition to soil investigation made by contractor. The main objective of Chapter 5 was to predict the load carrying capacity of a pile driven into the alluvial soil by using the continuous representative cone penetrometer data.

Method of load testing of piles, test procedure were summarized in Chapter 6. Interpretation of pile load tests results were made. Prediction of ultimate load of 12 No test pile were presented by using Chin's failure criteria.

### 1.3 Soil Data

Subsoil was divided into four different units from top to bottom as follows:

- 1- Gray colored, little mussel shelled , soft clay .
- 2- Gray colored, little fine gravely stiff-very stiff clay layer.
- 3- Sandy, very dense fine gravel and locally well cemented (conglomeratic) compact sand-gravel layer.
- 4- Gray - brown locally little fine gravely hard clay layer.

These layers were explained in detail as follows:

## 1- Gray colored, little mussel shelled soft clay

This formation takes place between 9-16 meters below sea level. This layer can be classified as CL (low plasticity clay) and locally CH (high plasticity clay). SPT values were  $N_{30}$  : 5 at the upper part of the layer, increasing up to  $N_{30}$  :15 at the lower part of the layer. The average unit weight was found around  $\gamma_n$  : 18 kN/m<sup>3</sup>. As an average the consistency limits are found as :  
LL = 35-55 , PL = 18-32 ,  $W_n$  = 35-45.

Unconfined compressive strength values are  $q_u$  : 100 kN/m<sup>2</sup> at the middle and  $q_u$  : 150 kN/m<sup>2</sup> through the bottom of the layer. The location of boreholes and soil profiling are shown in the Figure 1.1 and Figure 1.2 respectively.

Soil profiling will be checked in Chapter 2 by using computer outputs of program namely that MOSS. Soil properties which are used in calculation of pile capacity in Chapter IV could be given as follows :

$$C_u = 20 \text{ kN/m}^2, \phi_u = 5^\circ$$

## 2. Gray colored , little fine gravely stiff-very stiff clay layer.

This layer is present between -16 and -22 meters. This layer on the upper part , between -16 and -19 meters can be defined as gray colored, little fine gravely, calcereous nodules hard clay .

But on the lower part between -19 and -22 meters it can be define as again gray colored little fine gravely ,silty, rather hard clay layer . This layer can be classified as CL (low plasticity clay) and average SPT values are :  $N_{30}$  = 15-25.

Unit weight  $\gamma_n$  = 18.5-21.0 KN/m<sup>3</sup> and consistency limits are found as :

$$LL = 30-40 , PL = 15-20 , W_n = 20-30$$

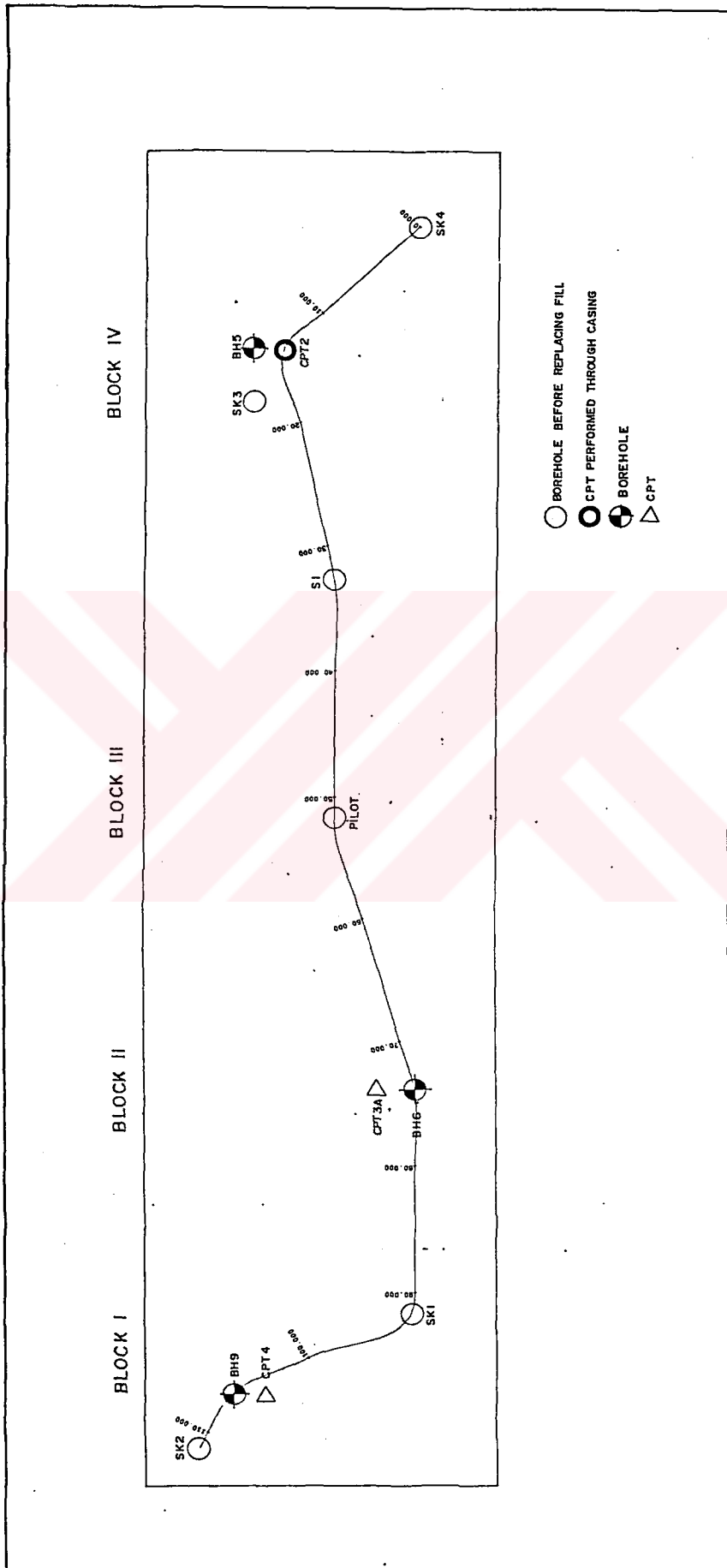


Figure 1.1 Location of Boreholes

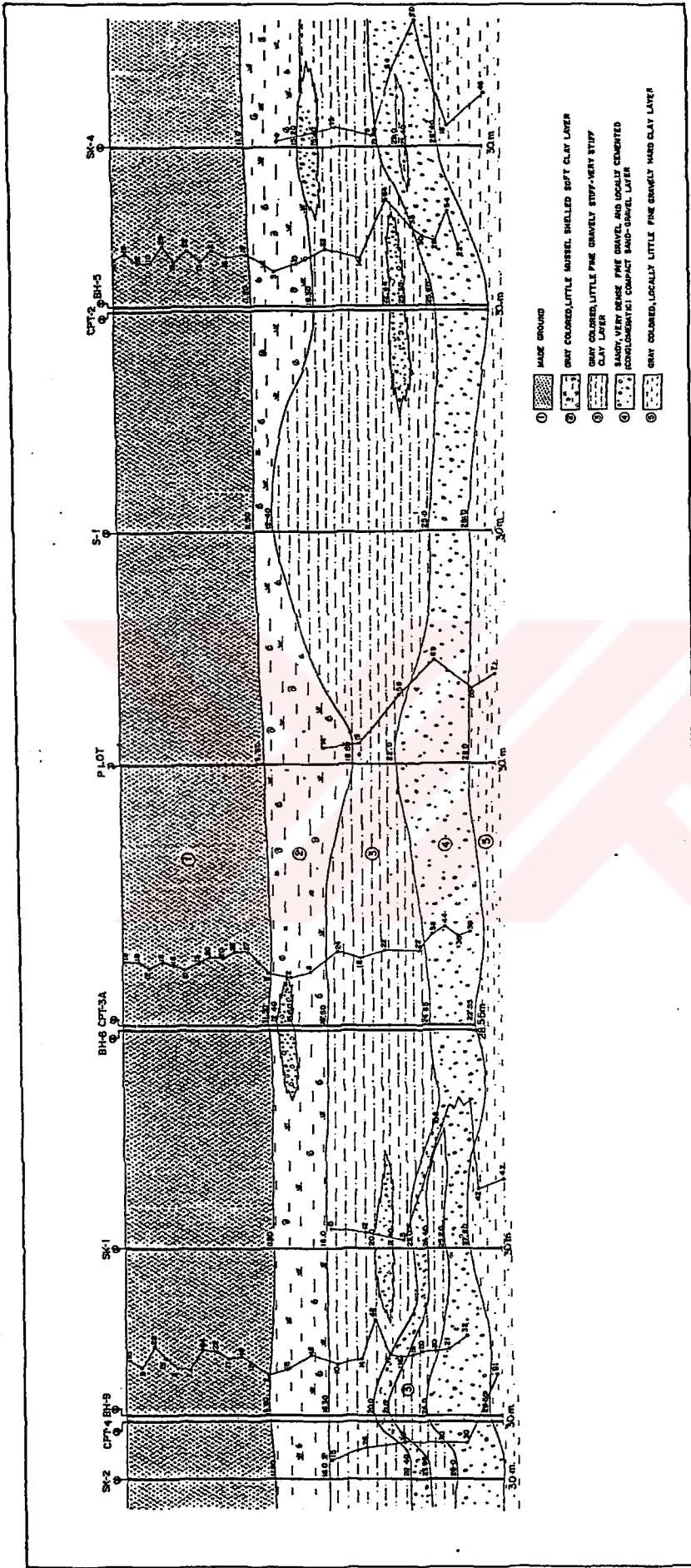


Figure 1.2 Typical Soil Profiling Under Silo Block Along the Line Between SK 4 and SK2

**Table 1.1 Idealized Soil Profiling and Soil Properties**

	DESCRIPTION	C <sub>u</sub> KN/m <sup>2</sup>	φ <sub>u</sub>	C KN/m <sup>2</sup>	φ	N <sub>30</sub>	γ KN/m <sup>3</sup>
②	GRAY COLORED, LITTLE MUSSEL SHELLED SOFT CLAY LAYER	20	5	-	-	5-15	18
③	GRAY COLORED, LITTLE FINE GRAVELY STIFF-VERY STIFF CLAY LAYER	40	8	-	-	15-25	185
④	SANDY, VERY DENSE FINE GRAVEL AND LOCALLY CEMENTED SAND AND GRAVEL LAYER	-	-	30	25	30-70	205-215
⑤	GRAY COLORED, LOCALLY LITTLE FINE GRAVELY HARD CLAY LAYER	-	-	80	10	-	185

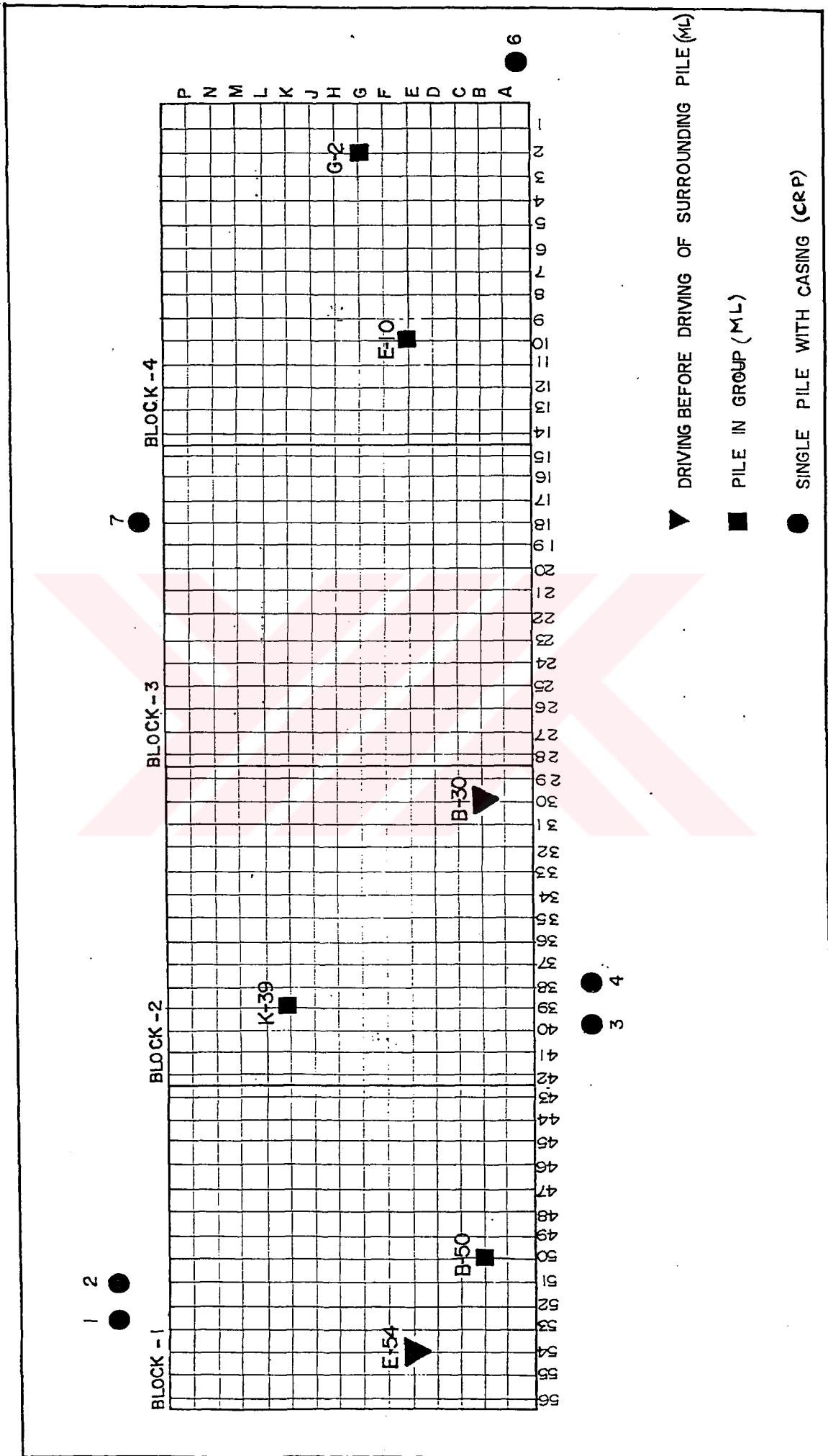


Figure 1.3 Location Of Test Piles

**Table 1.2 Outline Of Study**

PILE NO	TOTAL LENGTH (m)	LENGTH IN SOIL (m)	APPLIED MAX. LOAD (ton)	MAX. SETTLEMEN (mm)	XSECTION (cm <sup>2</sup> )	CHIN FAILURE (ton)	MAZURKIEW (ton)	RESIDUAL SETTLEMENT (mm)	BLOWS FOR LAST 60 CM PENETRATION
1	25.65	15.15	180	13.70	40x40	500	265	2.27	-
2	23.10	14.10	240	11.10	50x50	588	380	2.5	18,18,20,20,32,61
3	26.80	16.80	340	16.00	50x50	415	383	3.2	24,30,30,30,30,35
4	27.00	18.00	240	18.30	40x40	408	330	2.8	8,8,11,12,12,12
6	24.40	18.90	240	22.00	40x40	336	300	6	6,5,4,4,4,4
7	12.20	12.20	80	3.00	40x40	106	80		15,14,15,14,14,19
E-54		25.60	245	5.80	40x40		263	0.4	15,16,16,18,22,22
B-50		22.50	280	6.50	40x40		315	1	17,18,24,26,23,23
K-39		24.90	245	5.40	40x40		215	2.2	34,35,26,26,26,26
B-50		27.00	210	7.00	40x40	210	228	1.4	21,24,24,26,27,27
E-10		21.10	245	11.00	40x40	333	300	5.4	19,19,25,25,25,30
G-2		24.30	220	13.00	40x40	250	226	6.2	4,4,4,4,4,4

Unconfined compressive strength value is determined as :

$$q_u = 100-200 \text{ kN/m}^2$$

By considering the results of consolidation and triaxial compressive strength tests design values could be given as follows :

$$C_u = 20 \text{ kN/m}^2, \phi_u = 5^\circ$$

3. Sandy, very dense fine gravel and locally cemented (conglomeratic), compact sand - gravel layer .

SPT value vary between  $N_{30} = 30-70$  . It can be classified as GW (well graded gravel) , GW - GM (well graded silty gravel) and SC (clayey sand) the unit weight as found as  $\gamma_n : 20.5-21.5 \text{ KN/m}^3$  .The unconfine compressive

strength values at the upper parts are found as :

$$q_u = 100 - 150 \text{ kN/m}^2$$

The consistency limits and other values are determined as :

$$LL = 15-25, PL = 0-10, W_n = 5-15$$

$$C = 30 \text{ kN/m}^2, \phi = 25^\circ$$

4. Gray colored, locally littel fine gravely hard clay

SPT values are  $N_{30} : 30 - 70$  .

The following geotechnical properties can be given as :

$$\gamma_n = 18.5 \text{ KN/m}^3$$

$$q_u = 100- 380 \text{ KN/m}^2$$

$$LL = 30-45, PL = 15-25, W_n = 20-30$$

$$C = 80 \text{ KN/m}^2, \phi = 10^\circ$$

## CHAPTER II

### PILE DRIVING ANALYSIS

#### 2.1 Introduction

This section aims to study the pile driving data, 800 in number, to predict the load carrying capacity of piles. By using driving resistance versus depth relationship, soil profiling was also investigated to make partial elimination of uncertainties about soil profiling, since it was erratic.

This section does not aim to investigate the accuracy and precision of each dynamic formulae statistically and to perform risk analysis in order to properly assess the factor of safety. Since dynamic formulas simply represent conditions at the time of driving, they should not be used as only one item of design.

#### 2.2 Function of Dynamic Formulas

It is assumed in dynamic pile formulas that the ultimate bearing capacity is equal to dynamic driving force. Dynamic formula for single pile takes no account of the reduced value of a friction pile when in a group; and it takes no account of changes in soil structure and hydrostatic conditions induced temporarily during driving, or other short-or long-time adjustments in bearing value. Therefore the driving resistance is only one item of design information that must be considered .

Such a formula can apply only in the case of cohesionless strata, such as sand, gravel or permeable fill; in these strata the resistances acting while the pile is being driven bear a reasonably close relationship to those acting on a pile carrying a static load. In the case of driving piles in plastic material such as soft clay or fine-grained silt, relations between the temporary resistance to driving and permanent resistance to the applied load on the pile are uncertain. [20]

On the other hand, pile driving formulas, as one method of rapid determination of pile capacity and controlling it under job conditions, will still be needed where load tests and adequate soil investigations are not available.

For derivation of pile formulas, in general, the weight of hammer multiplied by stroke height is simply equated to the driving resistance multiplied by the net penetration per blow of the tip of the pile. In this study ultimate bearing capacities of piles were estimated by this simple concept and energy losses were also calculated as explained later. [20]

The only important difference between the many dynamic formulas is the classification and magnitude of the allowances made for energy losses. The resistance can be calculated by deducting various losses from the applied driving energy. These losses are generally agreed to be caused by:

- i) Impact
- ii) Compression of the driving cap
- iii) Compression of the pile
- iv) Deformation of the soil. [20]

Various dynamic formulas have been compared with measured load test results by various authors. (Poulos and Davis, 1981) and two of the more reliable have been shown to be the Danish and the Janbu formulas. Calculations of

dynamic capacities and energy losses were based on Janbu formula assumptions in the following sections.

In Michigan pile study, Housel (1966) demonstrated a difference in the relative accuracies of dynamic formulas at different load capacity levels. A considerable increase in the safety factor at higher load levels is demonstrated. For example, for the Gates formula safety factor ranged from 0.6 to 1 of loads in the range 0 to 100 t, but was as high as 1.3 to 2.5 for loads in the range of 200 to 350 t. It is probable that a similar variation applies to the Janbu formulae and if so, the actual capacities in this study may be as much as three times those determined from dynamic formulae.

## 2.3 Prediction of Pile Capacity from Pile Driving Data

### 2.3.1 Analysis and Results

Since the erratic nature of the soil, interpretation of the differences between the predicted capacity of project piles and measured capacity of the test piles was considerably difficult. Detailed information about the soil stratification would probably be helpful to overcome this difficulty. But this information can not be provided from the limited amount of borehole and cone penetrometer test results for the whole site. Therefore pile driving data could be used to predict soil profiling by knowing that significant increase in pile driving resistance shows the pile penetrates from a soft layer to hard layer-that is similar to dynamic penetration test.

Pile driving records were analyzed considering the stop-blow count for the last 10 cm penetration by using a professional software namely that MOSS. Contour lines are drawn which connect the piles which have equal stop-blow count

for the last 10 cm. penetration and equal toe elevation . It would seem obvious that the less distant the contour lines the less similar the pile behavior and soil condition exist. Program output shown in Figure.2.1 and Figure 2.2 provides a rough visualization of the soil stratification for the whole construction site.

Figure 2.3 has been prepared by considering pile driving data . In this figure, the piles are categorized as the friction or the end bearing type by using last 50 cm driving data and stop blow count as shown in Table 2.1 .

The following statements may be derived by the aim of Figure 2.1,Figure 2.2. Figure 2.3.

1- The soil profile is erratic .

2- Different zones can be classified as

a- Zone of piles which have the same toe elevations , but different stop blow count (ZONE I ,stratified ground)

b- Zone of piles with the different toe elevations but the same stop blow count (ZONE II , same soil layering at different depths).

c- Zone of piles with the different toe elevations and stop blow counts (ZONE III) .

d- Zone of piles with the same toe elevations and the same stop blow counts (ZONE IV , no stratification) .

Silo block II has the properties of ZONE IV . In this area the majority of the piles are friction type and embedded into a deep clay layer . The region of Silo Block III closer to that of ZONE I has piles having the same toe elevations but different stop blow count. These piles can be grouped as the piles driven into the sand layer in different depths. Resulting soil profiling is shown in Figure 1.1



Figure 2.1 Stop Blow Count of Piles in Whole Area.

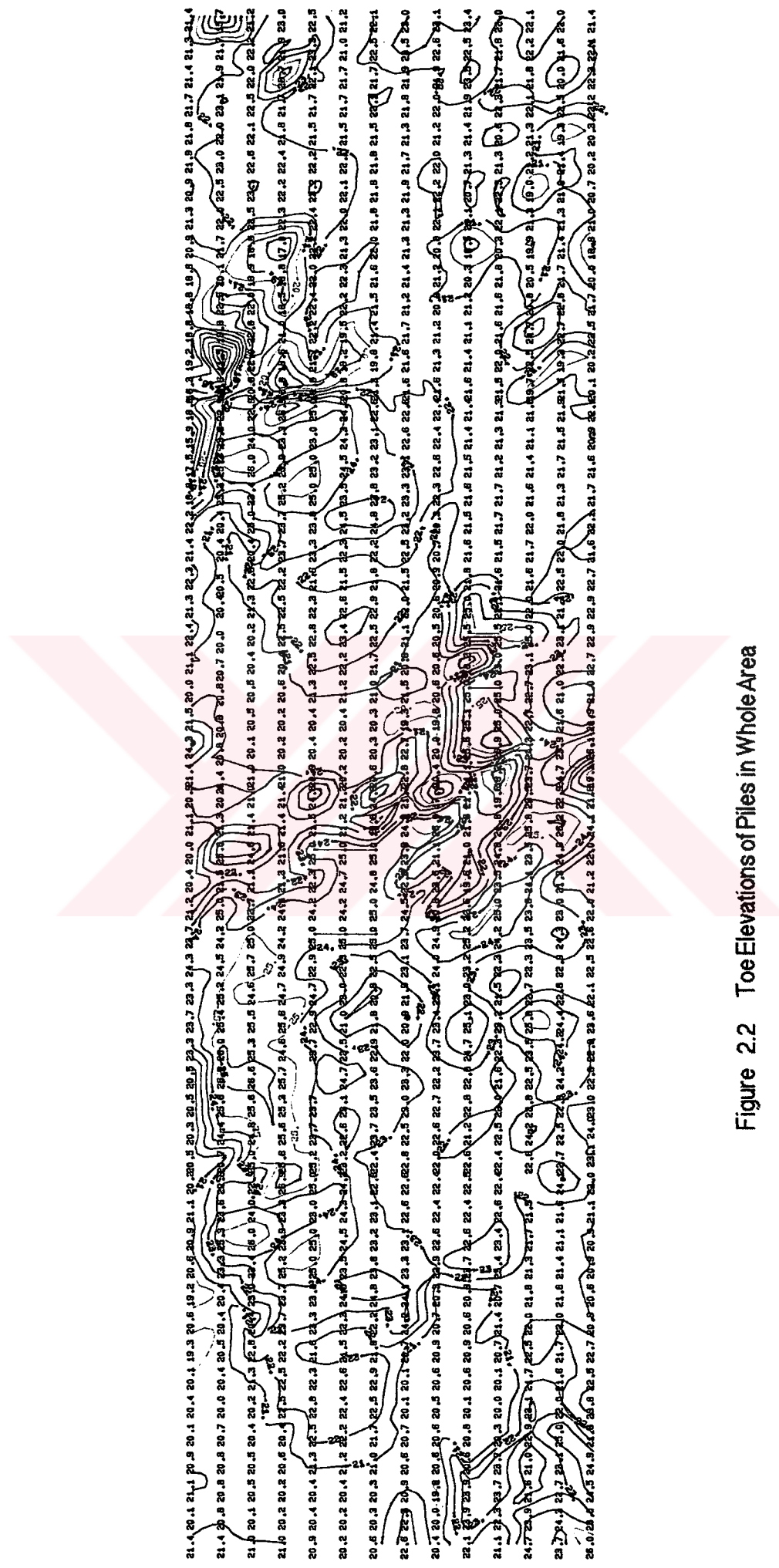


Figure 2.2 Toe Elevations of Piles in Whole Area

**Table 2.1 Method of Separation of End Bearing Piles**

NAME OF PILE	LAST FIVE BLOW COUNTS EACH FOR 10 CM. PENETRATION					PILES CATEGORISED AS
H-43	18	20	30	40	48	BLOW > 40
F-56	20	24	29	33	46	
C-42	28	39	45	56	59	
D-49	17	21	29	34	41	
P-39	14	17	25	35	49	
A-37	18	21	24	29	37	35<BLOW>40
B-35	18	18	26	29	39	
C-19	25	25	27	29	36	
E-51	16	20	28	29	36	
M-6	18	18	25	31	38	
P-42	14	18	19	27	33	30<BLOW>35
N-45	24	24	26	29	32	
J-39	19	24	24	29	34	
G-42	18	20	26	28	31	
C-2	18	18	23	28	31	
H-33	21	27	27	28	28	BLOW < 30
J-42	23	25	25	27	29	
K-28	21	22	22	24	27	
M-35	18	18	20	22	28	
N-41	16	16	22	26	29	
A-43	10	10	10	10	10	FRICTION PILE
A-29	20	24	24	24	24	
C-31	15	15	17	16	18	
E-37	20	20	20	21	21	
J-43	14	13	14	14	14	

BLOW : STOP BLOW COUNT FOR LAST 10CM.OF PENETRATION

Although there is considerable literature relative to pile bearing capacity prediction and many design methods are proposed, every skilled pile designer knows that accurate bearing capacity predictions are difficult. The discrepancies observed between real and theoretical bearing capacities are explained by the fact that generally design is based on the questionable and insufficient soil data.

That's why great attention was given to assessment based on soil profiling.

The shaft resistance and the tip bearing are the two main components of carrying capacity of a pile. The separation of these two components can not be measured from a classical pile test in which the load/settlement behavior of pile is measured. Although Van Wiele (1957) described a technique from load/settlement curve, it is tough not to be satisfactory. Such a separation can be satisfactorily done by installing more comprehensive instrumentation in the pile. But in this study, no instrumental test has been performed, therefore no sufficient data were available.

Therefore, pile driving data were further investigated to separate end bearing piles from frictional piles by considering the final five groups of blows, each for 10 cm. of penetration. The increasing trend in the last five groups of blow-counts have been showed that whether the pile was end bearing or friction type. To do this some judgement was needed to separate the piles, which are different in behavior. Examples for the method of separation were shown in Table 2.1.

Since, so many piles driven where the soil profile was so erratic, drawing of the distribution of similar piles in construction site would be very helpful to overcome the difficulties in the complex view of the case history.

All of the piles of the construction site were grouped into different categories in Figure 2.3. If the final five groups of blows, each for 10 cm. of penetration is rapidly increasing and their stop-blow count is between 35 and 40 and/or greater than 40 the pile is grouped as end bearing type. On the other hand, if blow number does not show a satisfactorily increasing trend and stop blow-count between 30 and 35 or less than 30 these piles can be considered to be both end bearing and friction type. Piles with blow numbers for last 50 cm. of penetration remains constant and the stop blow count is less than 30, this pile can be categorized as purely friction pile. Percent distribution of categorized piles according to blow-count in each silo block and in whole construction site were shown in Figure 2.4 and Figure 2.5 respectively.

These analyses suggest that not all piles are end-bearing on the sand/gravel layer, but are carrying a significant proportion of load in skin friction. 55% of piles is identified as end-bearing piles, 22% of piles is accepted as friction piles, the remaining 23% as probably end bearing but results are inconclusive.

Finally, the dynamic pile resistance versus depth graphs were plotted by using pile driving records. Graphs were shown in Figure 2.6 through Figure 2.11. These graphs were used to predict both the bearing capacities of piles in Block 4 and soil profiling in the whole construction site.

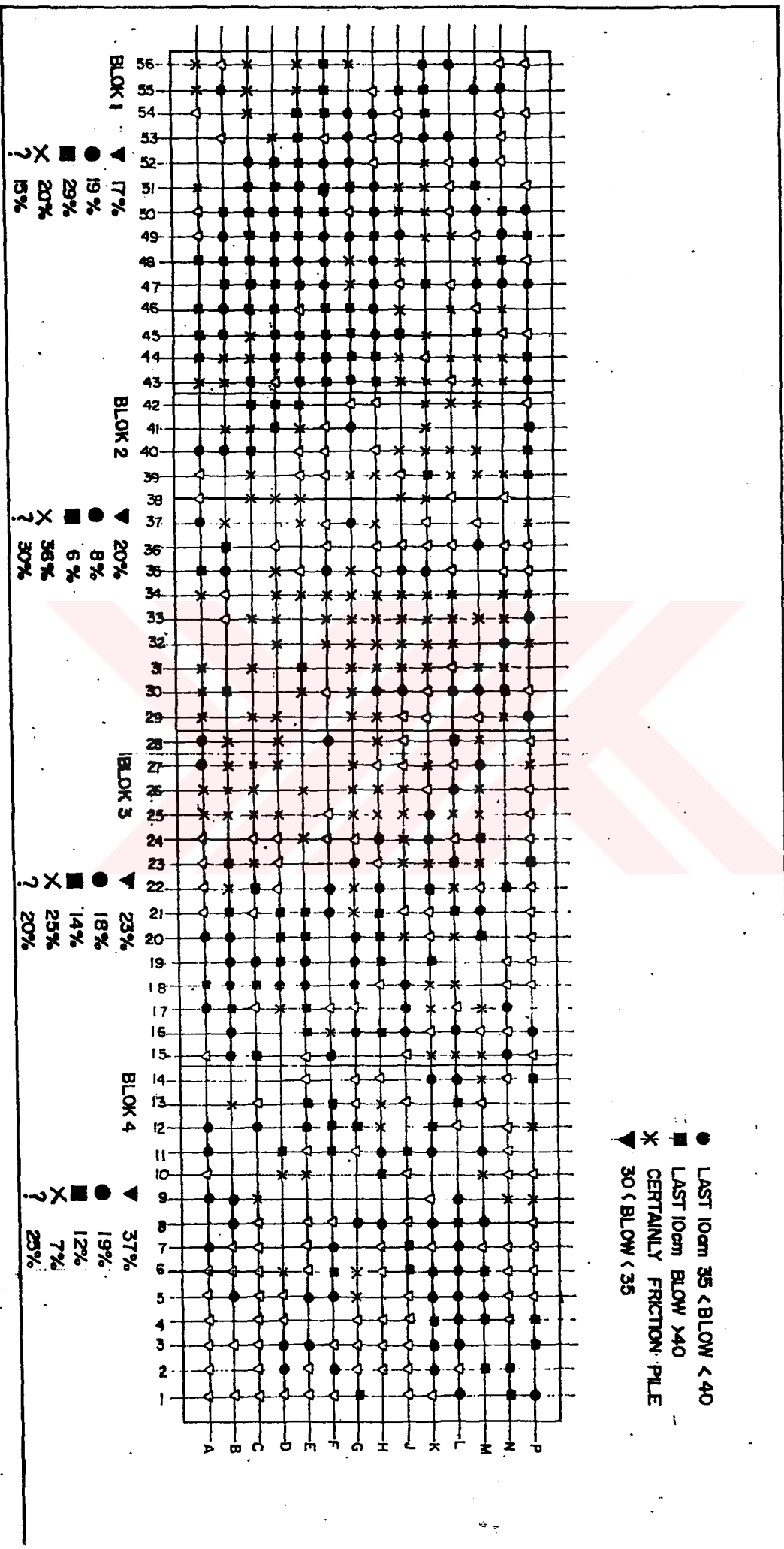


Figure 2.3 Plan View of Different Categories of Pile Groups According to Their Stop Blow Counts

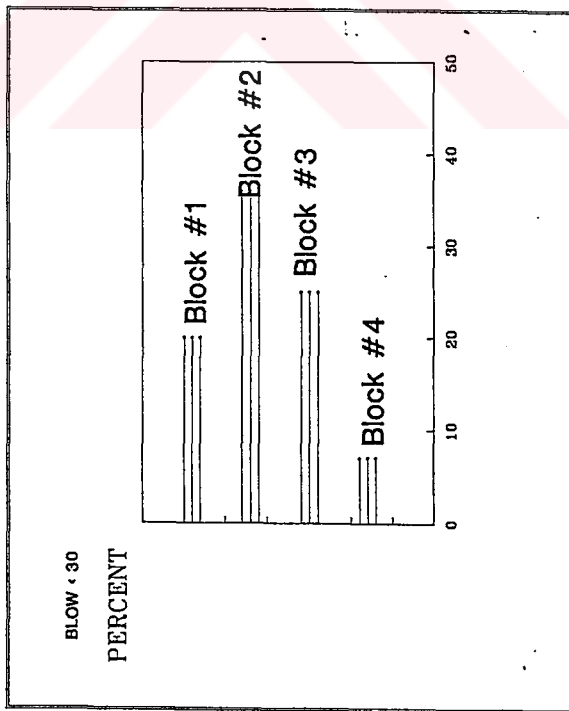
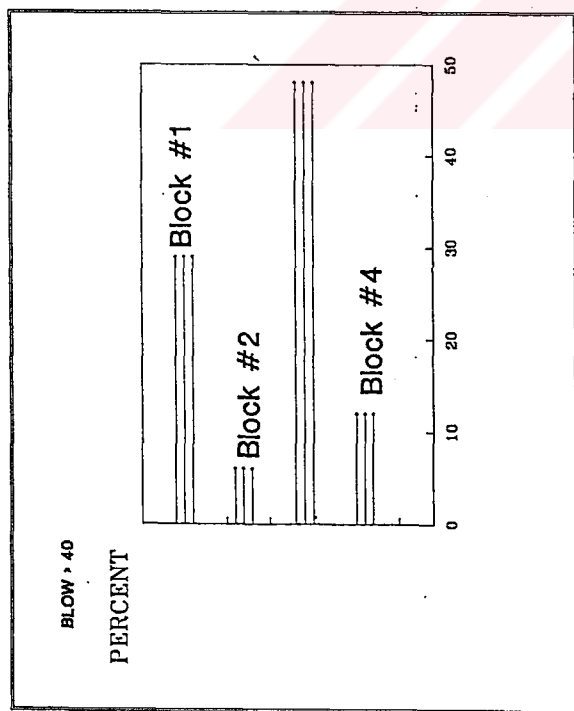
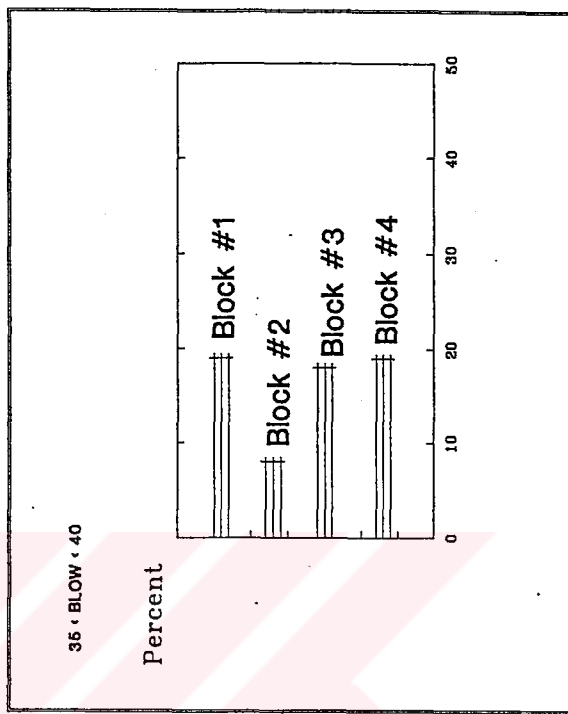
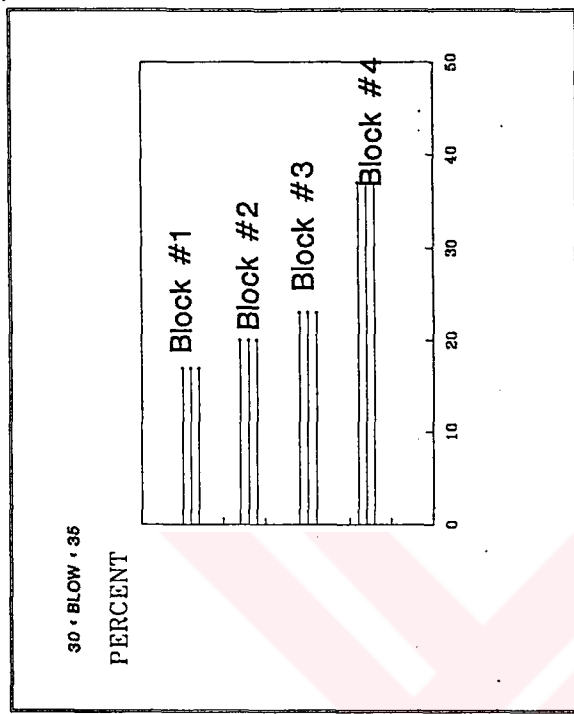


Figure 2.4 Percent Distribution of Piles in Each Silo Block According to Stop Blow Counts

**BLOW : No of blows for last 10 cm. penetration**

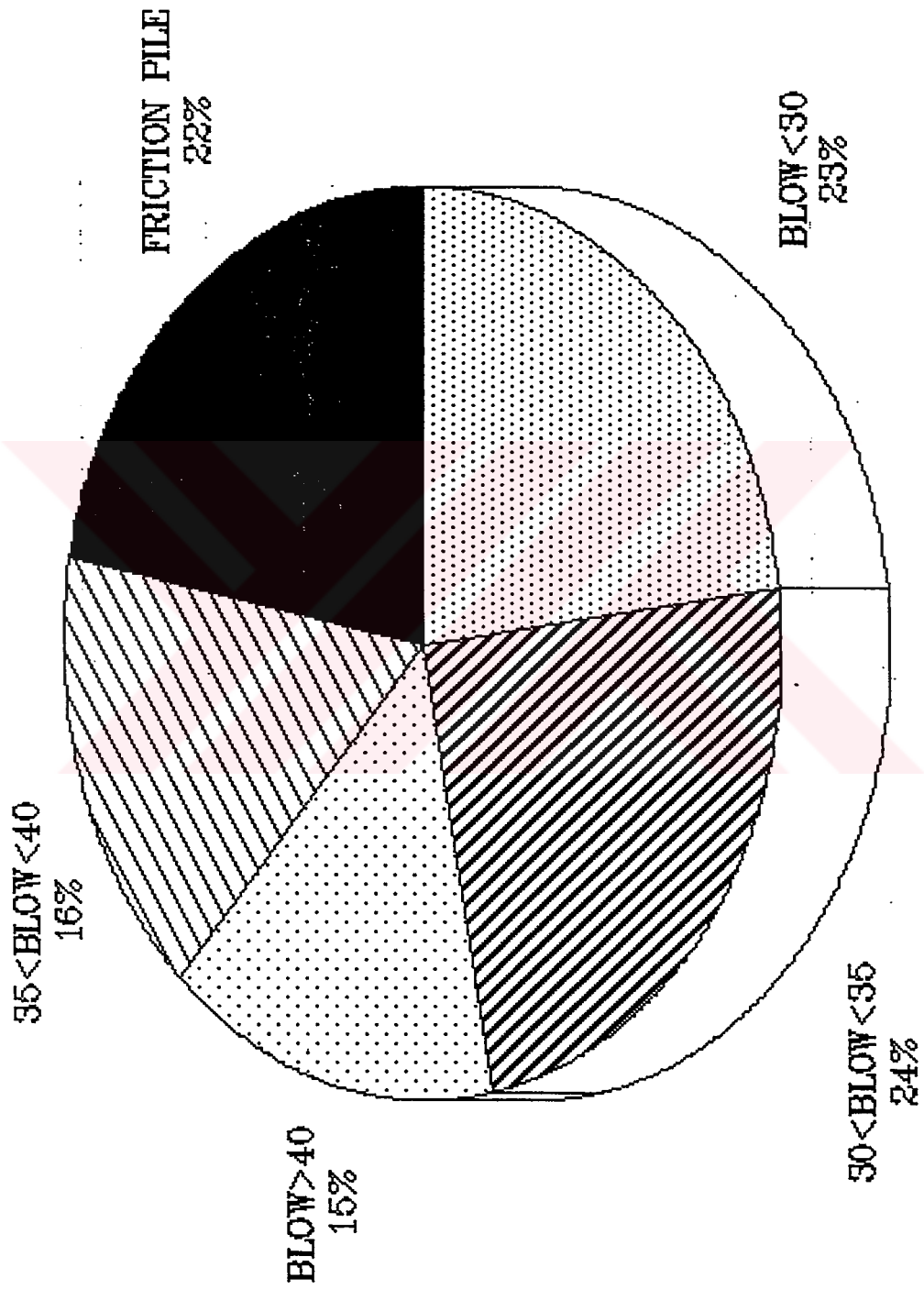


Figure 2.5 Distribution of Piles in All Blocks According to Stop Count

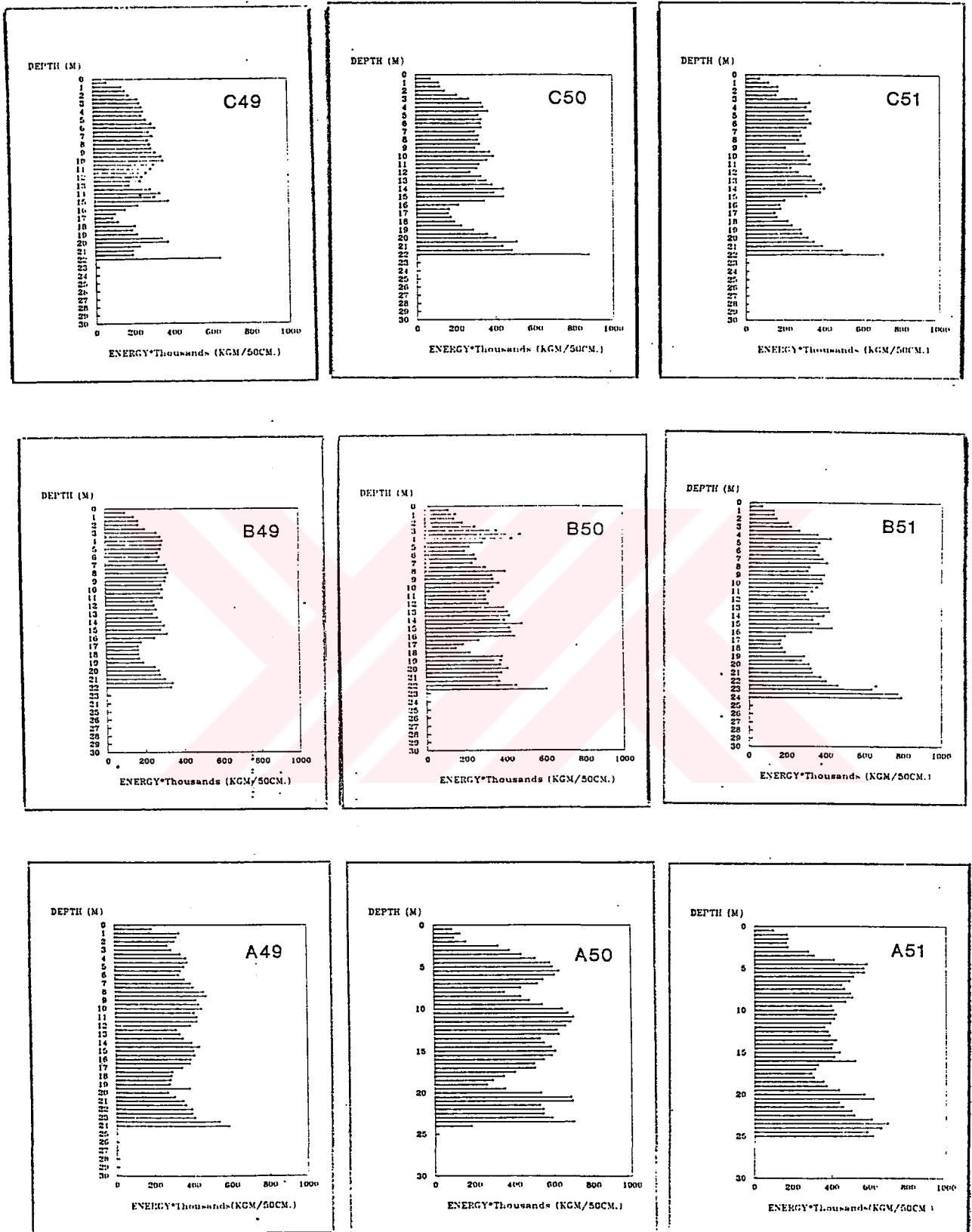


Figure 2.6 Pile Driving Records of Working Piles Around Test Pile B50

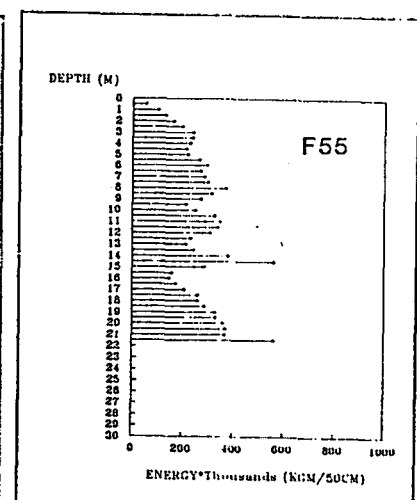
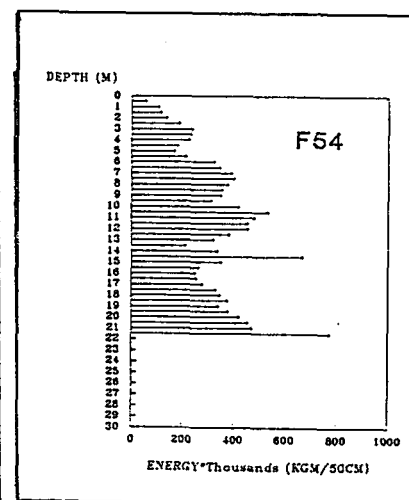
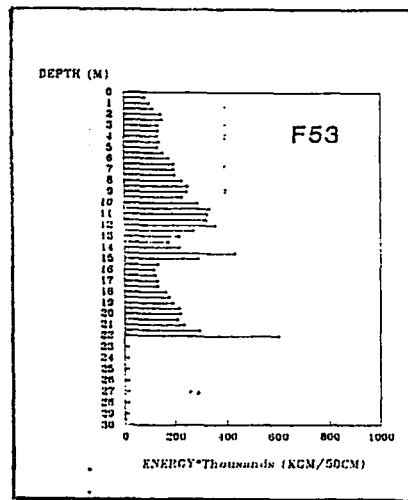
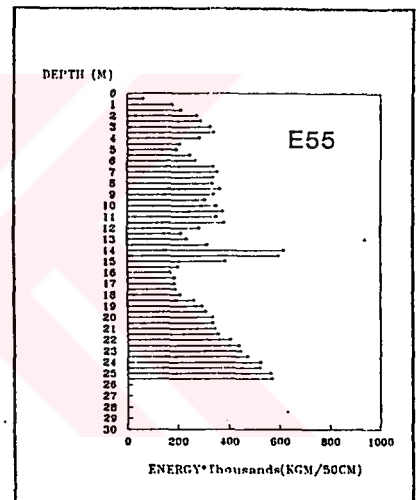
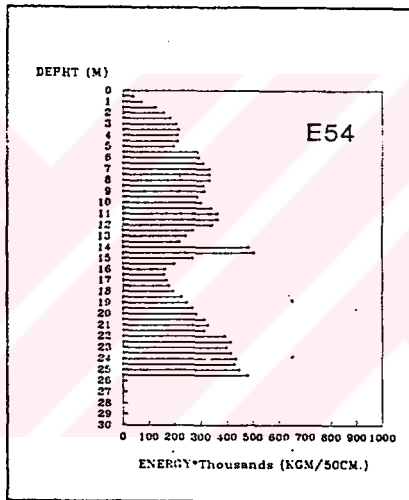
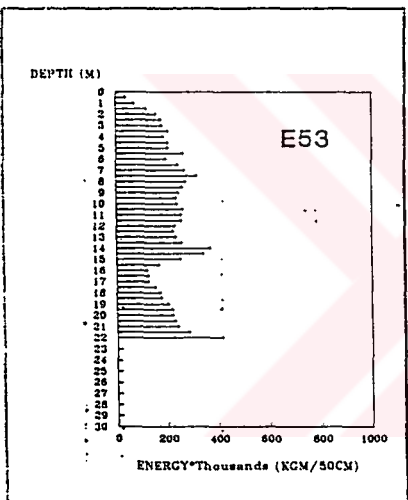
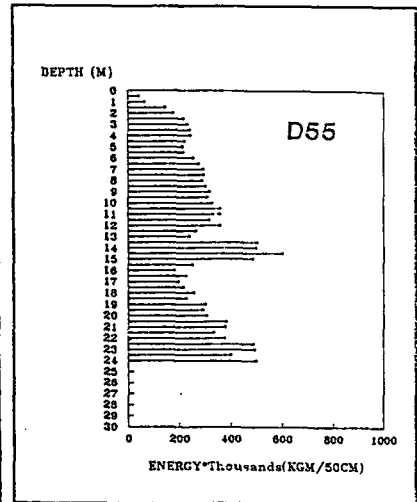
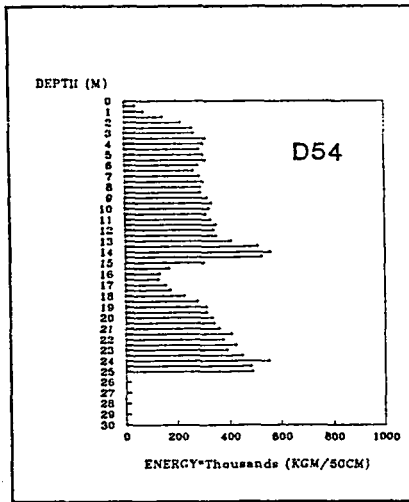
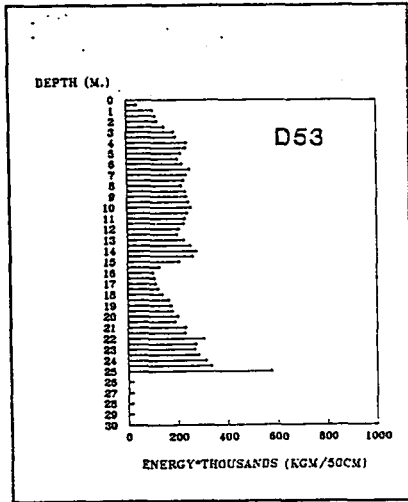


Figure 2.7 Pile Driving Records of Working Piles Around Test Pile E54

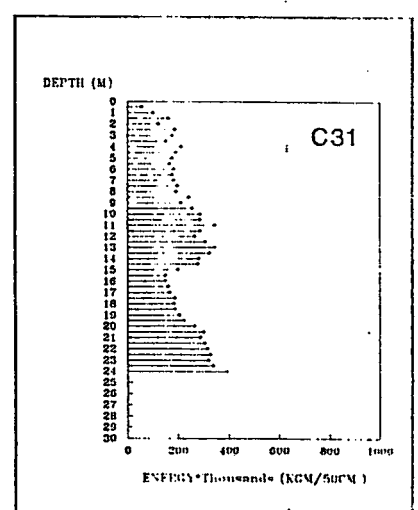
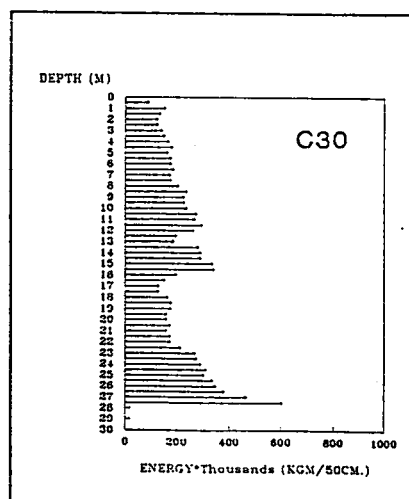
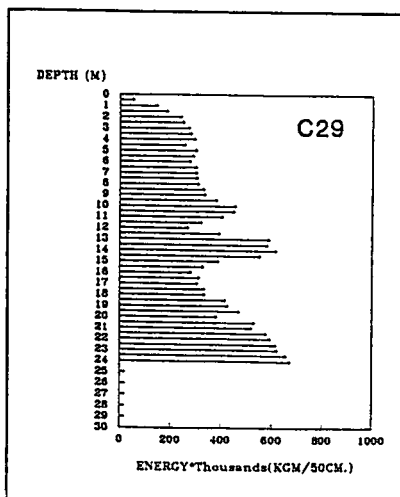
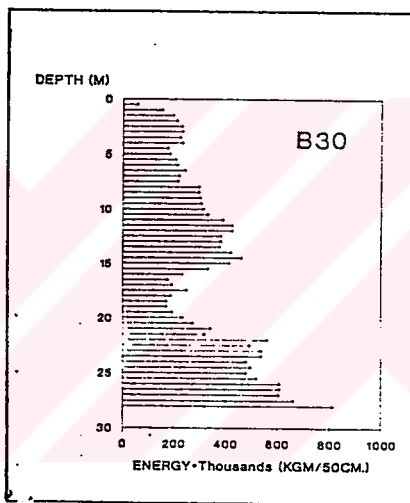
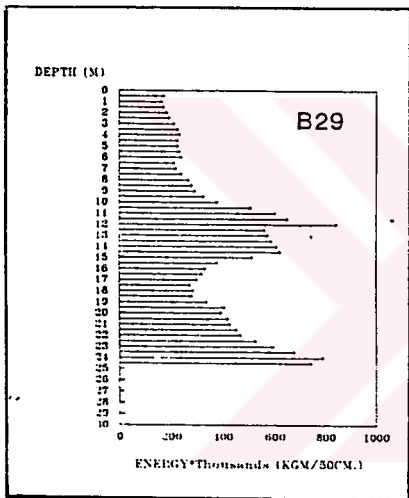
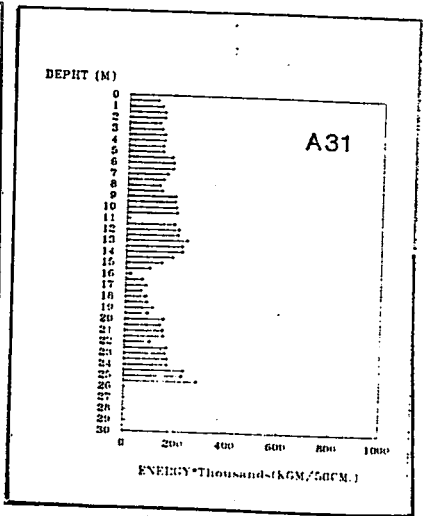
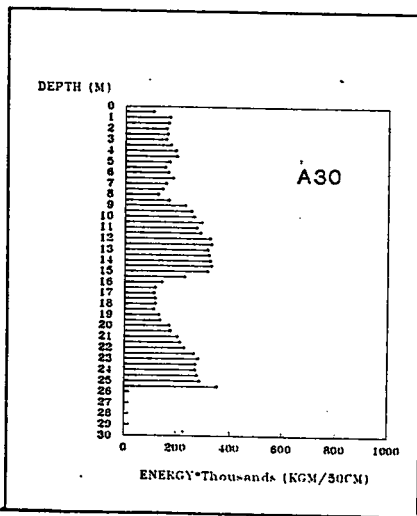
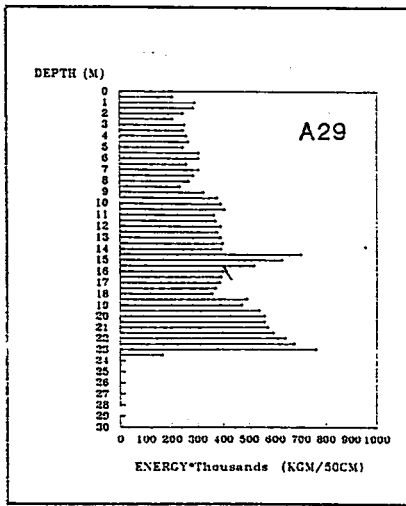


Figure 2.8 Pile Driving Records of Working Piles Around Test Pile B30

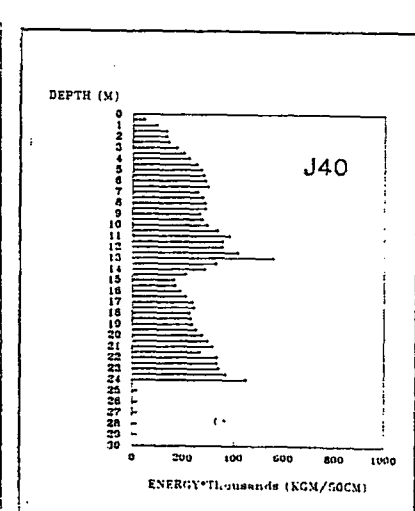
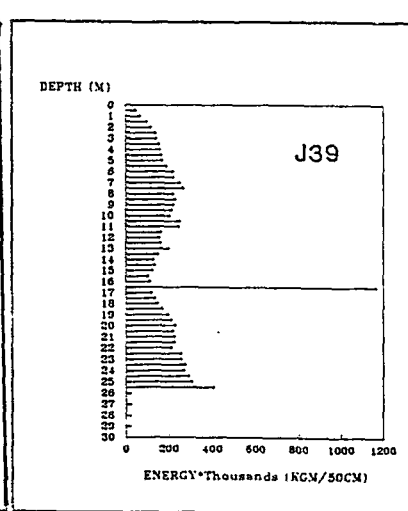
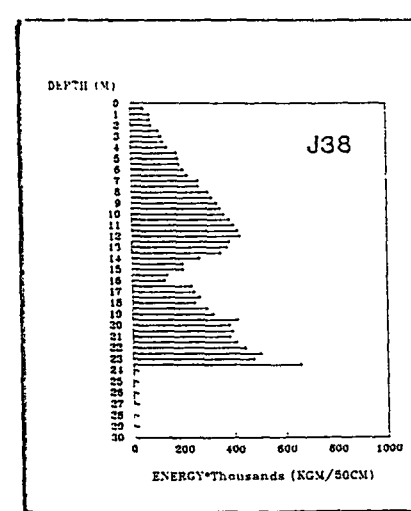
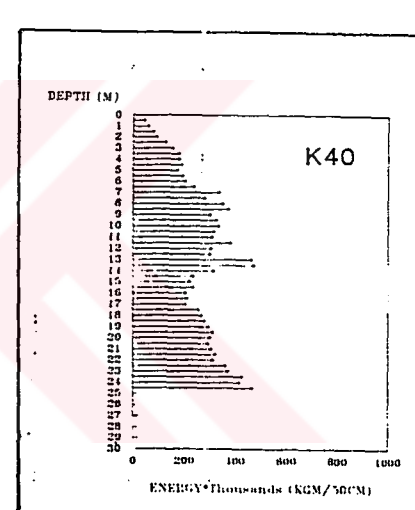
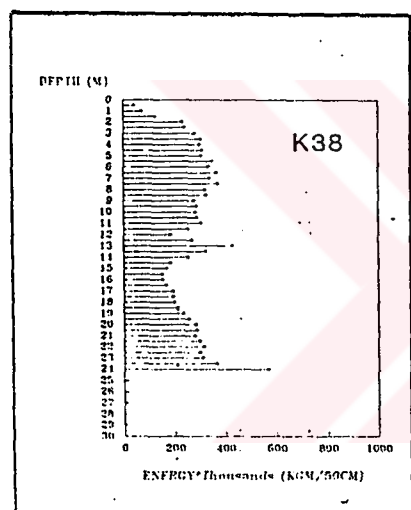
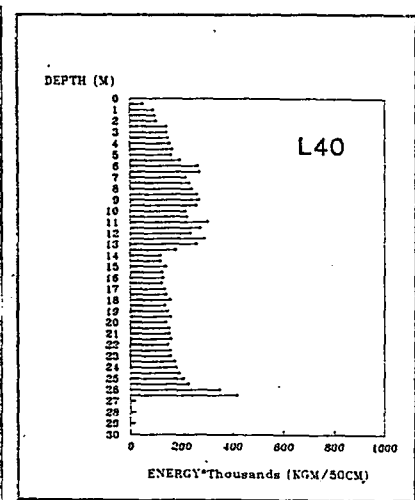
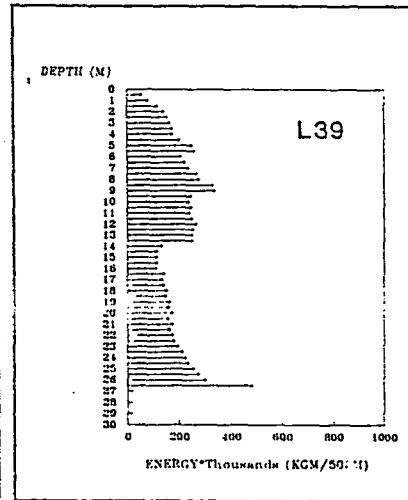
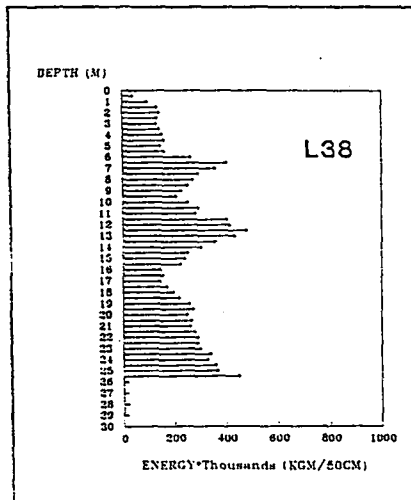


Figure 2.9 Pile Driving Records of Working Piles Around Test Pile K39

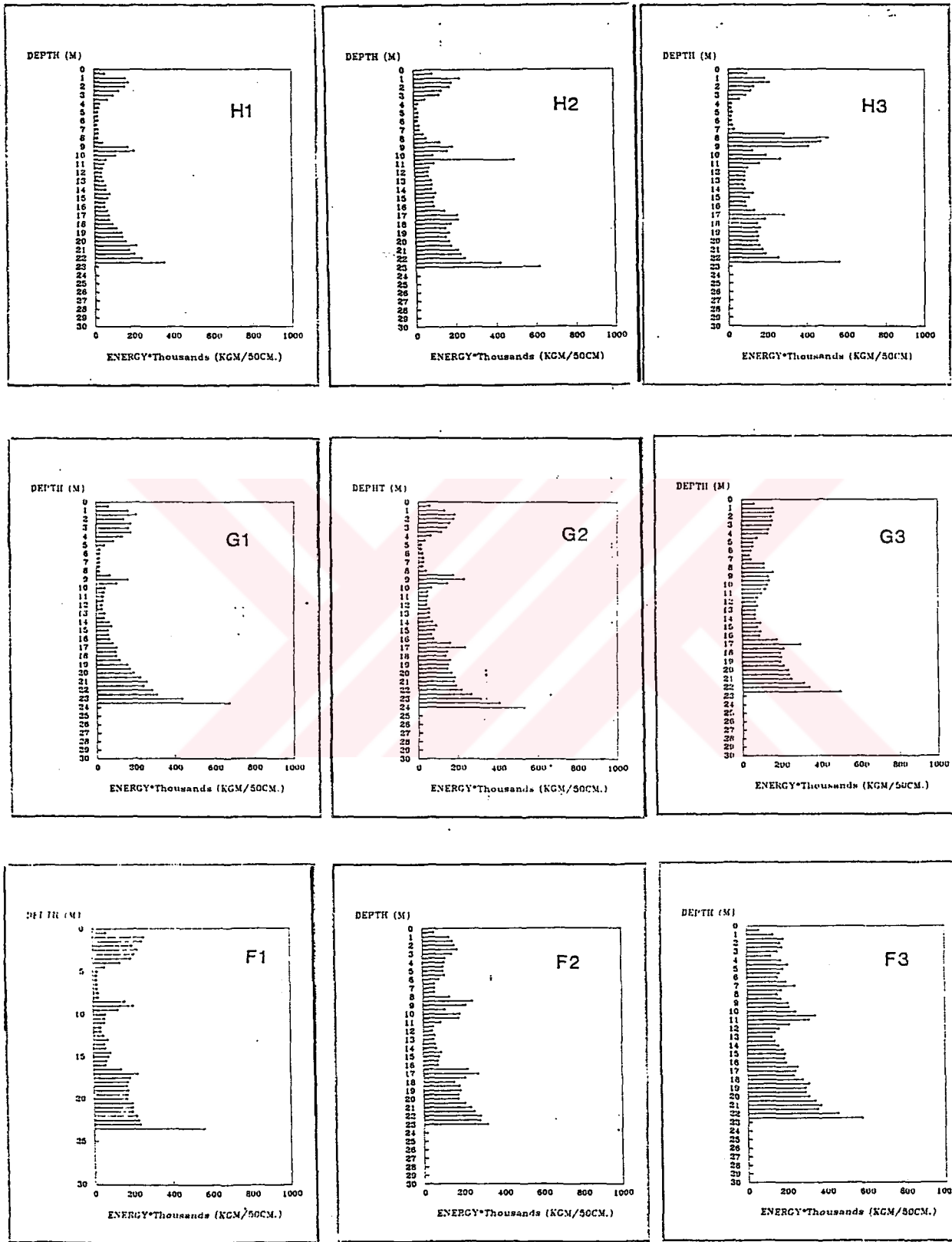


Figure 2.10 Pile Driving Records of Working Piles Around Test Pile G2

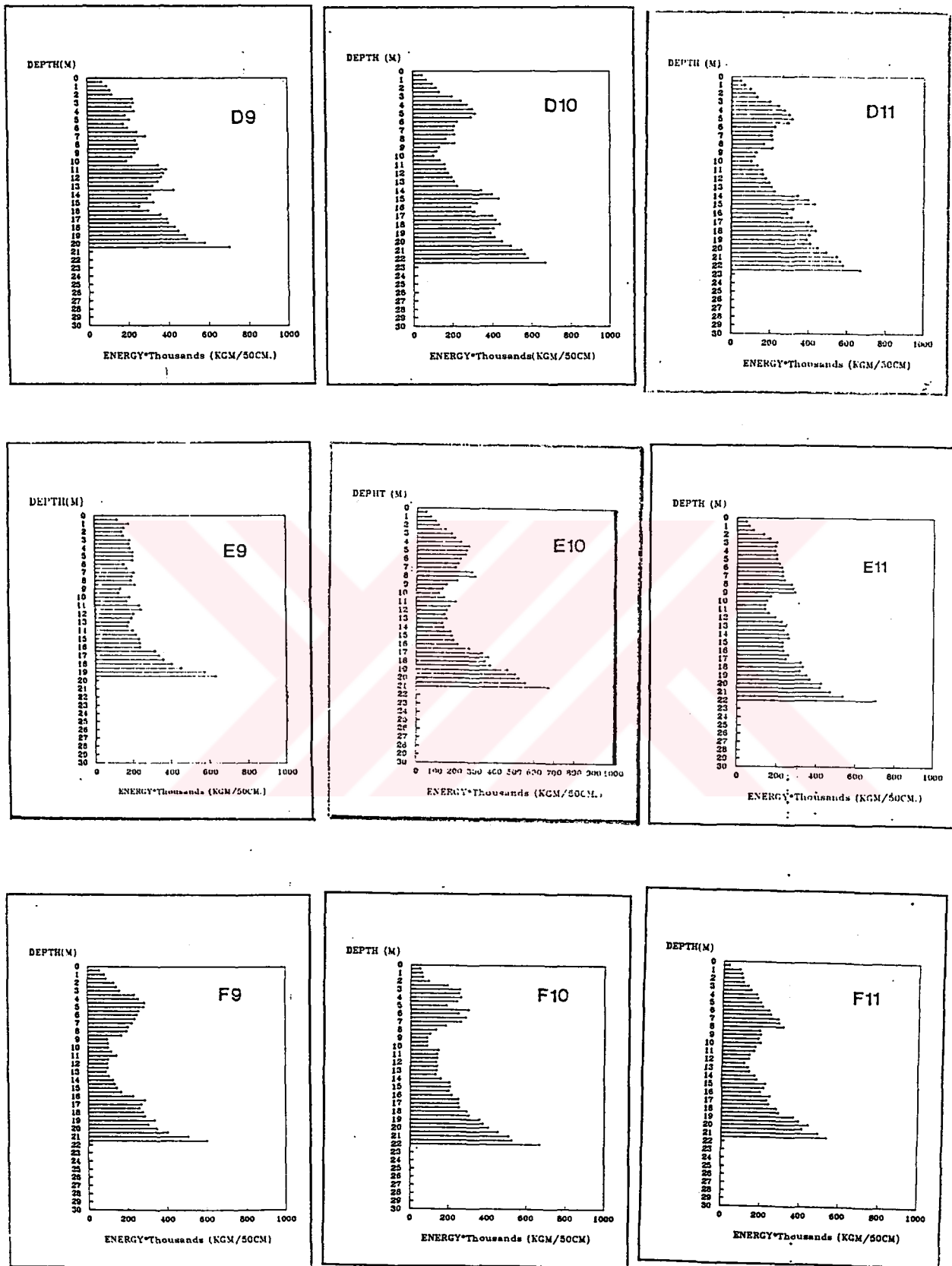


Figure 2.11 Pile Driving Records of Working Piles Around Test Pile E10

For example end bearing was identified as a rapid increase in load for negligible penetration. This is clearly seen in B30 in Figure 2.8. But in A31 in Figure 2.8, no such increase is apparent. Pile A31 in Figure 2.8 is therefore deemed to be carrying load predominantly in shaft adhesion due to relatively large penetration with no appreciable gain in pile capacity.

Pile driving records in Figure 2.9 can be used to predict the capacity of test pile K39, whose driving record is missing, assuming that the behavior of piles around this pile is similar.

These pile driving records also identify significantly different point of inflection at which loading again increases after fill is typically at a depth of 16 m for Block 1 in Figure 2.6, compared with 9 m. for Block 4 in Figure 2.10.

In summary, studies on driving records were performed:

i) to differentiate the piles with the same driving resistance. Piles with the same driving resistance were shown by the same contour line shown in Figure 2.1 and Figure 2.2.

ii) to differentiate the friction and end bearing piles. Because, dynamic pile formulas should not be used for friction piles driven into the soft clay. The number of blows per unit length of penetration for friction piles in clay are practically independent of depth. As a consequence, dynamic formulas if used in clay soils, may give such a wrong impression that the ultimate bearing capacity is independent of depth; on the other hand, it is known that the bearing capacity of friction piles increases with depth.[12]

iii) to detect major deviations in the geological profile. Because another way of exploration of subsoil stratification in a large extend can be as pile driving which is similar to dynamic penetration tests. Because in principal pile-driving is a way to detect the geological profile regarding its mechanical properties, but some restrictions are to be mentioned.

- Pile driving record is rough compared to a normal dynamic penetration tests sounding. Thin layers are not detected and the accuracy of positioning the separation of different layers can be beyond one meter depending on the pile diameter.

- The pile driving can cause a drastically change in the local soil properties compared to dynamic penetration test.

Although these restrictions present, pile driving can be accepted as a dynamic penetration test. It can detect the deviation in the geological profile. This information can be used to estimate proper input-data for common bearing capacity calculations. In this manner an indirect correlation between the dynamic and static behavior of a pile exists.

Prediction of ultimate bearing capacities of piles obtained from driving data by using Janbu driving formula in Block No.4 was shown in Figure 2.12. Variation of ultimate bearing capacities of piles in Block 4 was also shown in Figure 2.13. Results of Figure 2.13 and bearing capacities two test piles G2 and E10 in Block No 4 were summarized in Table 2.2. Dynamic capacities of these test piles are similar with the values obtained from compression load tests and static bearing

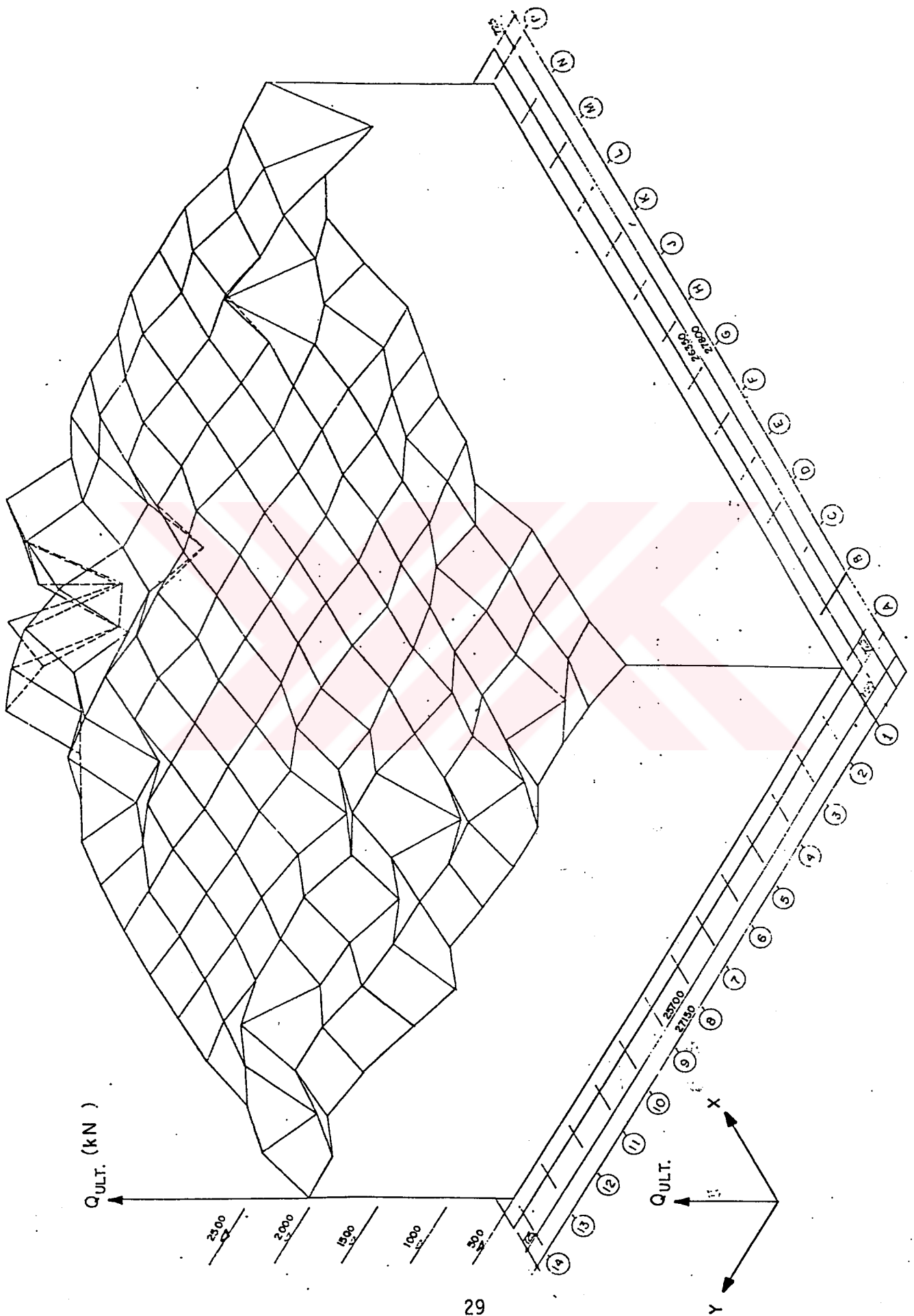


Figure 2.12 E Capacities Obtained From Data in Block No 4

DYNAMIC CAPACITY ( kN )

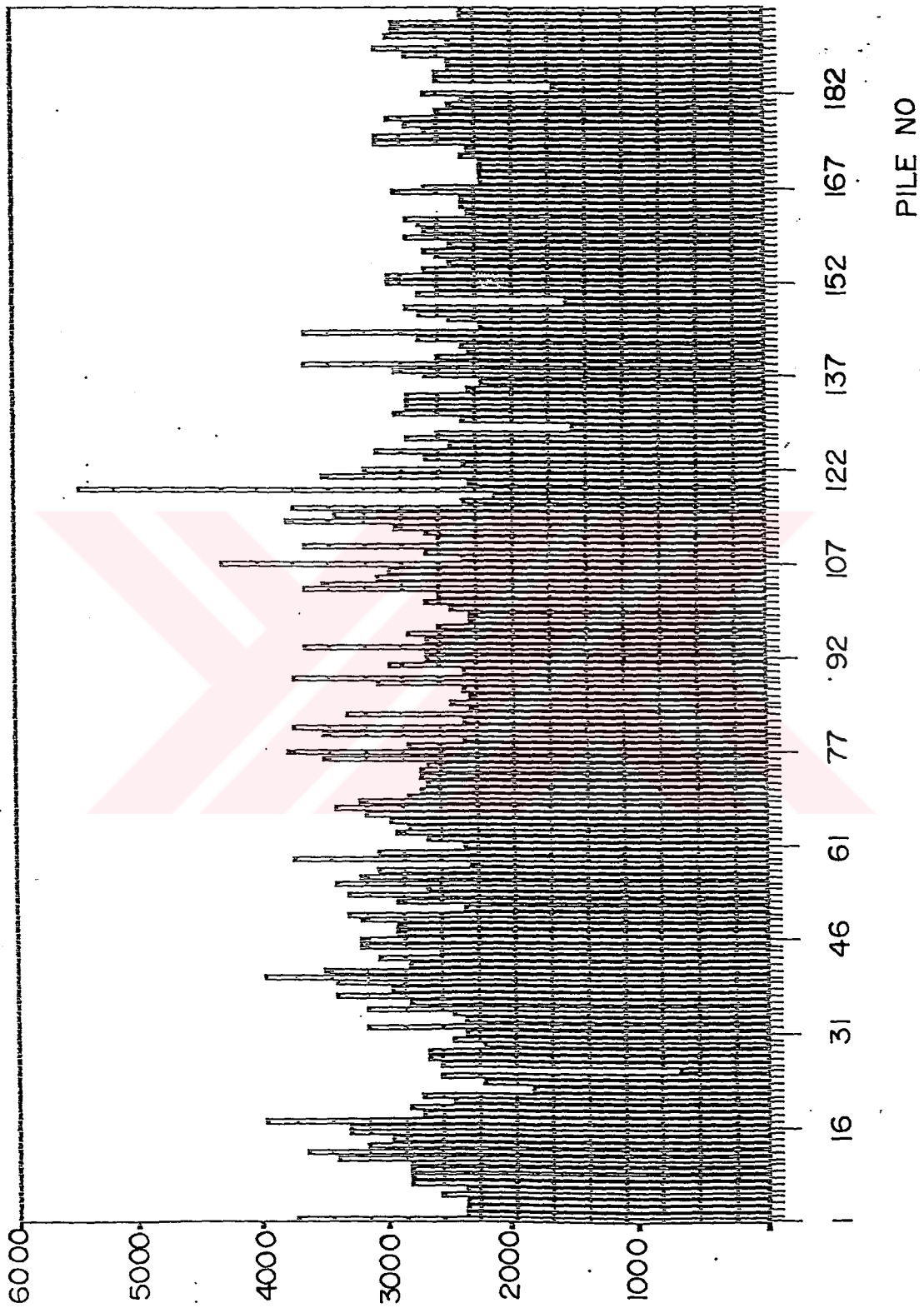


Figure 2.13 Distribution of Ultimate Capacities of Piles in Block No 4

**Table 2.2 Ultimate Dynamic Capacity of Test Pile G2 and E10 in Block No 4**

AVERAGE ULTIMATE DYNAMIC CAPACITY OF BLOCK NO 4 (kN)	STANDARD DEVIATION	TEST PILE IN BLOCK NO 4	BLOW FOR LAST 60 CM PENETRATION				HAMMER ENERGY AT GEAR 10th kNm / BLOW	ULTIMATE DYNAMIC CAPACITY OF THE PILE (kN)	
			21	24	24	26			27
2910	540.144	E10	21	24	24	26	27	27	2330
		G2	19	19	22	25	25	30	2590

capacity calculations. This prediction was made in only Block No.4. Because the existence of friction piles in Block No.4 is less, as shown in Figure 2.4

Bearing capacities of piles with the relation of penetration length was shown in Figure 2.14. In this figure, there was no clear connection between the penetration depth and the bearing capacity, in whole site of the Block No 4, because of the strong stratified ground. But at the middle of the block, a relation between toe elevation and bearing capacity of piles might be observed. This relation is as follows:

$$Q_{ult} = 1.6666 \cdot P + 250 \quad (2.1)$$

Where

$Q_{ult}$  = Dynamic capacity in Tons.

$P$  = Penetration Depth in meter.

This equation is valid for penetration depth of 15 to 25 m.

In summary, bearing capacity of piles in Block No 4 were not significantly different from results obtained from pile tests in Chapter 6 as well as from the fundamental soil mechanics approach in Chapter 4.

### 2.3.2 Calculation of Energy Losses

Value of energy losses for dynamic analysis were calculated as a representative of value given by Janbu formula. In calculation of average energy loss used for pile analyses and relations are shown in Figure 2.6, 2.7 and 2.8. Average pile length,  $L$ , and average stop blow-count,  $s$  of Block No.4 were taken. Average pile length,  $L$ , and average stop blow-count,  $s$  were shown in Figure 2.15

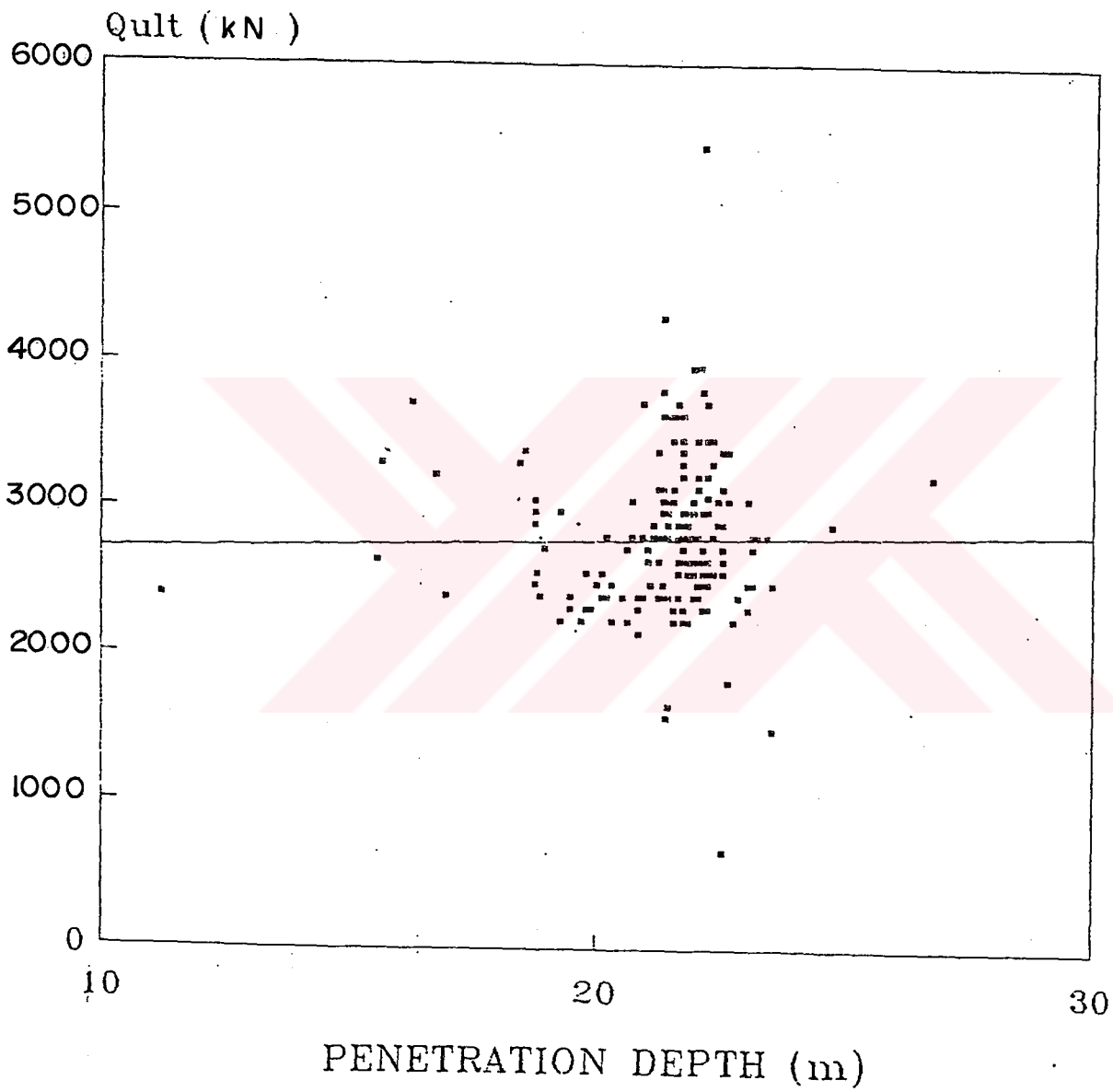
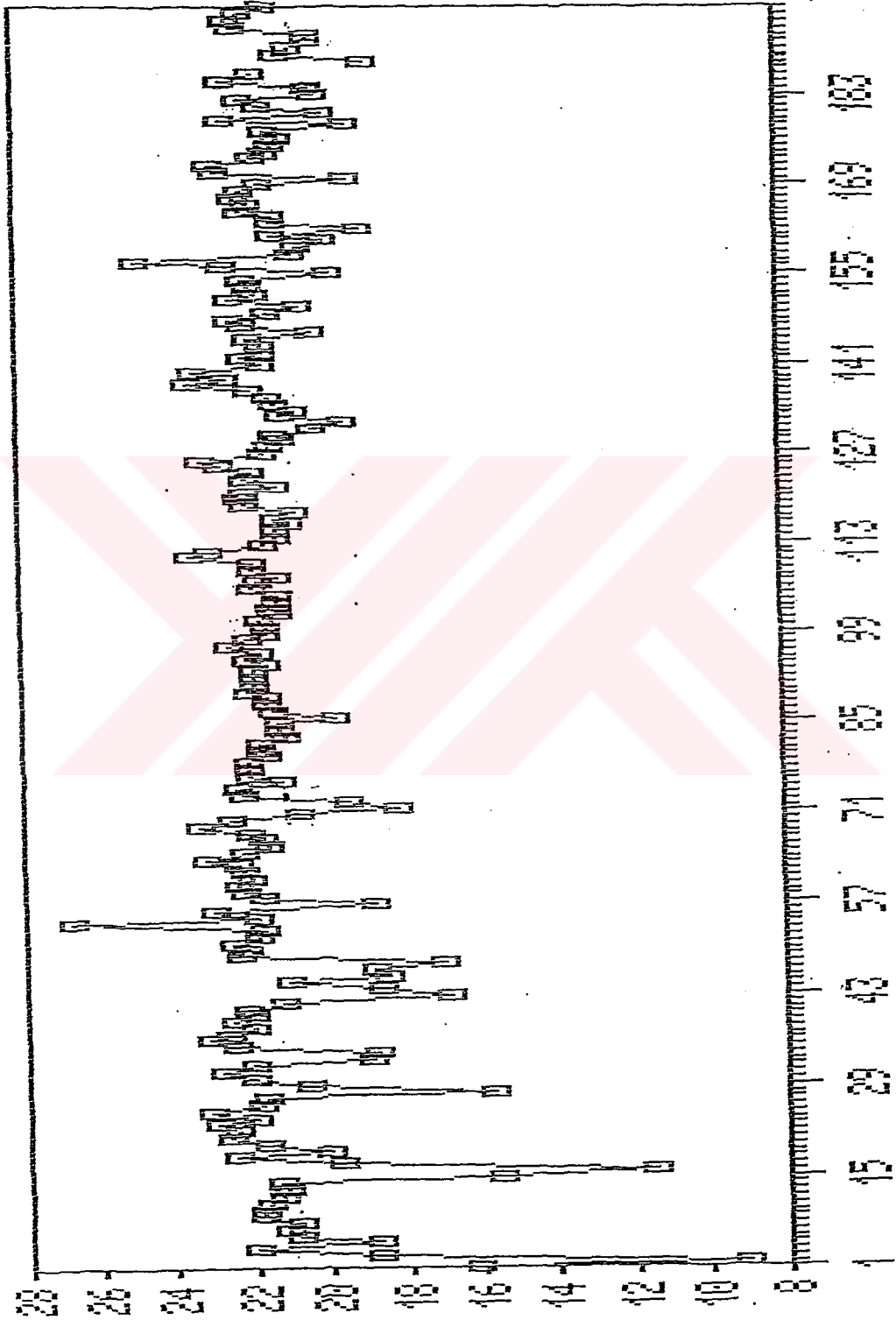


Figure 2.14 Bearing Capacities of Piles in Relation to the Penetration Length

BLOCK #4  
 STD. DEV. = 1.79 AVE. = 21.285 MAX = 26.7

TOE ELEVATIONS (M)



PILE NO

Figure 2.15 Variation of Toe Elevation of Piles in Block No 4

and Figure 2.16 respectively. Janbu Dynamic formula proposes ultimate bearing capacity as follows:

$$Q_{ult} = \frac{1}{k_u} \frac{E}{S}$$

$$k_u = C_d \left[ 1 + \sqrt{1 + \frac{\lambda}{C_d}} \right]$$

$$\lambda = \frac{EL}{AE_p s^2}$$

$$C_d = 0.75 + 0.15 \frac{W_p}{W}$$

where

$Q_{ult}$  = Ultimate bearing capacity of the pile

$E$  = Energy of hammer for one blow

$s$  = Penetration for one blow

$W_p$  = Weight of the pile

$W$  = Weight of the hammer

$L$  = Length of the pile

$A$  = Cross-sectional area of the pile

$E_p$  = Young's modulus of the pile.

The literature indicates that, the driving coefficient,  $C_d$ , included terms representing the efficiency of the pile hammer, the difference between the dynamic and static pile capacities and the rate of transferral of pile load into the soil with

Stop Blow-Count/10 cm

AVERAGE STOP BLOW-COUNT=34.66  
STANDARD DEVIATION=13.01

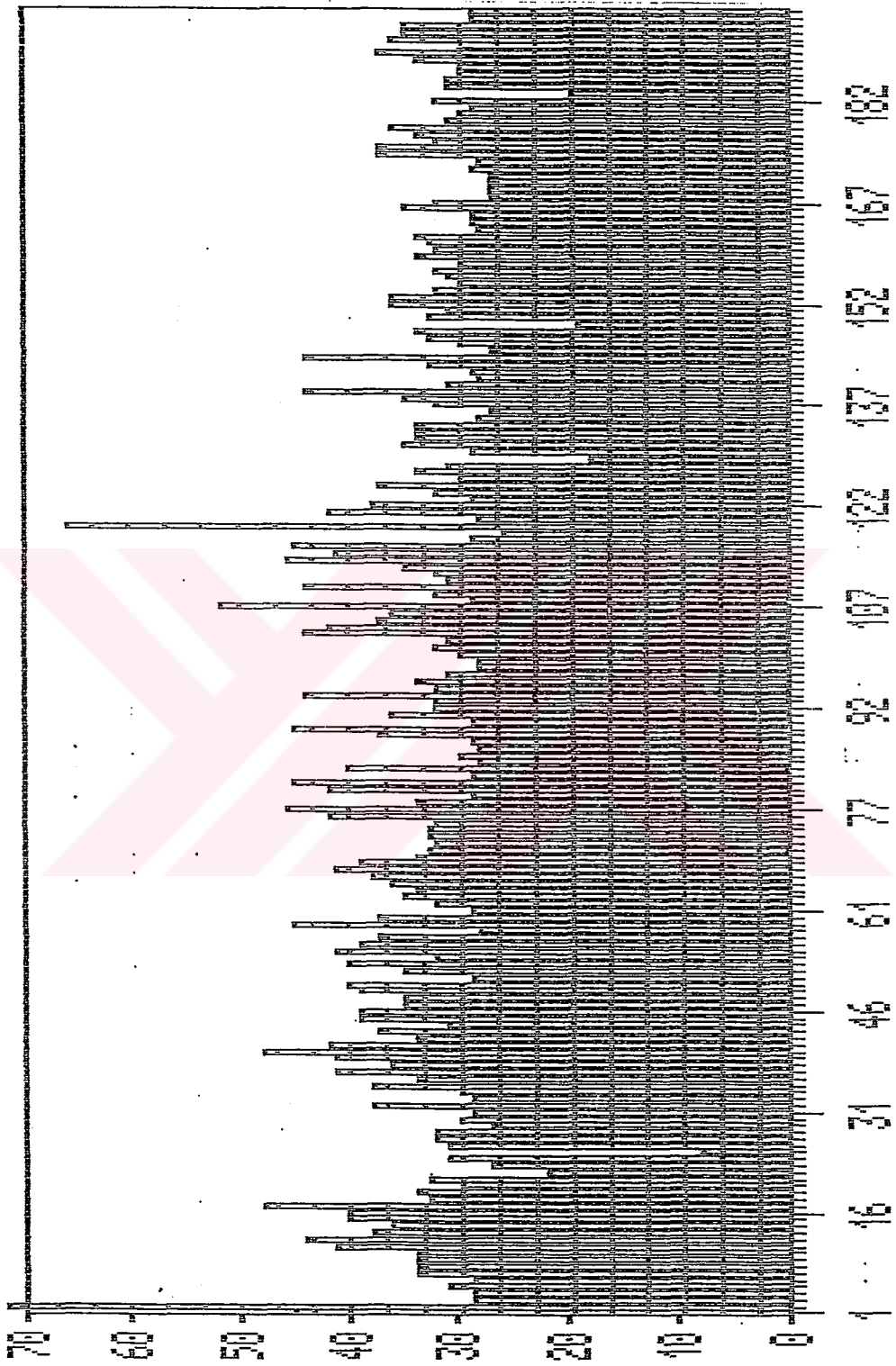


Figure 2.16 Variation of Stop Blow Count of Piles in Block No 4.

respect to depth. It also included the length and cross-sectional area of the pile, young's modulus for the pile and both the pile capacity and the set.

Janbu correlated his driving coefficient,  $C_d$ , with the ratio of the weight of the pile to the weight of the falling parts of hammer,  $W_p/W$ . The influence of the ratio  $W_p/W$  on the value of  $C_d$  has been investigated by Sorensen and Hansen (1975) with the conclusion that there occurs no significant variation in  $C_d$  variation in  $W_p/W$  as shown in Figure 2.17.

By making trial, influence of  $s$  on  $\lambda$  was also investigated. As a result it was decided to take average value of  $s$  and  $L$  in Block No.4 for calculation of average energy loss.

By taking

$$E = 5500 \times 10^{-2} \text{ kNm/blow (10}^{\text{th}} \text{ Gear)}$$

$$S_{\text{avg}} = 0.10 \text{ m/35 blow} = 0.286 \times 10^{-2}$$

$$W = 50 \text{ kN}$$

$$W_p = 21.3 \times 0.4^2 \times 25 = 85 \text{ KN.}$$

$$W_p / W = 1.7$$

$$L_{\text{avg}} = 21.3 \text{ m.}$$

$$E_p = 32000000 \text{ kN/m}^2$$

$$A = 0.4 \times 0.4 = 0.16 \text{ m}^2$$

$$W = 50 \text{ kN}$$

$k_u$  was found to be 6.38. This means 15% of reduction was made in Block No.4. For making check, variation of coefficient  $k_u$  was found to be 6.4 by using Figure 2.18.

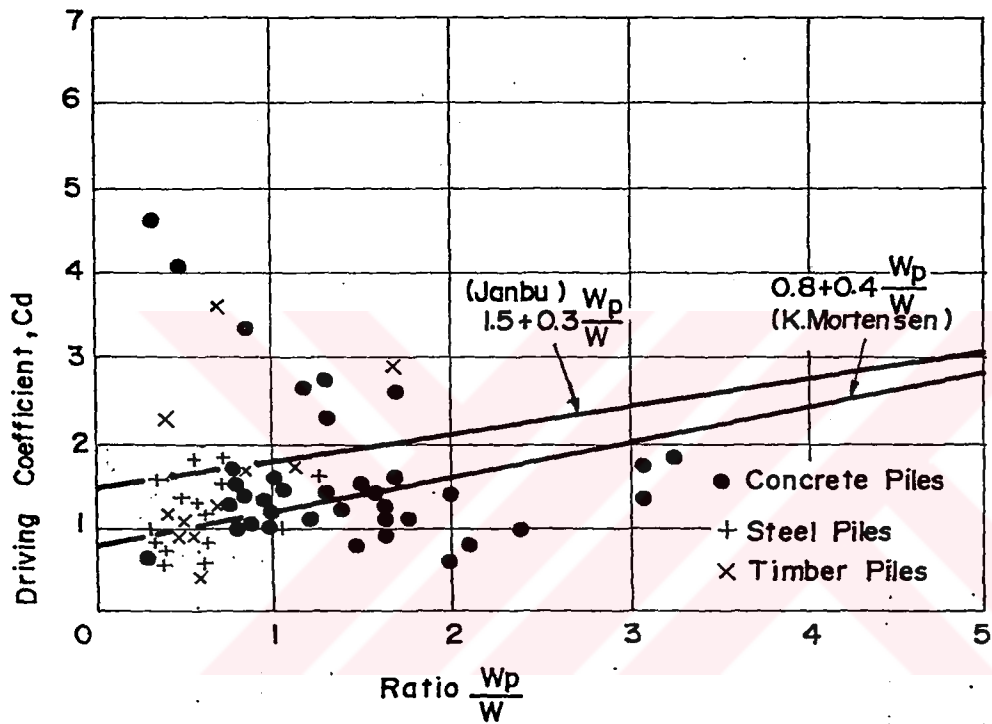


Figure 2.17 Influence of Ratio  $\frac{W_p}{W}$  on Driving Coefficient  $C_d$  in Janbu

Driving formula (After Sarsenen and Hansen , 1957)

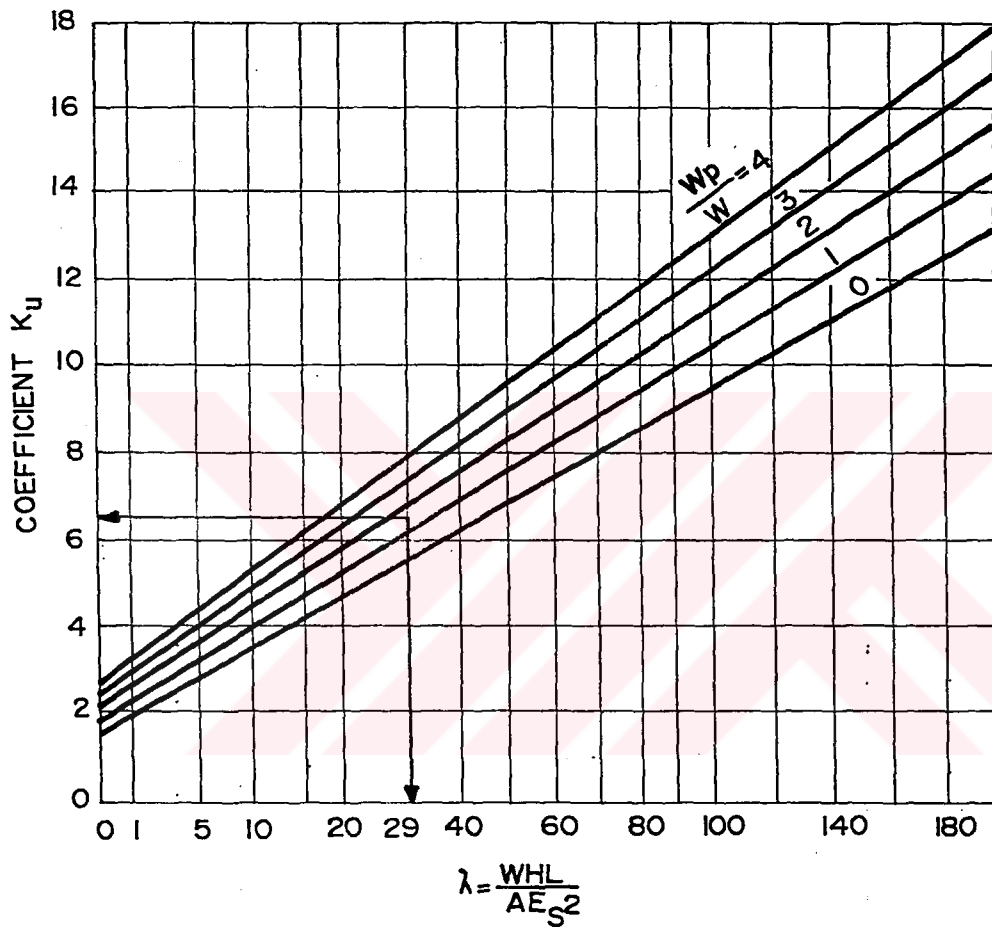


Figure 2.18 Diagram for the Determination of  $k_u$  in Janbu Driving

Formula (After Flaate, 1964)

## 2.4 Correlation Between Dynamic and Static Behavior of a Pile

In literature many trials to find such a correlation are reported. Hundreds of measured piles have been considered. Yet no satisfactory relation could be derived.

In this study, there is a purely empirical form valid for a specific situation. This relation is as follows:

$$(Q_{ult})_{dynamic} / (Q_{ult})_{static} = 0.898$$

A direct correlation between the pile driving resistance and static bearing capacity does not exist. Since

- Pile-driving causes dynamic excess pore pressures. This phenomenon is generally measured in sand layers. It can be expected likewise in less permeable soil layers on the contrary static behavior of a pile is not affected by such temporary excess pressures.

- The distribution of side and toe resistance appears to differ significantly for during driving and static bearing capacity test.

- The area of soil mobilized due to the pile behavior in a static and dynamic loading environment is principally different with respect to the area size and the nature of the response. [13]

## CHAPTER III

### GROUND DISPLACEMENT DUE TO PILE DRIVING

#### 3.1 Introduction

The aim of this chapter is to describe the relative density change caused by piles driven into the soil with upper 10 m fill is overlying the fully saturated silty, sandy clay. An analysis of the two different test piles shown in Figure 3.2 indicates quite satisfactorily the general trend of increasing of load carrying capacity due to pile driving. It may be pointed out that the difference in load carrying capacities for the same settlement of these test piles are due to compaction of fill only, since clay was fully-saturated.

#### 3.2 Action of Soil Around a Driven Pile

When a pile is driven into sand and cohesionless soil, the soil is usually compacted by displacement and vibration, resulting in permanent rearrangement and some crushing of the particles. Penetration tests results in sand prior to the pile driving and after pile driving indicate significant densification of the sand around the pile. Increasing density results in an increase in the internal friction angle. Driving of a pile displaces soil laterally and thus increases the horizontal stress acting on the pile. Horn (1966) summarized the results of studies of horizontal effective stress,  $\sigma_h$ , acting on the piles in sand. It may be useful to point out that the wide

range in horizontal stresses in Table 3.1. It would seem logical that  $K$  must exceed 1 and a value around 2 would seem to be reasonable (Lambe and Whitman 1969).

Robinsky and Morrison conducted a careful series of model pile tests in sand. It was found that in an initially very loose sand (Relative density,  $D_r = 17\%$ ), soil movement extended 3 to 4 pile diameters from the side of the pile and 2.5 to 3.5 diameters below the pile tip. In medium dense sand ( $D_r = 35\%$ ), the extent movement was somewhat larger, extending 4.5 to 5.5 diameter from the side and 3 to 4 diameters below the tip. [15]

### 3.3 Action of Soil Around a Pile in Group

When group of piles are driven into loose sand, if the pile spacing is sufficiently close (less than about six diameters), the ultimate load capacity of the group may be greater than the sum of the capacities of the individual piles—that is, the efficiency of the group is greater than 1. (Lambe and Whitman 1969).

Some field measurements of the amount of compaction caused by the driving of a group in granular soil, in which standard penetration tests have been carried out before and after driving of groups have been reported by Philcox (1962). The test results are shown in Figure 3.1. Cases (c) and (d) show that the increase in  $N$  becomes less at the point considered becomes more distant from the center of the group. [15]

Table 3.1 Horizontal Stress on Pile Driven In Sand.

Reference	Relationship	Basis of Relationship
Brinch, Hansen, and Lundgren (1960)	(a) $\sigma'_h = \cos^2 \phi' \cdot \sigma'_v = 0.43 \bar{\sigma}_v$ if $\phi' = 30^\circ$ (b) $\sigma'_h = 0.8 \sigma'_v$	(a) Theory (b) Pile test
Henry (1956)	$\sigma'_h = K_p \cdot \sigma'_v = 3 \sigma'_v$	Theory
Ireland (1957)	$\sigma'_h = K \sigma'_v = (1.75 \text{ to } 3) \sigma'_v$	Pulling tests
Meyerhof (1951)	$\sigma'_h = 0.5 \sigma'_v$ ; loose sand $\sigma'_h = 1.0 \sigma'_v$ ; dense sand	Analysis of field data
Mansur and Kaufman (1958)	$\sigma'_h = K \sigma'_v$ ; $K = 0.3$ (compression) $K = 0.6$ (tension)	Analysis of field data

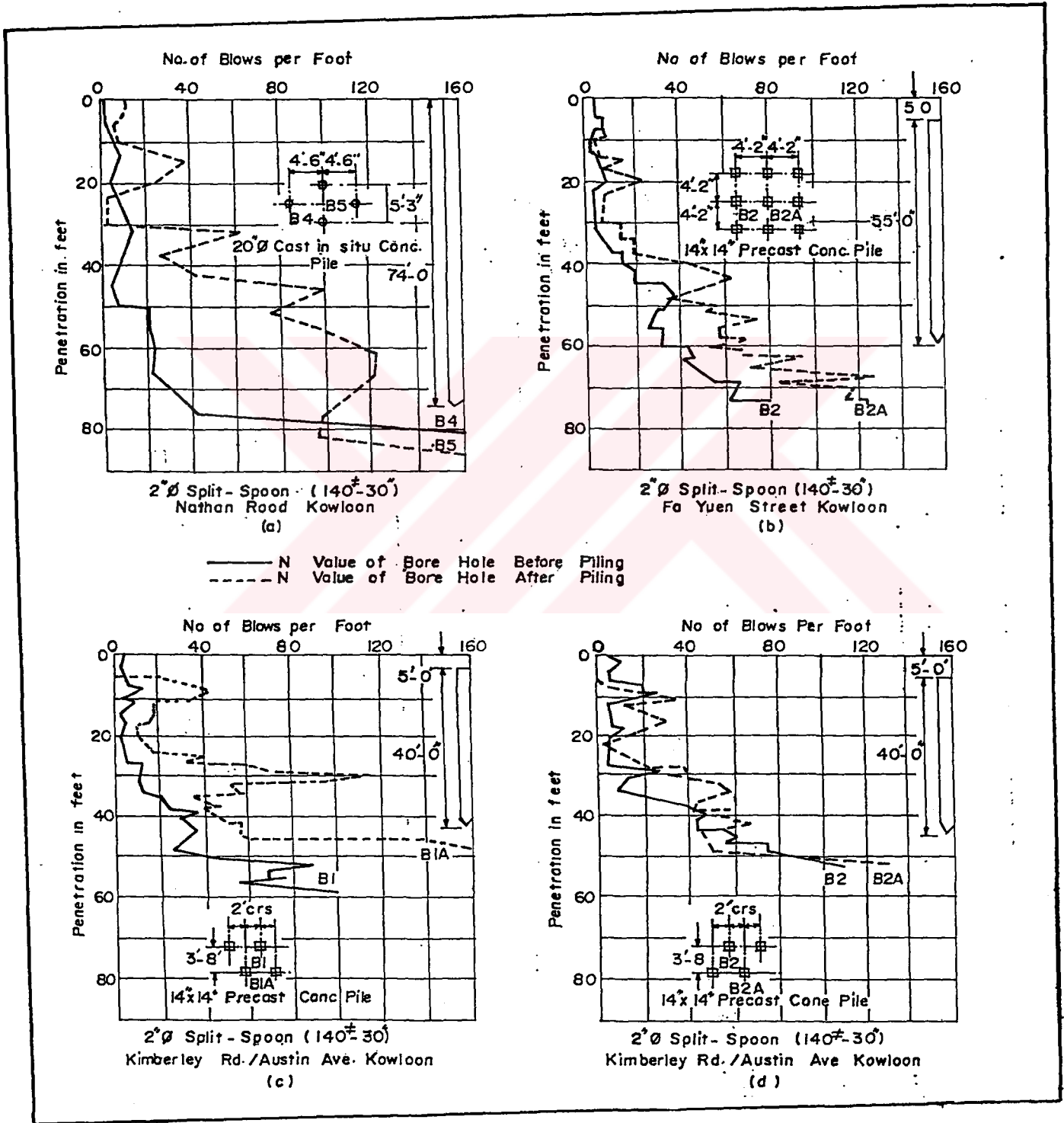


Figure 3.1 A comparison of N Values Before and After Driving Piles (Philcox, 1962)

### 3.4 Difference in Bearing Capacity Behaviour Between Single Pile and Pile in Group

Two test piles, shown in Figure 3.2 have the same geometry and about the same soil profiling. Therefore it is expected that the static capacities of these driven piles are similar. But unlike the test pile K39, the test pile B30 in Figure 3.2 was tested before the driving of neighboring piles in group and it could be assumed to carry less load than the other due to less compaction of soil. In general, the ultimate shaft friction of a pile is mobilized at very small deformation; less than 5mm. relative movement between the soil and the pile. End bearing resistance is not fully mobilized until large settlements occur, numerically up to 20% of the base diameter in sand and 10% in clay.[5] The shaft friction of test pile K39 is equal to 235 tons, when the pile tip settlement is about 5mm. The friction of second test pile B30 is mobilized at a value of 165 tons, when the pile tip settlement is about 5mm. In order to relate the change in shaft resistance to the change in  $\sigma'$  and  $K_s$  the following formula is given.

The subscripts 1 and 2 in the following formulas denote the single test pile K 39 and test pile B30 in group cases respectively.

$$\Delta Q = \sigma_{v0} \times \Delta K_s \times \Delta \tan \tau \quad (3.1)$$

$$\text{or} \quad \Delta Q = \Delta f_s = (f_{s2} - f_{s1}) * A_s \quad (3.2)$$

$\Delta Q$  = Difference in shaft resistance of test piles

$\sigma_{v0}$  = Effective overburden stress

$\Delta K_s$  = Difference in the ratio of horizontal to vertical

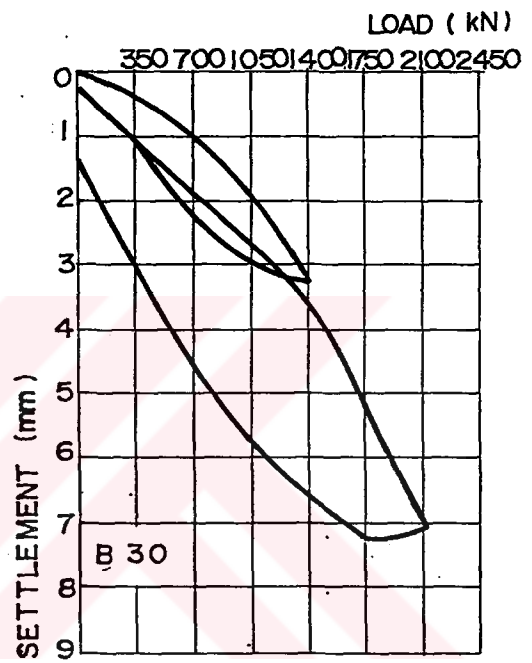


Figure 3.2 Load-Settlement Behaviour of Two Test Piles.

effective stresses, of single pile and pile in group

$\Delta\tau$  =Difference in angle of wall frictions of single pile and pile in group

$f_s$  = Ultimate shaft resistance of the pile.

$A_s$  = Shaft area of the pile along the fill.

Equation (3.2) can also be evaluated by the following expression.

$$f_{s2} - f_{s1} = \sigma_{v0} \times (K_{s2} - K_{s1}) \times (\tan \tau_2 - \tan \tau_1) \quad (3.3)$$

Difference in  $K_s$ ,  $\Delta K$ , and difference in  $\tau$ ,  $\Delta\tau$ , will be explained in the following paragraphs.[10]

### 3.5 Prediction of the Amount of Compaction

Densification of soil can be interpreted by the angle of internal friction angle and internal friction can be estimated from the intermediate parameter of relative density.

It must be pointed out that in process of predicting the increase in relative density, a number of errors occur, due to the natural variability of the soil; this is tied to fact that the pile load tests and the soil tests are not performed at the same location.

The cone penetrometer test (CPT) and standart penetration test (SPT) have an important role in exploration of cohesionless soil because there is a lack of satisfactory alternative methods.

In this study, before pile driving CPT and SPT have been carried out on construction site. Thus initial relative density have been estimated from cone penetrometer and standard penetration test results.

For evaluating relative density of soil from CPT soundings various methods have been suggested by Durgunoğlu and Mitchell (1975), Trofimenkof (1974), Schmertman (1977) Schmertman (1978) as shown in Figure 3.3 through Figure 3.6. In Table 3.2, relative density or internal friction angle have been estimated by using these methods with Cone Penetrometer Test Results. Additionally, the prediction of those parameters have been summarized by using various methods have been suggested by Thorburn (1963), Gibbs and Holtz, DeMello (1971), after Gibbs and Holtz as shown in Figure 3.7 through Figure 3.10. Kishida (1967) suggests that  $\phi'$ , and N may be related by the following expression.[9]

$$\phi = \sqrt{20N + 15} \quad (3.4)$$

In Table 3.3,  $\tau$  and  $K_s$  values are given.

In this study, SPT and CPT field measurements have not been carried out after driving of groups. Consequently, the amount of compaction, in other words increase in relative density, caused by the driving of groups was not known. As in the case of this project, if any parameter related with void ratio or relative density is not available than engineering judgement and/or approximate method may be necessary to find the amount of compaction. Because design of driven piles, unlike the bored piles, without considering the amount of compaction leads to conservation.

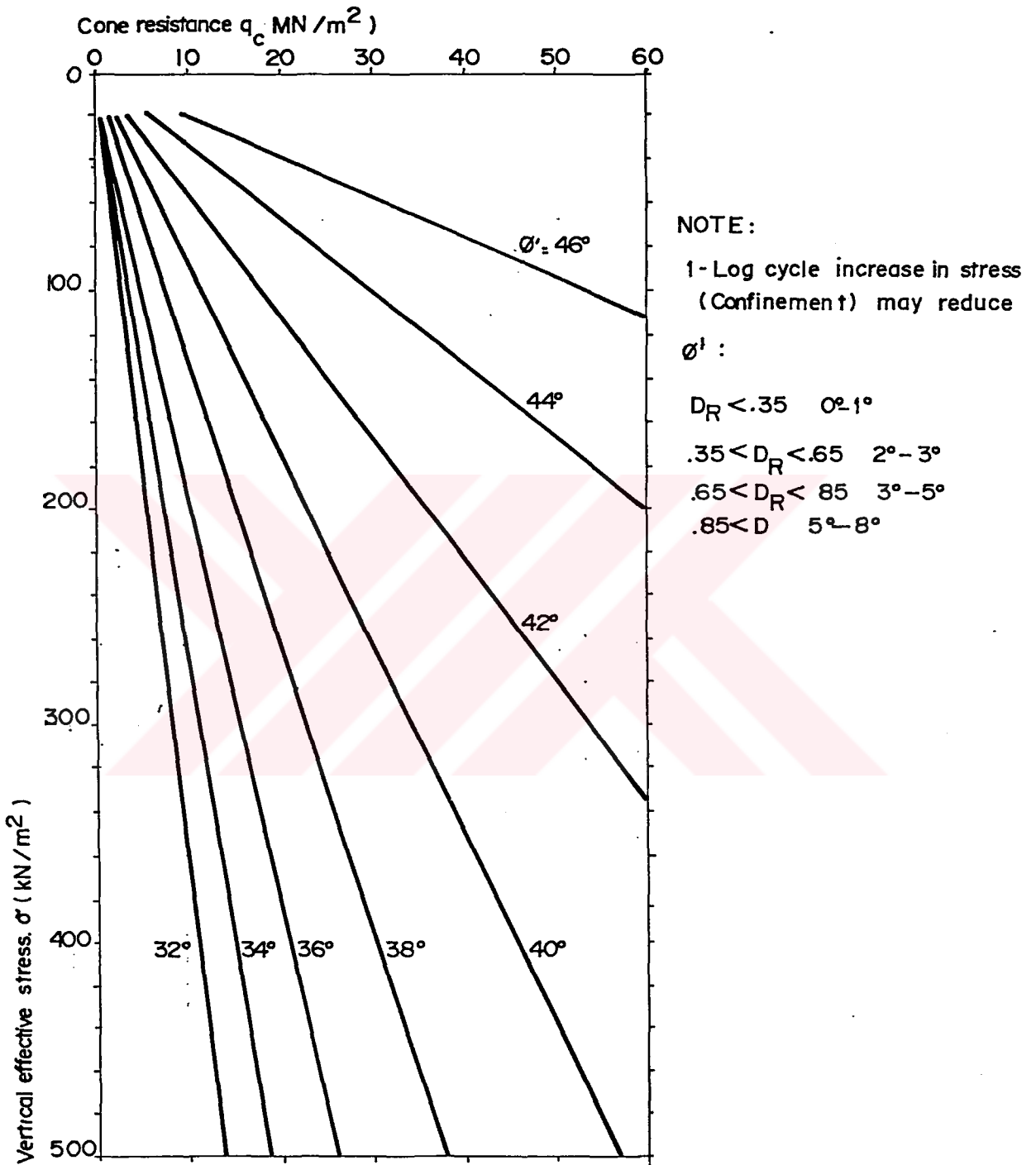


Figure 3.3 Relationship Between Angle of Shearing Resistance and Cone Resistance (After Durgunoglu and Mitchell, 1975)

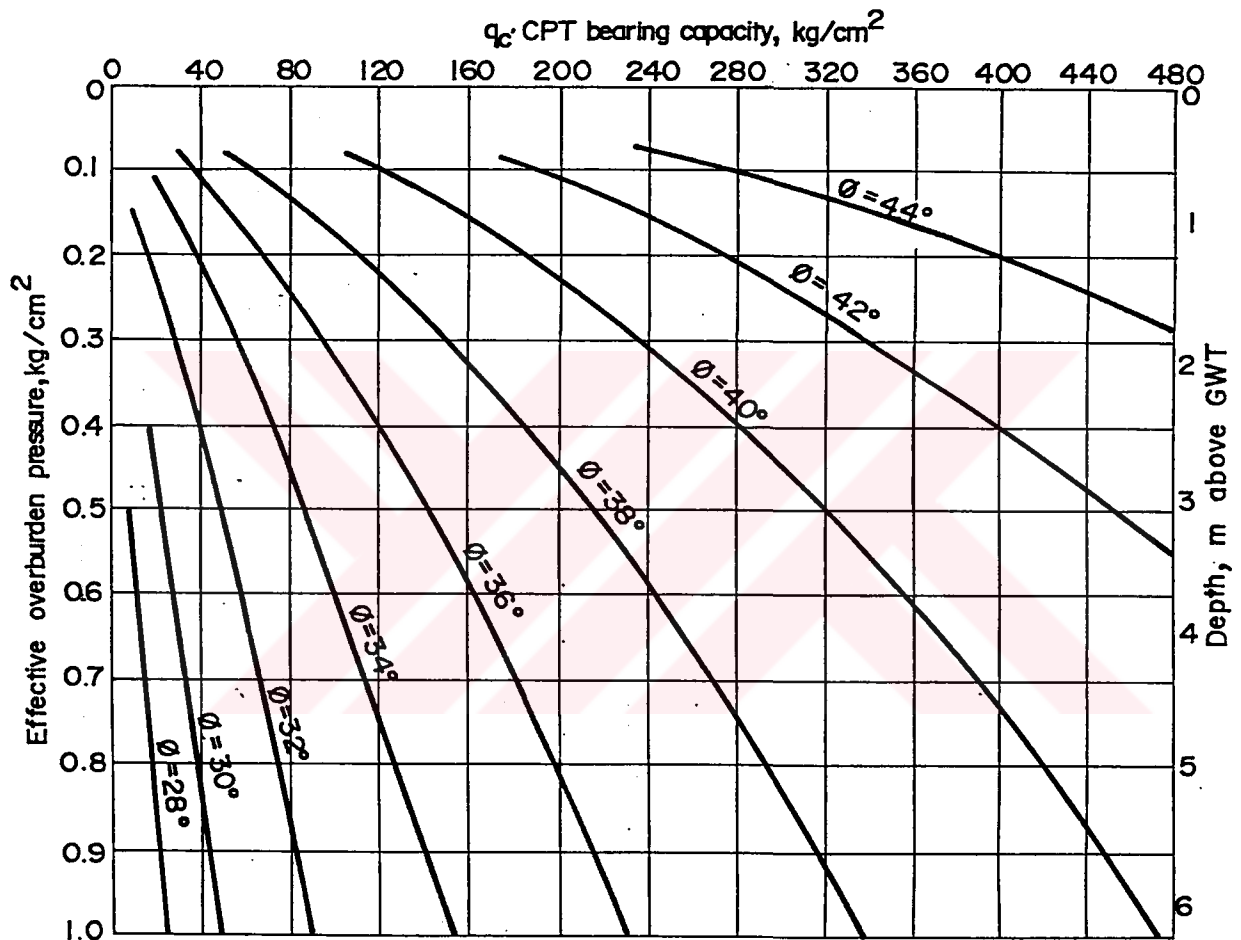


Figure 3.4 Correlation Between Effective Overburden Pressure  $q_c$  and  $\phi$

(Trofimenkov, 1974)

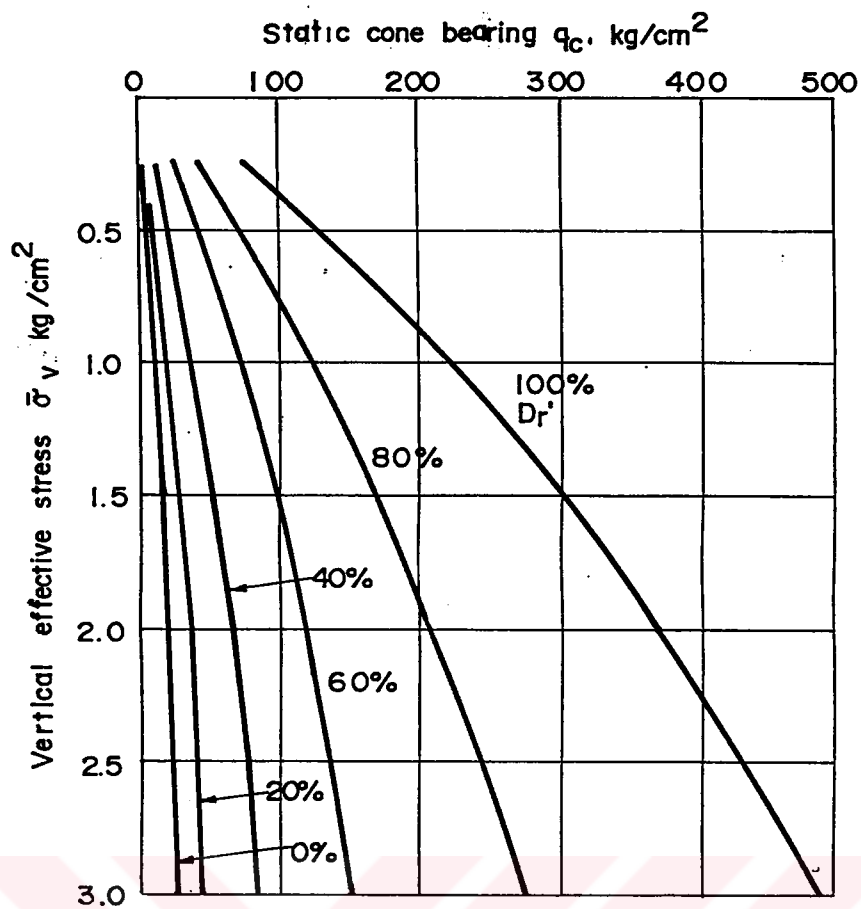


Figure 3.5 Static Cone Resistance  $q_c$  Versus  $D_r$  (Schmertman, 1977)

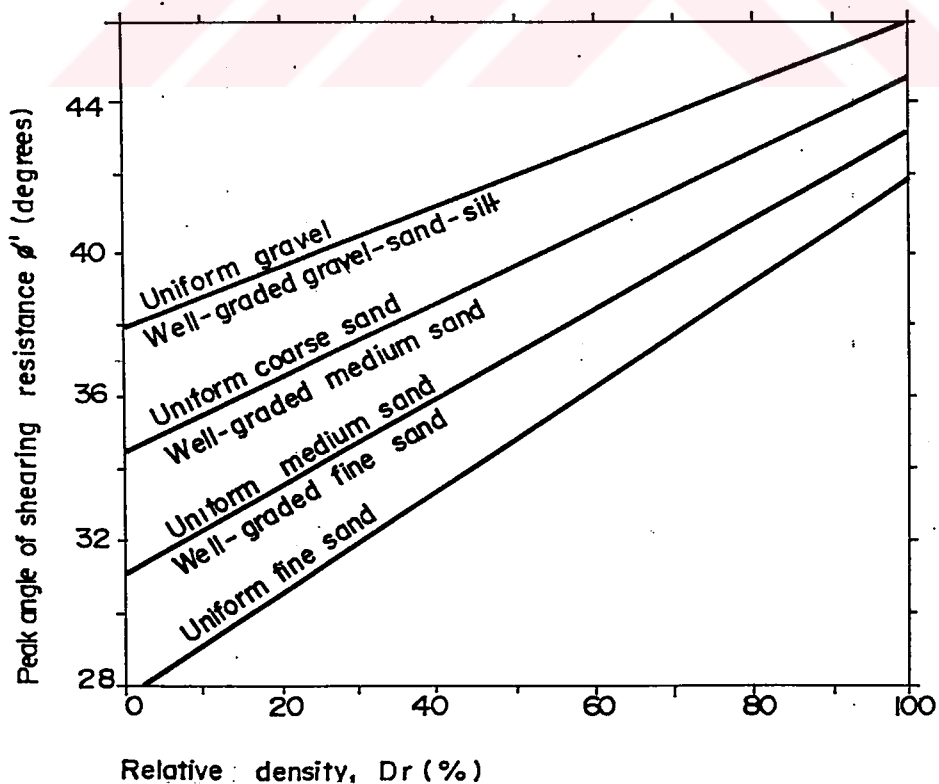


Figure 3.6 Relationship Between Peak Angle of Shearing Resistance and Relative Density (Schmertman, 1978)

**Table 3.2 Relation Between Cone Resistance and Relative Density**

METHOD	$q_c=40$ kg/cm <sup>2</sup>	$q_c=50$ kg/cm <sup>2</sup>	$q_c=60$ kg/cm <sup>2</sup>	$q_c=80$ kg/cm <sup>2</sup>	$q_c=100$ kg/cm <sup>2</sup>
DURGUNOGLU & MITCHELL (1975)	$\phi' = 32$	$\phi' = 34$	$\phi' = 36$	$\phi' = 38$	$\phi' = 39$
TROFIMENKOF (1974)	$\phi' = 28.5$	$\phi' = 29$	$\phi' = 30$	$\phi' = 31$	$\phi' = 32$
SCHMERTMAN (1977)	$D_R = 40\%$	$D_R = 45\%$	$D_R = 50\%$	$D_R = 60\%$	$D_R = 68\%$
SCHMERTMAN (1978)	$\phi' = 30$	$\phi' = 34$	$\phi' = 34.5$	$\phi' = 36$	$\phi' = 37$

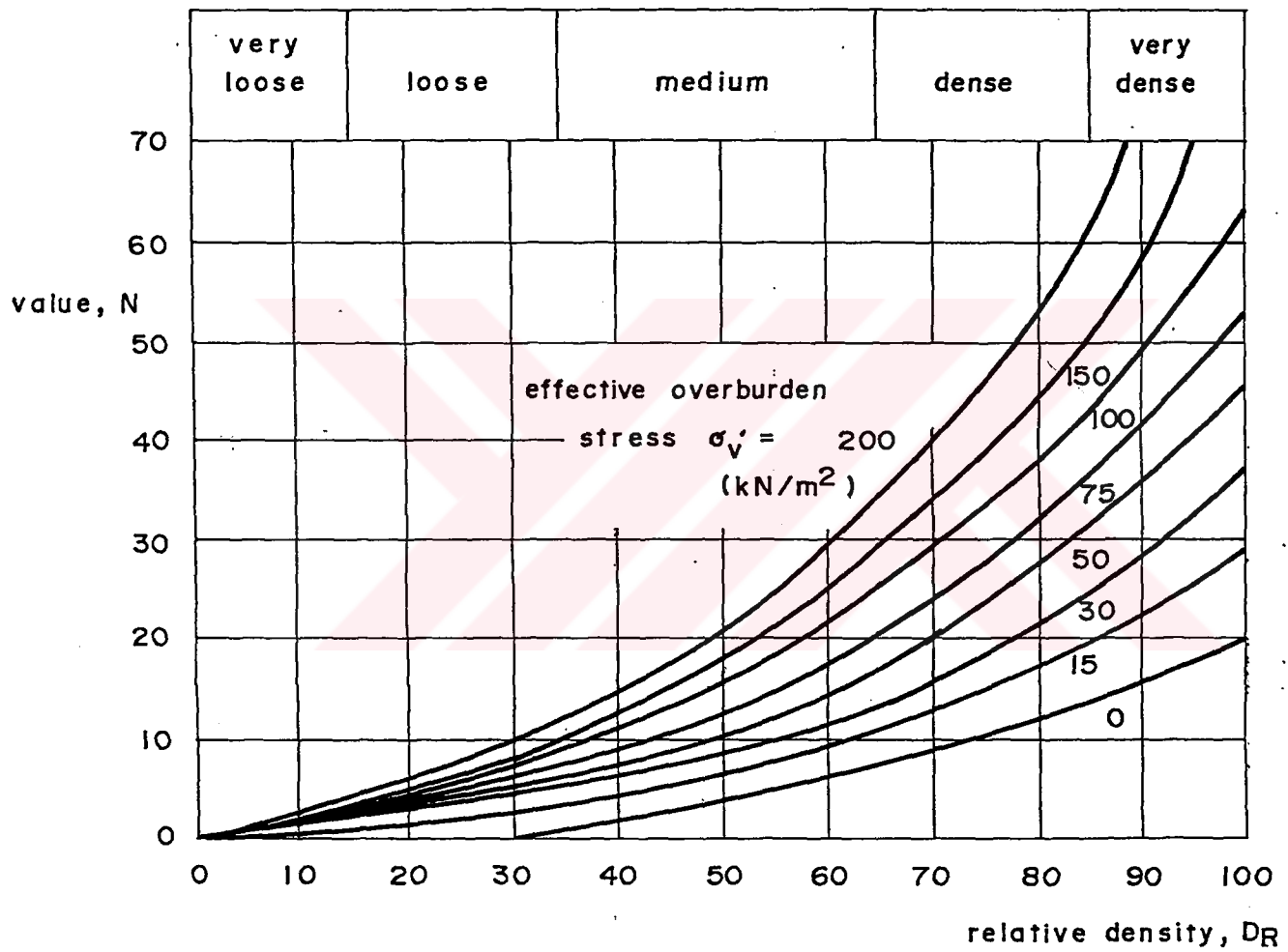


Figure 3.7 Correlation of SPT Value With Relative Density (Thorburn, 1963)

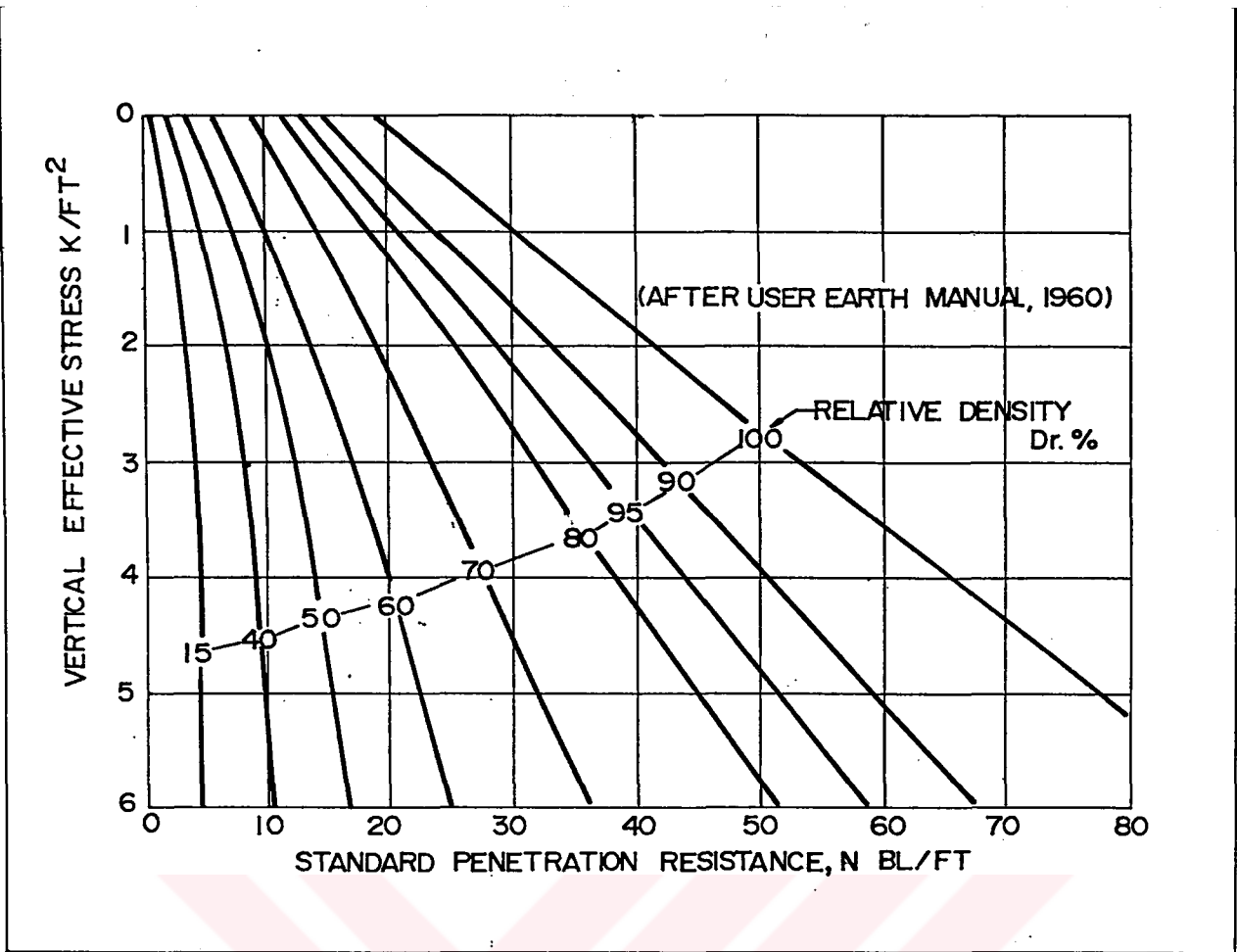


Figure 3.8 Correlation Between Relative Density and Standard Penetration Resistance in Accordance With Gibbs and Holtz.

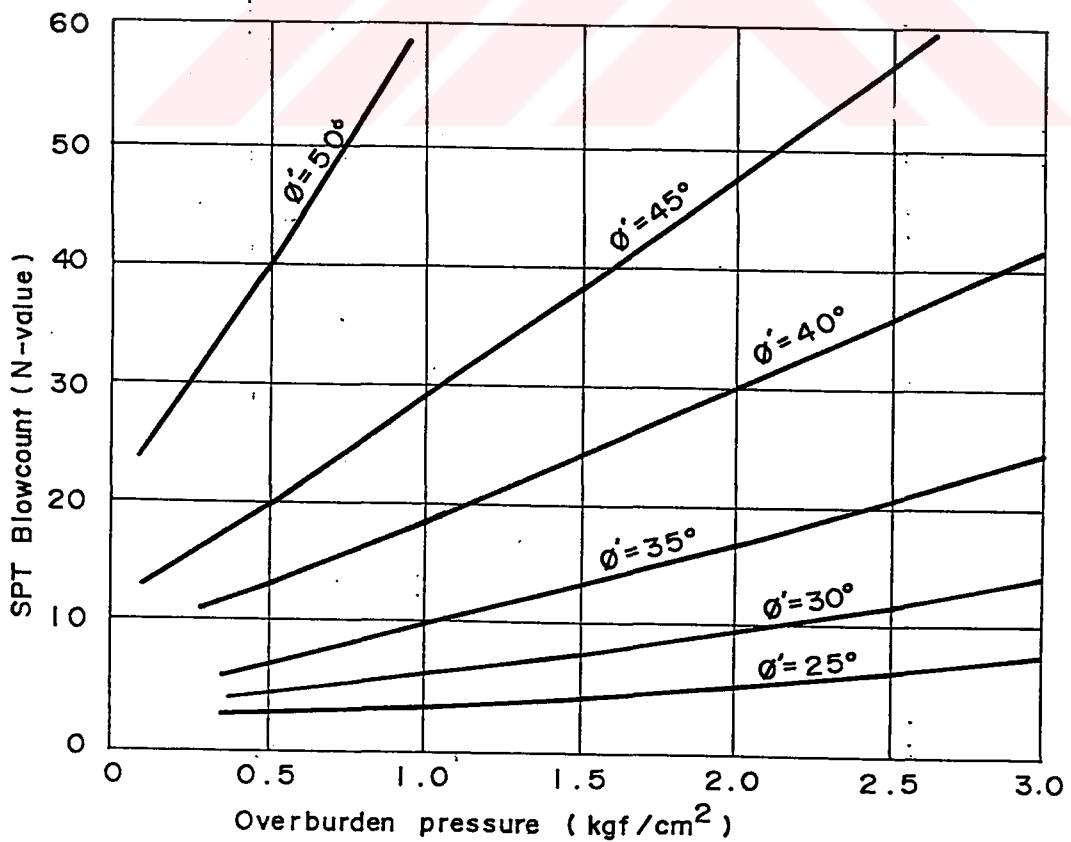


Figure 3.9 Method for Estimating  $\phi'$  From SPT (DeMello's, 1971)

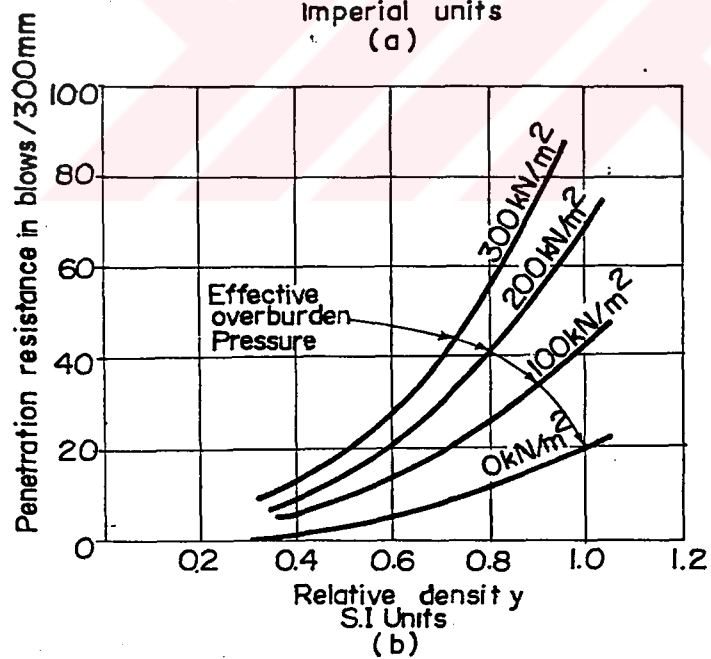
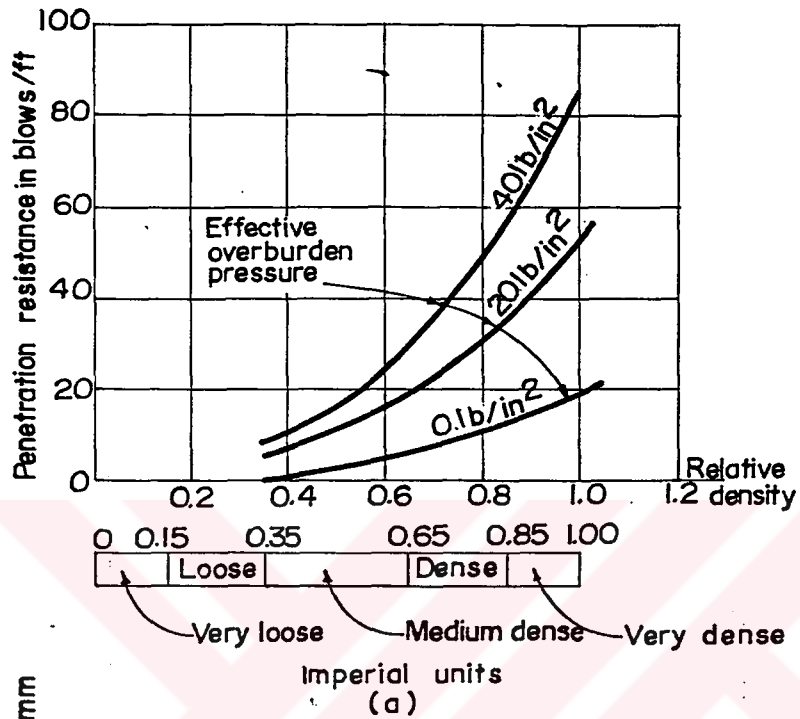


Figure 3.10 Relative Density Obtained From Standard Penetration Test N-Values (After Gibbs and Holtz)

**Table 3.3 Angle of Wall Friction Between Pile and Soil**

Pile type	$\delta$	$K_s$ for	
		Low relative density	High relative density
Steel	20°	0.5	1.0
Concrete	3/4 $\emptyset$	1.0	2.0
Wood	2/3 $\emptyset$	1.5	4.0

As an example of the approximate methods for predicting the amount of compaction of soil due pile driving, Tomlinson gives the relationship between relative density and average unit skin friction in Figure 3.11. Initial average unit skin friction,  $f_{s1}$ , can be estimated from Equation 3.5 Initial internal friction angle is friction,  $f_{s1}$ , can be estimated from Equation 3.5 Initial internal friction angle is obtained from CPT and SPT results.

$$f_{s1} = \sigma'_{v0} \times K s_1 \times \tan \tau_1 \quad (3.5)$$

### 3.5.1 Evaluation of the Relative Density

From figure 3.2, difference in shaft resistance of test piles,  $\Delta Q$ , can be taken as 70 tons, when the pile tip settlement is about 5mm. Depth of fill is approximately 10 m.

$$\Delta Q = (f_{s2} - f_{s1}) A_s \quad A_s = 0.4 \times 4 \times 10 = 16 \text{ m}^2$$

$$\tau = 3/4 \phi$$

$$\phi = 32$$

$$\Delta K_s \text{ max} = 1$$

$$f_{s2} - f_{s1} = \sigma'_v \times \Delta K_s \times \Delta \tan(\tau)$$

$$70 = 8 \times 10 \times 1 \times \Delta \tan(\tau)$$

$$\Delta \tan(\tau) = 0.1094$$

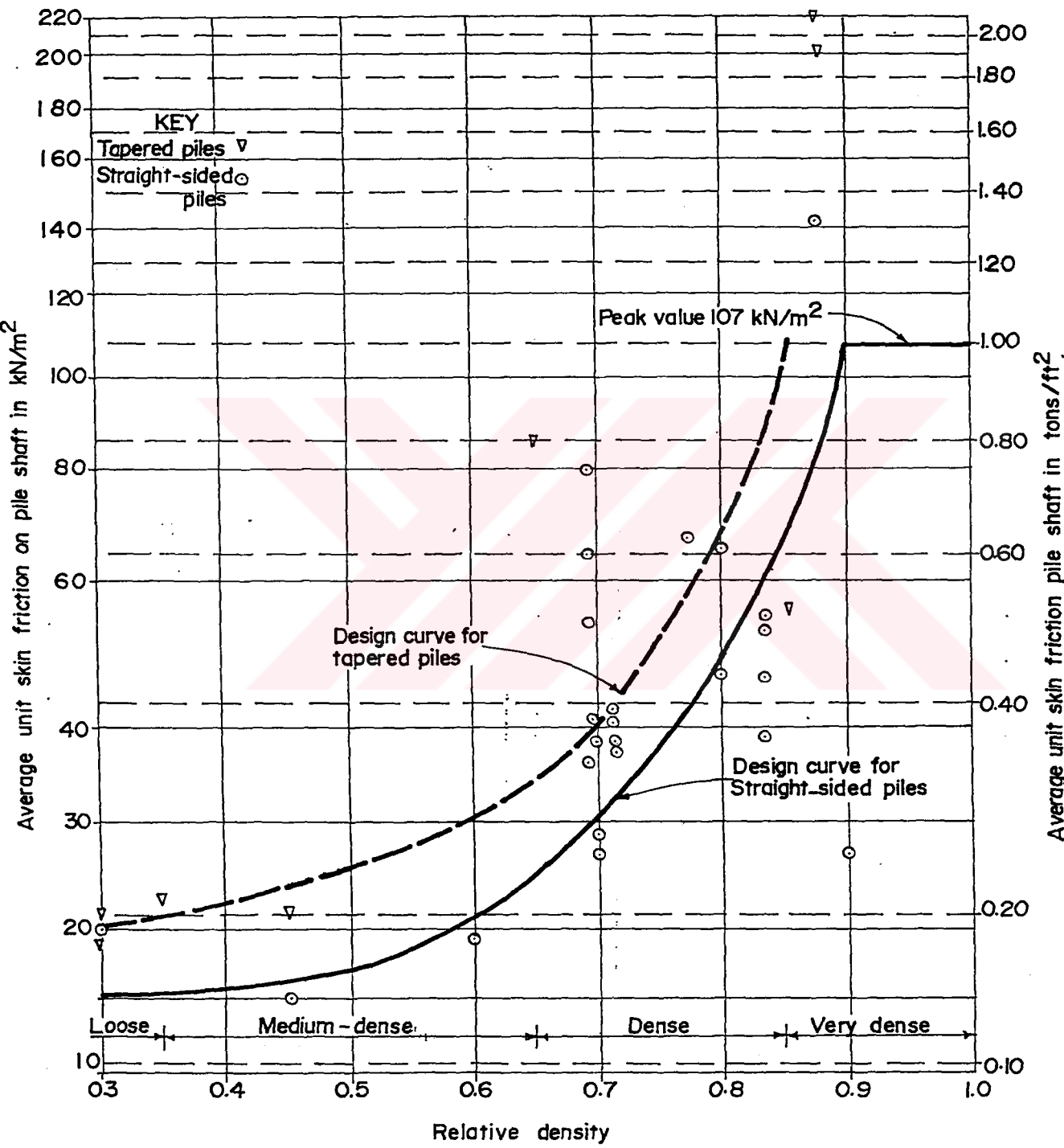


**Figure 3.11 Average Unit Skin Friction on Driven Piles in Cohesionless Soils Related to Relative Density**

$$\begin{aligned} \tan \tau_2 - \tan \tau_1 &= 0.1094 \\ \tan \tau_2 &= 0.1094 + \tan (3/4 \times 32) \\ \tan \tau_2 &= 0.555 \\ \tau_2 &= 29 \quad \Rightarrow \quad \phi = 38.7^\circ = 39^\circ \end{aligned}$$

From Table 3.2

$$\phi_1 = 32^\circ \quad (D_{R1}) = 40 \%$$

$$\phi_2 = 39^\circ \quad (D_{R2}) = 68 \%$$

Analysis and results which were explained above was used as a guide only, it was concluded that increase in relative density was approximately 28% and increase in shaft resistance is approximately 70 Tons, when the difference in Ks value was maximum ( $\Delta K_s = 1$ ).

## CHAPTER IV

### PREDICTION OF AXIAL PILE CAPACITY BY STATIC FORMULA

#### 4.1 Axial Capacity of Piles

A pile subjected to load parallel to its axis will carry the load partly by shear generated along the shaft and partly by normal stresses generated at the base of the pile. The ultimate capacity,  $Q$ , of the pile under axial load is equal to the sum of the base capacity,  $Q_b$ , and the shaft capacity,  $Q_s$ . Thus,

$$Q = Q_b + Q_s = A_b q_b + A_s \tau_s \quad (4.1)$$

where

$A_b$  = area of the pile base

$q_b$  = end bearing pressure

$A_s$  = area of the pile shaft

$\tau_s$  = average limiting shear stress down the pile shaft.

Methods of estimating values of the end bearing pressure,  $q_b$ , and the skin friction,  $\tau_s$ , is divided into two categories, those based on fundamental soil properties such as shear strength or angle of friction, and those based directly on in-situ measurements such as Dutch cone or standard penetration tests.

It should be emphasized that estimation of pile capacity is still largely based on empirical methods, derived from correlations of measured pile capacity

with soil data of variable quality. There is generally a wide scatter in the correlations, and different approaches suit different soil types better than others.

## 4.2. Capacity of a Driven Pile in Cohesionless Soil

### 4.2.1. Skin Friction

Chandler (1968) described an approach, considering the bond between pile and soil as purely frictional in nature, with the resulting skin friction a function of the normal effective stress,  $\sigma'_v$ , and an interface friction angle,  $\phi'$ . The normal stress was related to the effective overburden stress,  $\sigma'_v$ , by a factor,  $K_s$  to give

$$\tau_s = \sigma'_n \tan \phi' = K_s \sigma'_v \tan \phi' \quad (4.2)$$

For piles in soft, normally or lightly overconsolidated clay, Burland (1973) and Parry and Swain (1977) have suggested values of  $K_s$  lying between  $(1 - \sin \phi')$  and  $\cos^2 \phi' (1 + \sin^2 \phi')$ . Neither these suggestions takes due account of the stress changes which occur during and after pile installation. [5]

Francescon (1982) showed from instrumented model pile tests, where the normal effective stress acting on the pile was measured directly; the angle of friction between soil and pile was consistent with that measured in simple shear tests, being somewhat lower than that measured in triaxial compression tests. Denoting this angle by  $\phi'_{ss}$ , the skin friction was thus given by

$$\tau_s = 1.5 K_o \sigma'_v \tan \phi'_{ss} \quad (4.3)$$

#### 4.2.2 End Bearing

In the estimation of base resistance, it is assumed that penetration of the strata in which the toe of the pile is situated is sufficient for mobilization of base resistance. In practise it is generally assumed that a penetration of at least 5D into granular deposit will be achieved. [5]

Therefore 40 x40 working piles penetrate at least 2m into granular band.

On the other hand sand bands in alluvial deposit are generally less than 2m. and this depth is not sufficient for mobilization of base resistance . Inorder to predict a base resistance of piles penetrate the sand band with a depth greater than 2m , it is necessary to establish a value of the bearing capacity factor  $N_q$ . The factor varies with the depth to base area ratio of the pile and also the angle of shearing resistance of the soil.  $\phi'$  is estimated after the pile installation and it is the representative of the soil . Most methods suggested for calculation of  $\phi'$  are based on an estimate of in-situ  $\phi'$  prior to pile installation. If, as a first approximation, the  $\phi'$  value is estimated from in-situ tests, it is common to employ the Peck, Hanson and Thornburn relationship between N value and  $\phi'$ . For the derivation of  $N_q$  from  $\phi'$ , methods available include those due to Terzaghi and Peck, Meyerhof and Berezantsev et.al (1961). [5]

Consistent estimates of  $N_q$  are not found from these alternative methods. For instance, if  $\phi' = 35^\circ$ , the following values of  $N_q$  are predicted:

Terzaghi and Peck (deep footing)	$N_q = 40$
Berezantsev (driven pile)	$N_q = 60$
Meyerhof (driven pile)	$N_q = 200$

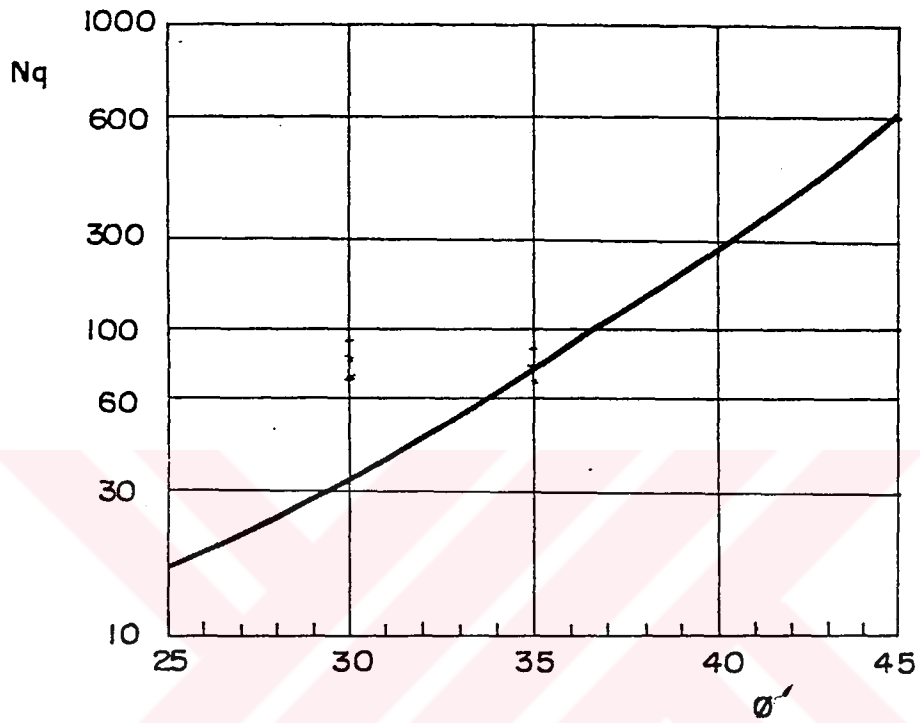


Figure 4.1 Variation of  $N_q$  With  $\phi'$  (Berezantzev et al., 1961)

It is generally considered that the Terzaghi and Peck value is conservative, while the Meyerhof value, being based on a definition of "failure" (or ultimate load) may lead to excessive settlement at working loads if traditional factors of safety of 2 to 3 are employed. Work by Norlund and Vesic supports the view that the Berezantsev values in Figure 4.1 are of most practical application for driven piles.[5]

Finally the end bearing pressure,  $q_b$ , may be expressed in terms of the effective vertical stress,  $\sigma'_v$ , and end bearing capacity factor,  $N_q$  as:

$$q_b = N_q \sigma'_v \quad (4.4)$$

### 4.3 Capacity of a Driven Pile in Cohesive Soil

#### 4.3.1 Skin Friction

Most piles in clay develop a high proportion of their overall capacity along the shaft. Whereas the ratio of end-bearing pressure to skin friction may be typically 50-100 for piles in sand, the corresponding range is 10-20 for piles in clay. As such, considerably more effort has been devoted to developing reliable methods for estimating values of skin friction for piles in clay, than has been the case for sand. [5] Historically, the skin friction around a pile shaft has been estimated in terms of undrained shear strength of the soil, by means of an empirical factor,  $\alpha$ , (Tomlinson, 1957) giving:

$$\tau_s = \alpha C_u \quad (4.5)$$

### 4.3.2. End Bearing Pressure

The long-term, drained, end bearing capacity of a pile in clay will be considerably larger than the undrained capacity. However, the settlements required to mobilize the drained capacity would be too large to be tolerated by most structures. In addition, the pile must have sufficient immediate load-carrying capacity to prevent a short-term failure. For these reasons it is customary to calculate the base capacity of piles in clay in terms of the undrained shear strength of the clay,  $C_u$ , and a bearing capacity factor,  $N_c$ .

Thus the end-bearing pressure is

$$q_b = N_c C_u \quad (4.6)$$

For depths relevant for piles, the appropriate value of  $N_c$  is 9 (Skempton, 1951). A linear interpolation should be made between a value of  $N_c = 6$  for the case of the pile tip just reaching the bearing stratum, up to  $N_c = 9$  where the pile tip penetrates the bearing stratum by 3 diameters or more. [5]

### 4.4 Capacity of Pile Groups

A group of piles may be viewed as providing reinforcement to a particular body of soil. Failure of the group may occur either by failure of the individual reinforcing members (the piles) or as failure of the overall block of soil. When considering failure of the individual piles, it must be remembered that the capacity of each pile may be affected by the driving of subsequent piles in close proximity. This has been demonstrated experimentally by Vesic (1974) and Lo

(1976), who showed that the shaft capacity of piles driven into sand could increase by a factor of 2 or more. Physically, this may be attributed to higher normal effective stresses acting on piles driven in a group, than for single piles. Vibration and soil displacement due to driving of subsequent piles is likely to reduce the tendency for the soil to arch around each pile, leading to higher contact stresses, and thus shaft capacities, than for single pile. [5]

In other situations, the capacity of a pile within a group may be reduced by comparison with a single, isolated pile. In particular, for piles driven into sensitive clay, the effective stress increase in the surrounding soil may be less for piles in a group, than for individual piles. This will result in lower shaft capacities.

#### 4.5 Pile Groups in Clay

Groups of friction piles in clay, the efficiency is unity at relatively large spacing, but decreases as the spacing decreases. For point bearing piles, the efficiency is usually considered to be unity for all spacing—that is, grouping has no effect on load capacity, although in theory the efficiency could be greater than unity for closely-spaced piles that are point bearing, for example, in dense gravel. For piles that derive their load capacity from both side-adhesion and end bearing, Chellis (1962) recommends that the group effect be taken into consideration for the side-adhesion component only. [5]

Model test on groups carried out by Whitaker (1957) confirmed the existence of the two types of failure. For a given length and number of piles in a group, there was a critical value of spacing at which the mechanism of failure changed from block failure to individual pile failure. For spacing closer than the

critical value, failure was accompanied by the formation of vertical slip planes joining the perimeter piles, the block of clay enclosed by the slip planes sinking with the pile relative to the general surface of the clay. For wider spacings, the piles penetrated individually into the clay.[5]

#### 4.6 Pile Groups in Sand

There is less information on pile groups in sand than on groups in clay, but it has been fairly well established that group efficiencies in sand may often be greater than 1. Vesic (1969) measured the point load separately from the shaft resistance, and in the light of his measurements, he concluded that when the efficiency of closely spaced piles was greater than unit, this increase was in the shaft rather than the point resistance.[5]

The broad conclusion to be drawn from the above explanation is that unless the sand is very dense or the piles are widely spaced, the overall efficiency is likely to be greater than 1. The maximum efficiency is reached at a spacing of 2 to 3 diameters and generally ranges between 1.3 and 2.[5]

#### 4.7 Bearing Capacity Calculation for a Single Pile

In this study, ultimate bearing capacities of the piles under axial load which is the sum of the base capacity and the shaft capacity was estimated for a idealized profile shown in Figure 4.3 to Figure 4.12.

Trial test piles were in out side the construction site and behave as a single pile which were driven through a casing for the upper 12 m. to eliminate the

effect of skin friction within the fill. Casing was considered in calculations by taking minus sign for bearing capacities within fill. Results were summarized in Table 4.1

Table 4.1 Prediction of Ultimate Bearing Capacity of Test Piles

PILE NO	ULTIMATE BEARING CAPACITY	
	STATIC (TON)	DYNAMIC (TON)
E10	207	233
E54	259	190
B30	324	224
B50	288	198
K39	200	276
G2	257	259
#1	231	HAMMER ENERGY IS MISSING
#2	253	
#3	227	
#4	239	
#6	230	

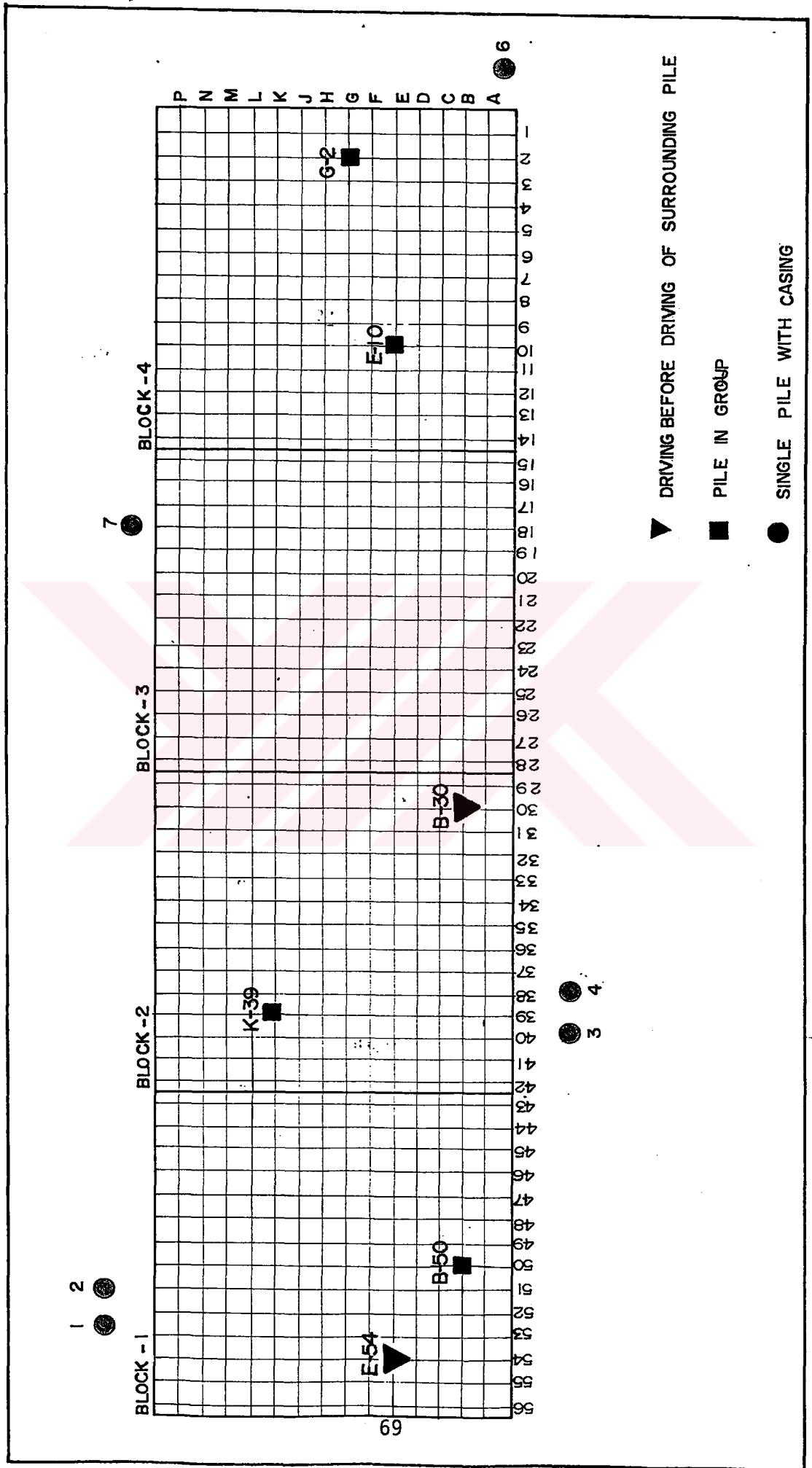


Figure 4.2 Location of Test Piles

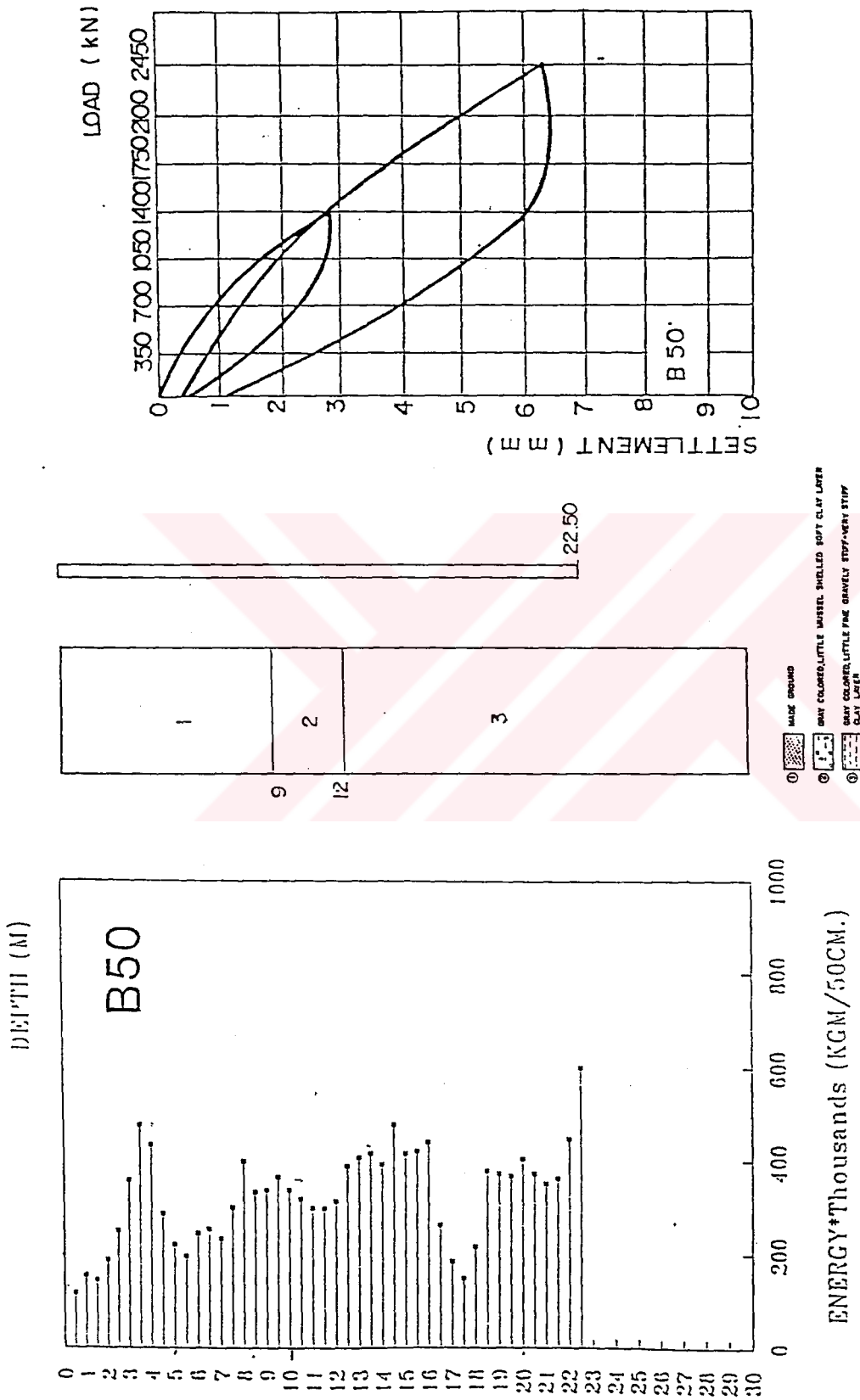
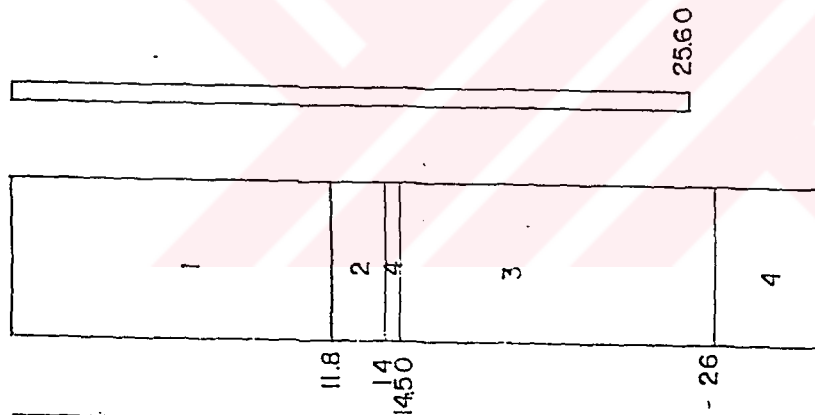
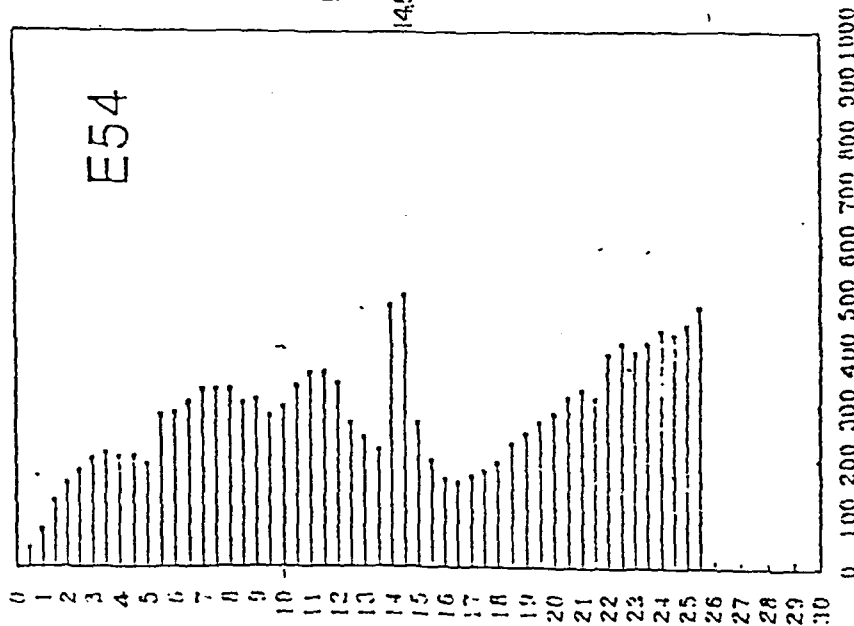


Figure 4.3 Static Bearing Capacity of Test Pile B50.

DEPTH (M)



- ① MAKE GROUND
- ② SANDY FINE GRAVEL AND LOCALLY CEMENTED
- ③ SANDY VERY DENSE FINE GRAVEL AND LOCALLY CEMENTED
- ④ CLAY LAYER
- ⑤ SANDY COLORED LITTLE FINE GRAVEL VERY STIFF
- ⑥ SANDY COLORED LITTLE MEDIUM SOFT CLAY LAYER
- ⑦ MAKE GROUND

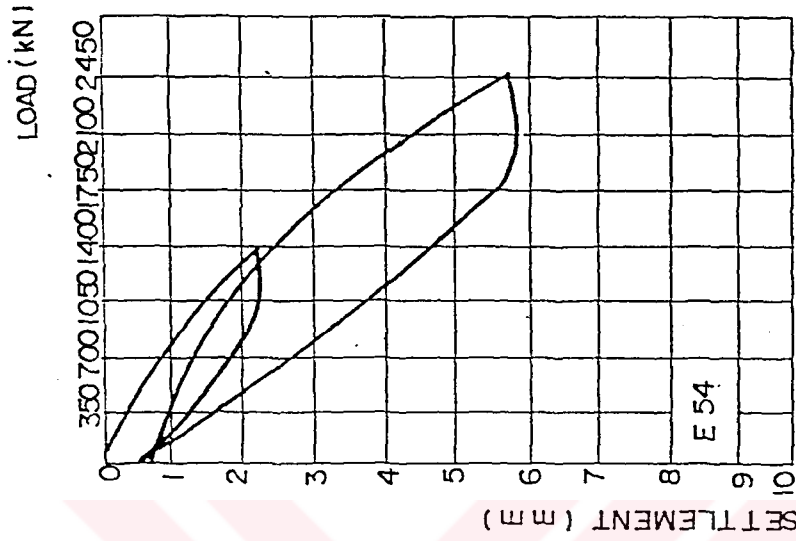
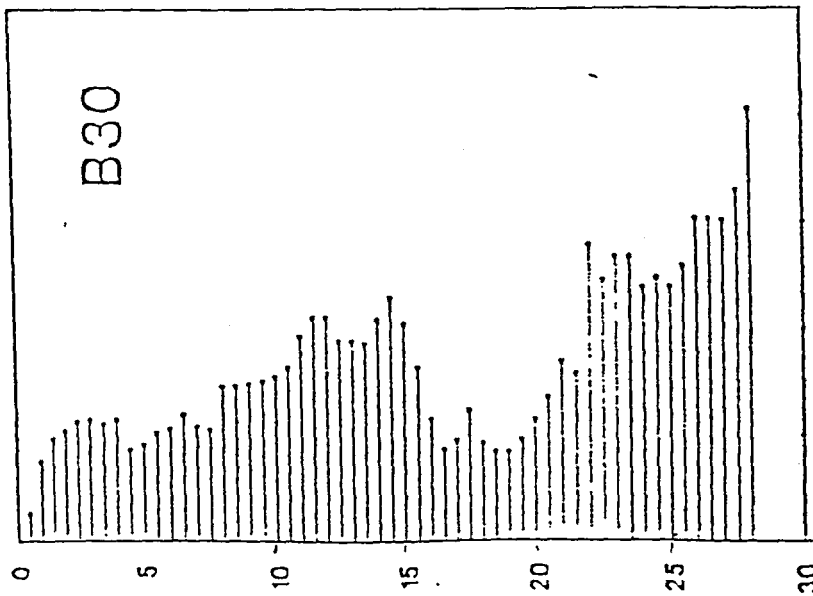
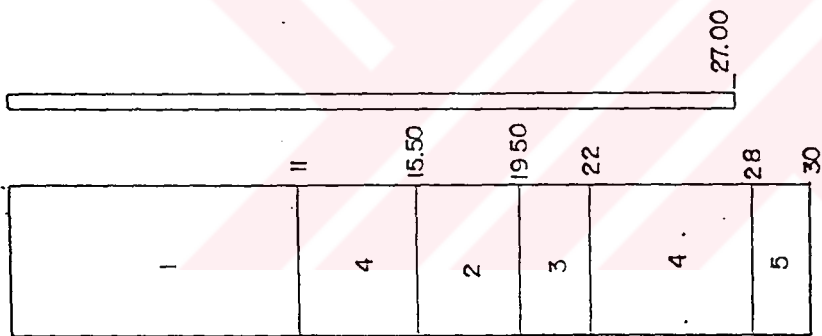


Figure 4.4 Static Bearing Capacity Of Test Pile E54

DEPTH (M)

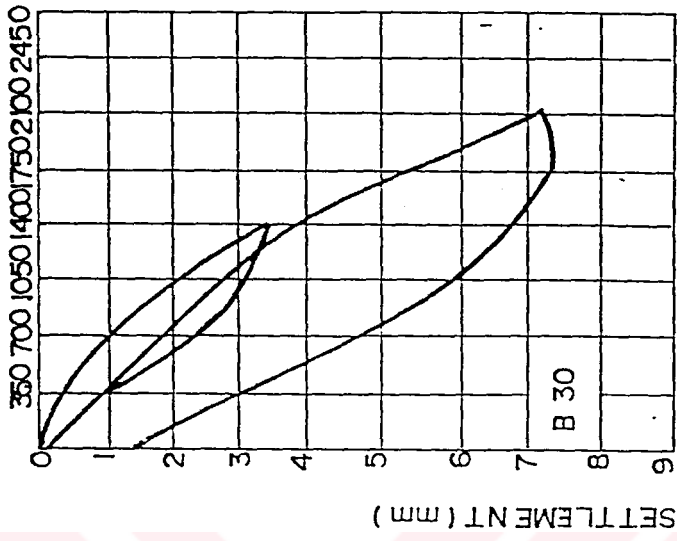


ENERGY (Thousands (KGM/50CM.))



- ① BARE GROUND
- ② GRAY COLORED, LITTLE MASSIVE, SHELLED SOFT CLAY LAYER
- ③ GRAY COLORED, LITTLE FINE GRAVEL, STIFF-VERY STIFF CLAY LAYER
- ④ SAND, VERY DENSE, FINE GRAVEL AND LOCALLY CEMENTED (CONCREMENTAL) COMPACT SAND-GRAVEL LAYER
- ⑤ GRAY COLORED, LOCALLY LITTLE FINE GRAVEL, HARD CLAY LAYER

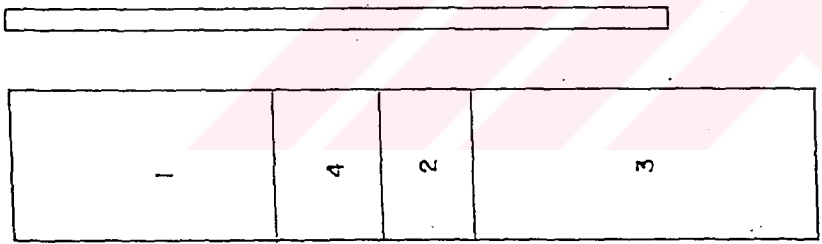
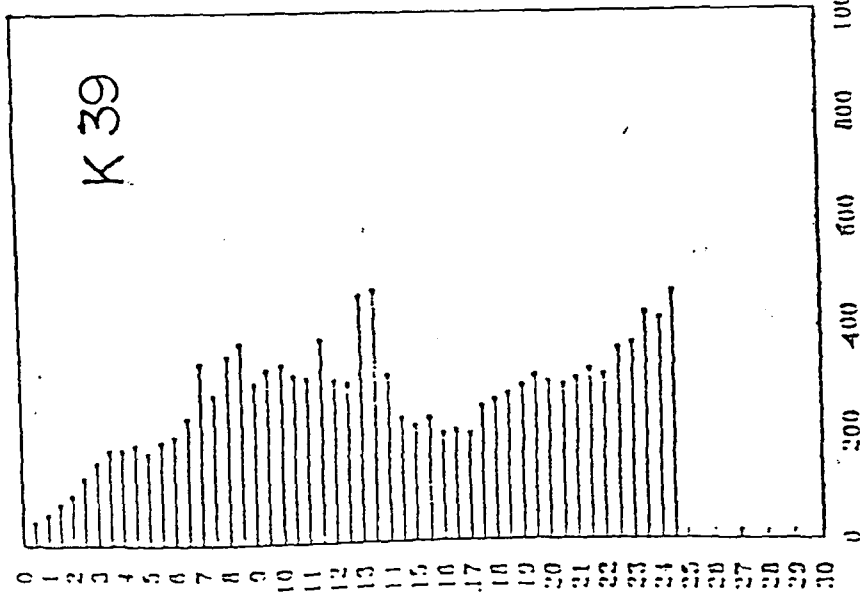
LOAD (kN)



SETTLEMENT (mm)

Figure 4.5 Static Bearing Capacity Of Test Pile B30.

DEPTH (M)



- ① MAKE GROUND
- ② SAND COLORED, LITTLE SHELLS, SOFT CLAY LAYER
- ③ SAND COLORED, LITTLE FINE GRAVEL, STIFF-VERY STIFF CLAY LAYER
- ④ SAND, VERY DENSE, FINE GRAVEL AND LOCALLY CEMENTED
- ⑤ HOMOGENEOUS, COMPACT SAND-GRAVEL LAYER

LOAD (kN)

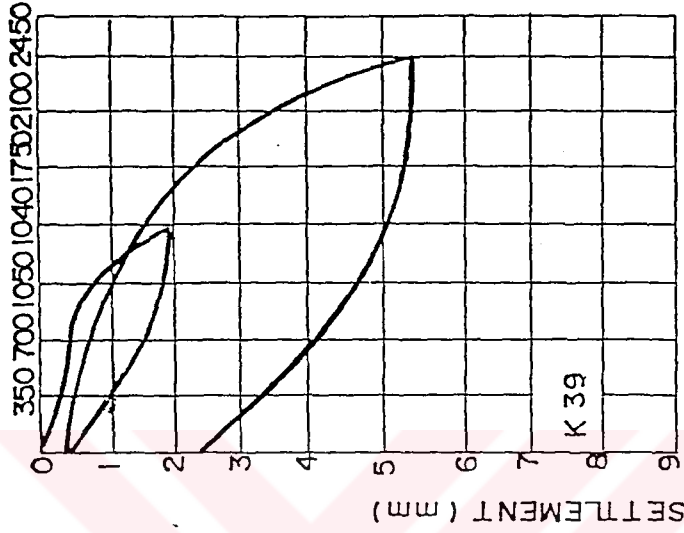
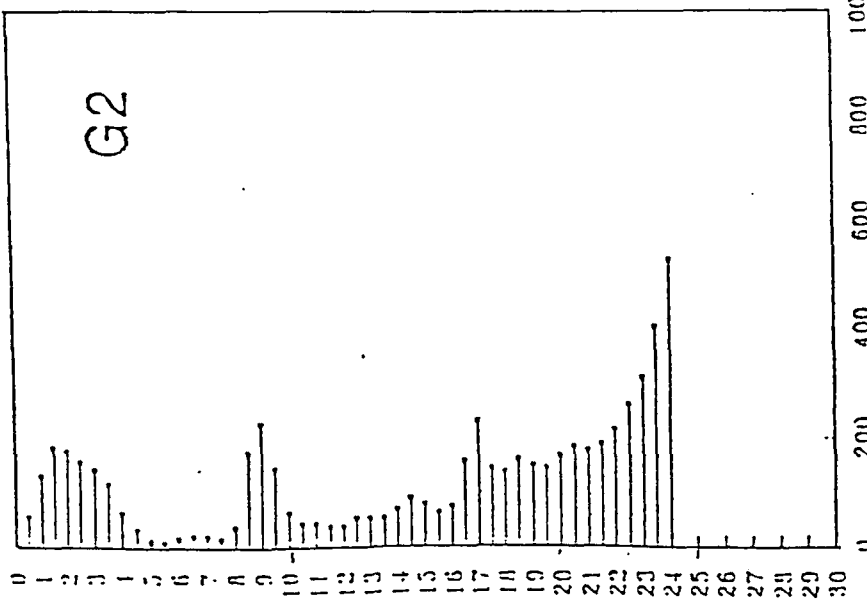


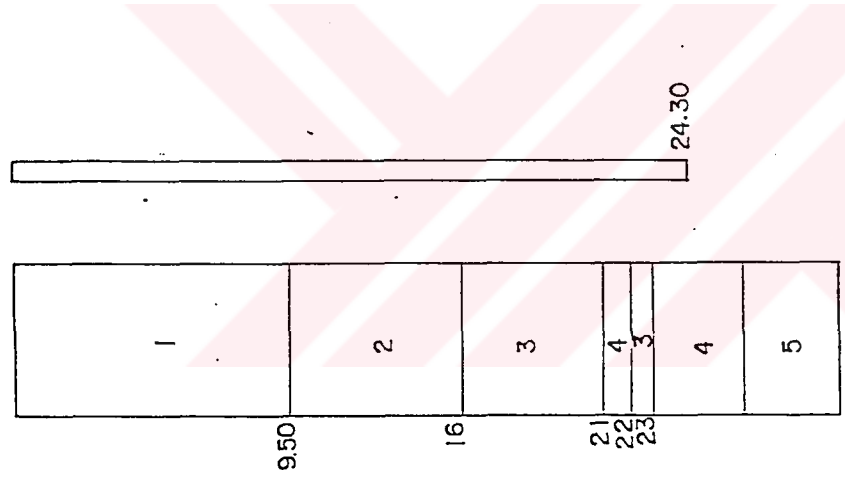
Figure 4.6 Static Bearing Capacity Of Test Pile K39

DEPTH (M)



G2

ENERGY \* Thousands (KG)/50CM.



- ① DARK BROWN
- ② GRAY COLORED, LITTLE MUSSEL, SHELLED, SOFT CLAY LAYER
- ③ GRAY COLORED, LITTLE FINE GRAVELLY STUFF-HEAVY STUFF CLAY LAYER
- ④ SANDY, VERY DENSE, FINE GRAVEL AND LOCALLY CEMENTED SAND- GRAVEL LAYER
- ⑤ GRAY COLORED, LOCALLY LITTLE FINE GRAVELLY HARD CLAY LAYER

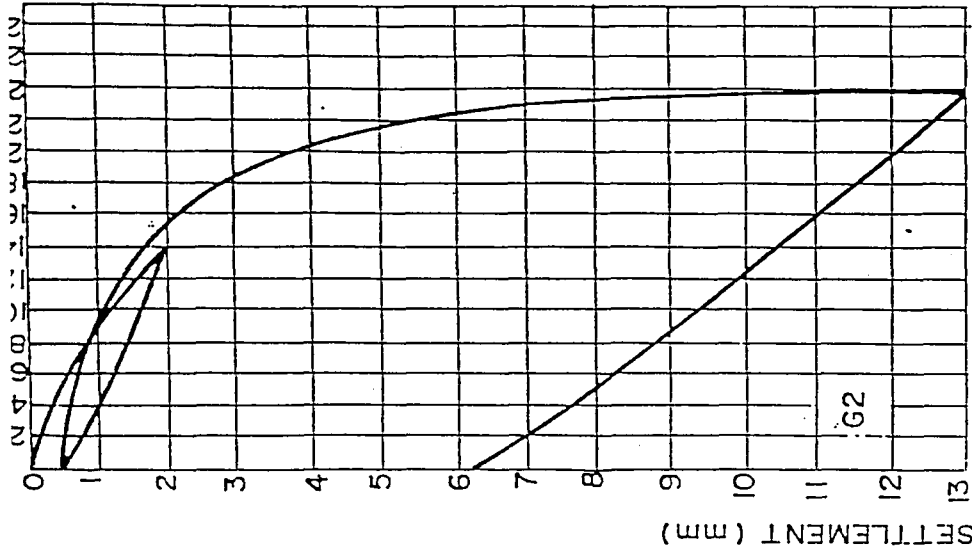
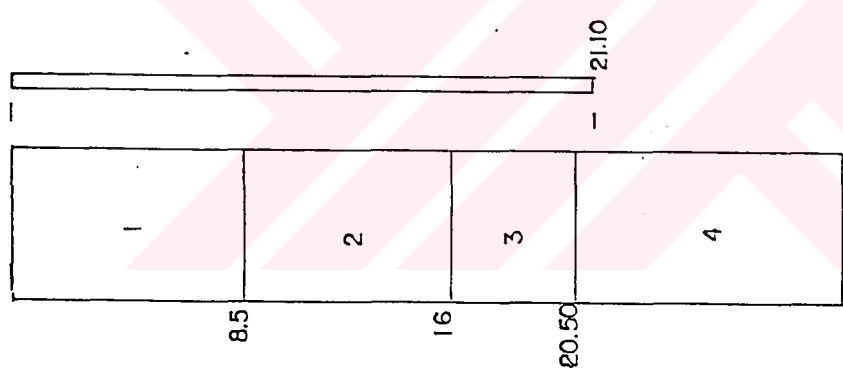
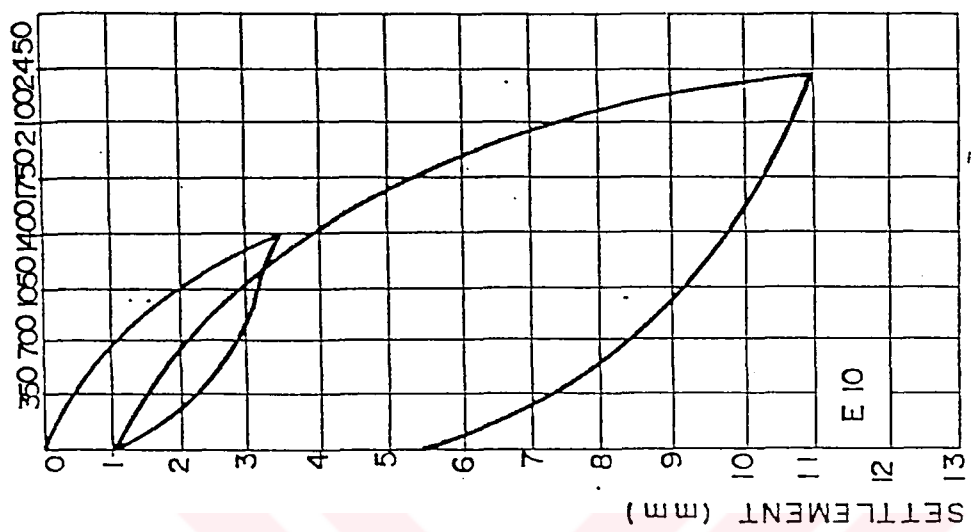


Figure 4.7 Static Bearing Capacity Of Test Pile G2

LOAD ( kN )



- ① MAKE GROUND
- ② GRAY COLORED, LITTLE RUBBLE, SHELLED SOFT CLAY LAYER
- ③ GRAY COLORED, LITTLE FINE GRAVELLY STIFF-VERY STIFF CLAY LAYER
- ④ SANDY, VERY BENE, FINE GRAVEL, AND LOCALLY CEMENTED (CONGLOMERATE) COMPACT SAND-GRAVEL LAYER

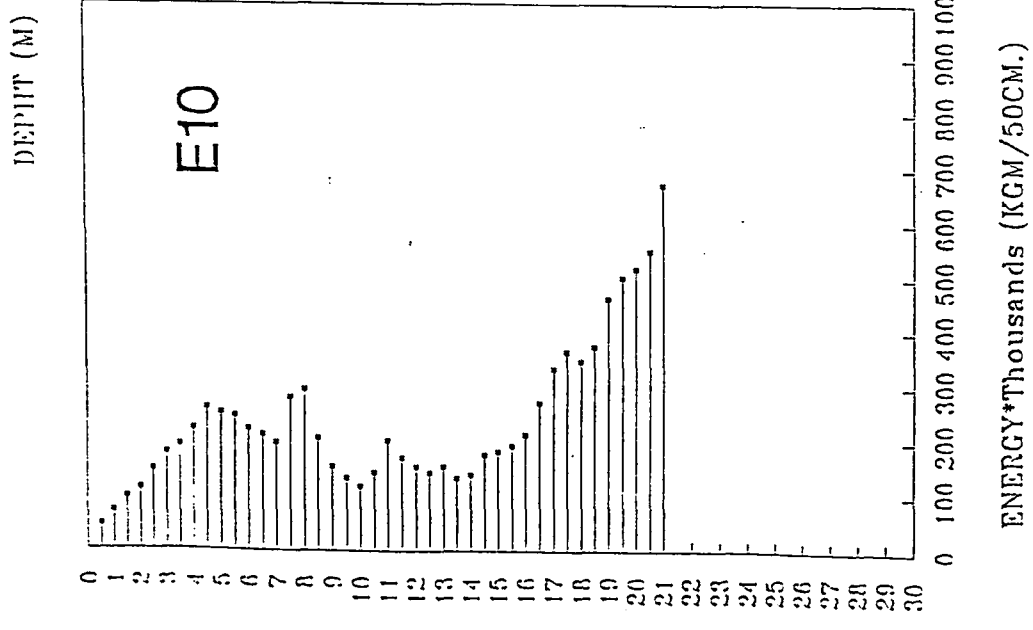


Figure 4.8 Static Bearing Capacity Of Test Pile E10

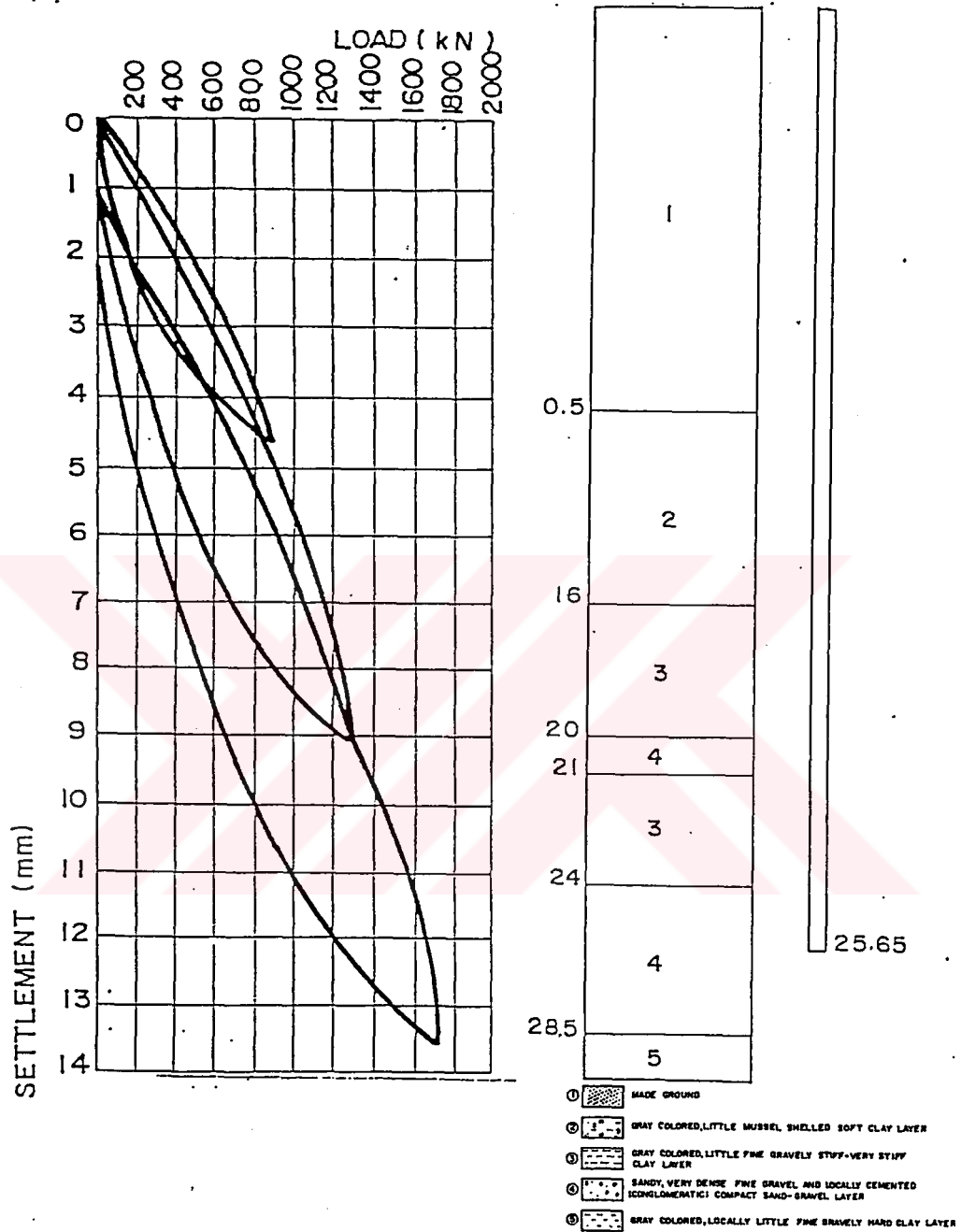


Figure 4.9 Static Bearing Capacity Of Test Pile No 1

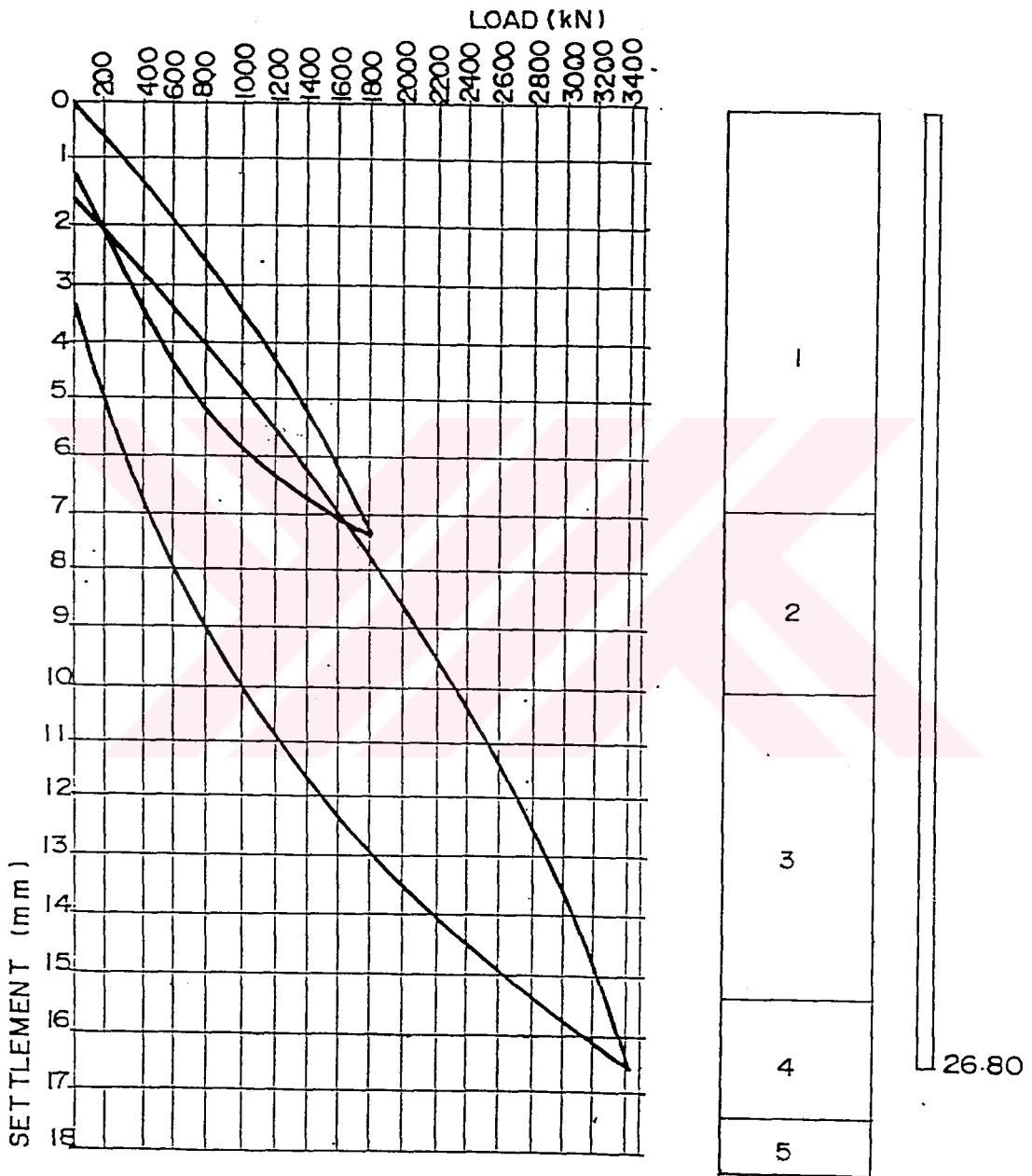


Figure 4.10 Static Bearing Capacity Of Test Pile No 3

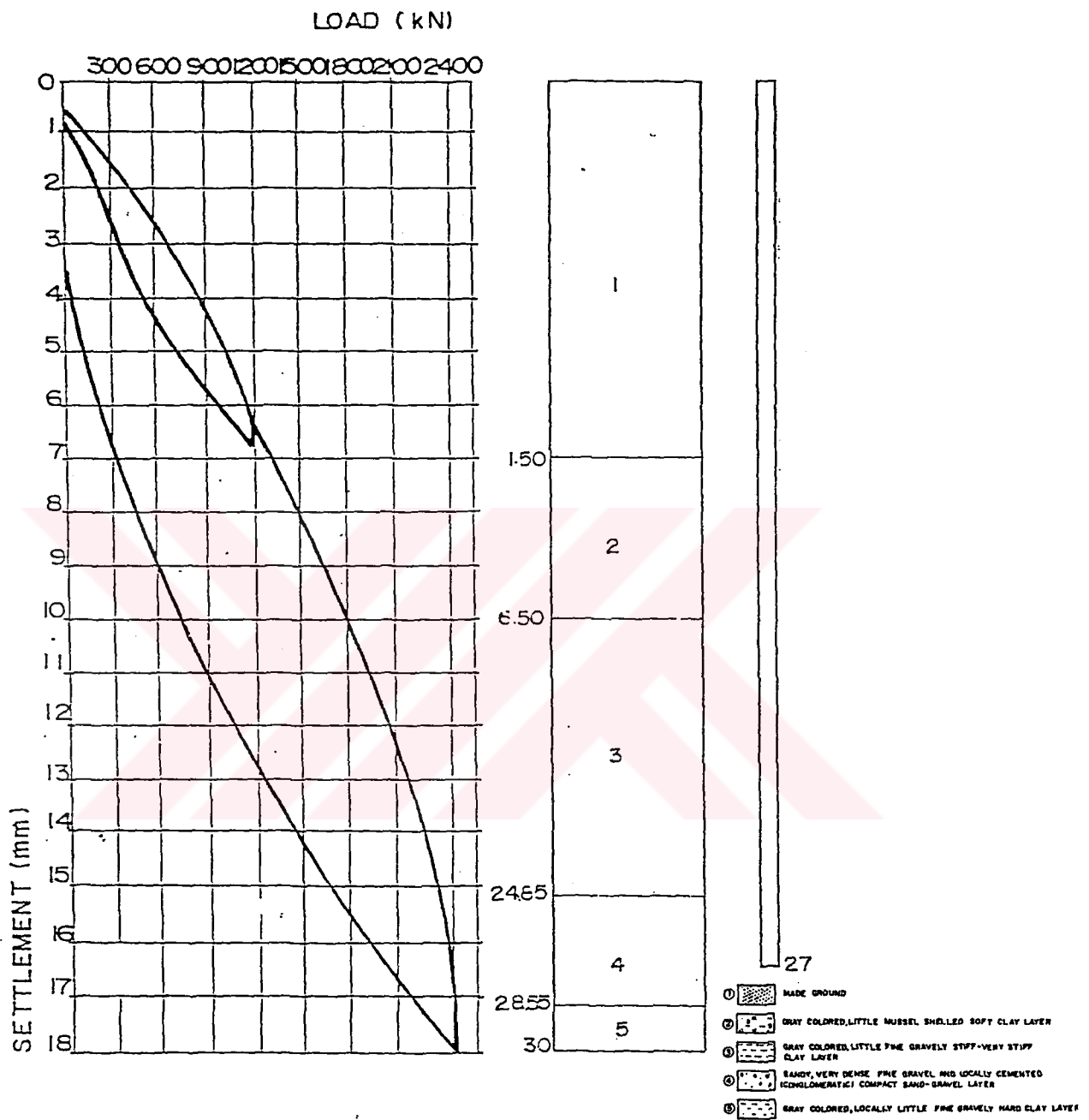


Figure 4.11 Static Bearing Capacity Of Test Pile No 4

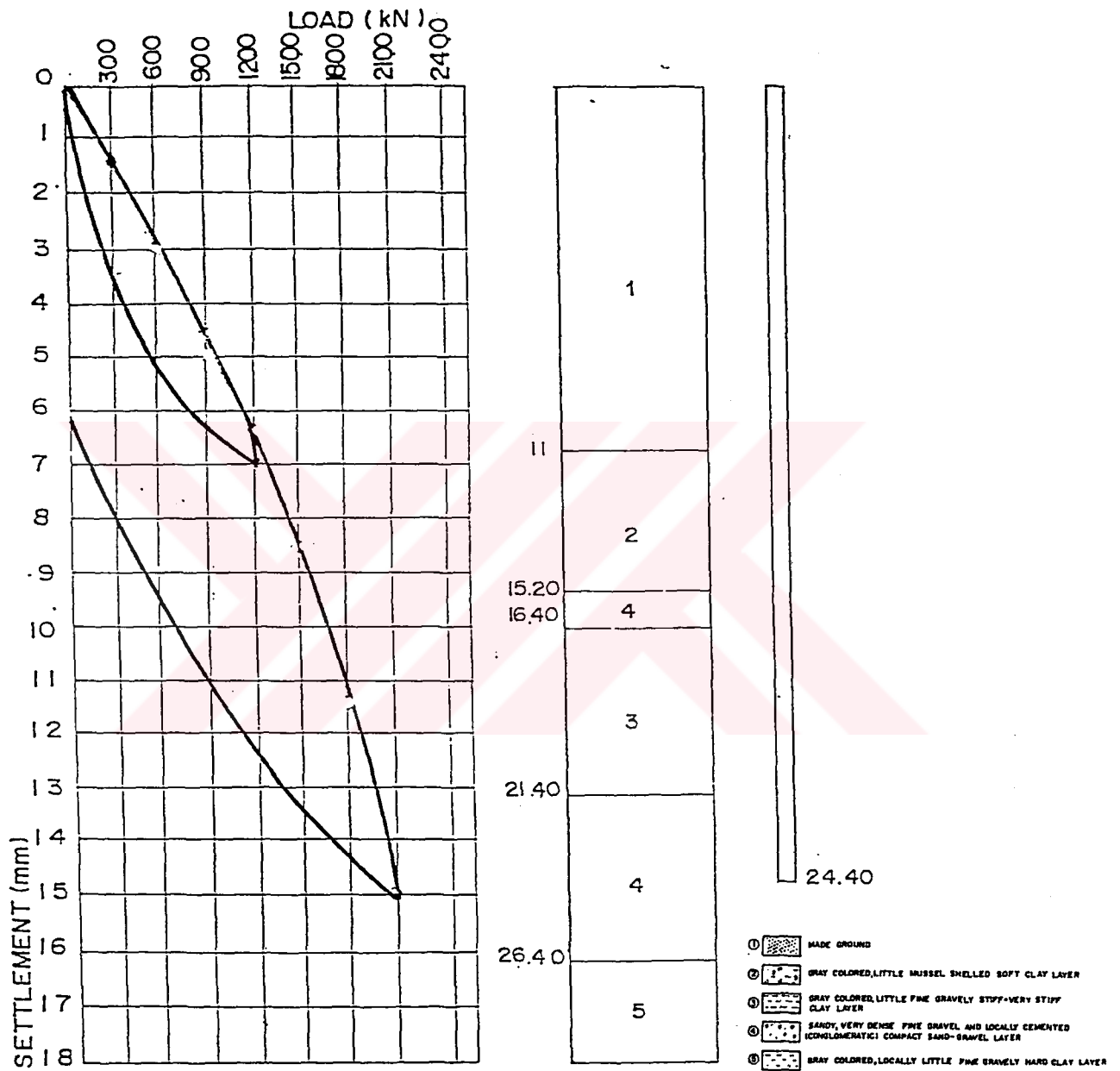


Figure 4.12 Static Bearing Capacity Of Test Pile No 6

## CHAPTER V

### THE PRACTICAL USE OF THE CPT IN SOIL PROFILING AND IN PREDICTION OF AXIAL PILE CAPACITY

#### 5.1 Introduction

The main objective of this section was to investigate the possibility of using the cone penetrometer data to predict the load carrying capacity of piles driven in alluvial soils.

The prediction of axial pile capacity is complex engineering problem. In order that a pile foundation may be designed safely and economically, its behaviour under load must be accurately predicted and ideally a full scale pile load test should be performed. Full scale load tests are, however, very expensive and are therefore often impractical. Also predictive methods for pile capacity require an accurate assessment of the properties of the soil into which the pile is to be placed.

However, cone penetration testing provides a means by which continuous representative field data is obtained. Therefore CPT is generally accepted as a rapid and simple method for the determination of the bearing capacity of soils under applied load, especially in areas with soft soil deposits.

## 5.2 Difference in Behaviour Between Cone Penetrometer Results and Test Piles

Cone penetrometer has been considered as a model pile and used to predict the skin friction and point resistance for the pile. But the stress field encountered during the penetration of cone is quite different from that of pile under loading. It is well known that the pile driving will densify the surrounding soil if it is driven through loose or medium loose sand. But in the same soil, the densification caused by CPT is lesser so that CPT would under-estimate the density or strength parameters of the sand ground of the actual pile. In soft clay, the penetration of cone generates large excess pore pressure in the vicinity of the cone. The faster the penetration speed, the lower the cone resistance will be. But, the clay around a driven pile, after set, will recover its strength due to reconsolidation. Therefore, in soft clay, CPT would also underestimate the shear strength. The difference of effect between CPT and pile, in dense sand and firm clay, thus might be in reverse. Therefore all CPT methods use some kind of correction factor or technique. The need for such reduction factors is due to a combination of the following influences:

- size effect
- rate of loading effect
- difference of insertion technique
- difference in soil displacement. [14]

In Norway a correction factor of 1/2 is used in all situations, while in USSR, same correction factor is used but for evaluating the allowable load corresponding to 8 mm settlement. [9]

## 5.3 Review of Existing Methods

### 5.3.1 Ultimate End Bearing From Cone Resistance In Granular Soils

For evaluating end resistance of pile embedded in sand various methods have been suggested by Meyerhof (1975), Te Kamp (1977), De Beer (1971, 1972), Thorburn (1979), and Nottingham (referred to Schmertman, 1975) et.al. The main difference among the various methods is how to interpret the cone resistance at pile toe level, including: the range around pile toe in which cone resistances should be counted; the weight factor of cone resistances at various levels. If in an uniform sand layer with a constant limit cone resistance, the pile has been embedded to a sufficient depth, then all above mentioned methods will give same interpreted cone resistances. [14]

The tip bearing capacities were estimated by a procedure similar to the Dutch method as explained and applied by Nottingham. This procedure is a recent version of the one suggested by Beqemann.

The unit tip bearing,  $q_0$  of the piles were then calculated as follows:

$$q_0 = \frac{(q_{b1} + q_{b2})/2 + q_a}{2} \quad (5.1)$$

where

$q_{b1}$  = Average of  $q_c$  values 4D below the pile tip

$q_{b2}$  = Average of minimum  $q_c$  values 4D below pile tip.

$q_a$  = Average of minimum  $q_c$  values 8D above pile tip

The difference between this procedure and the recent version

of Dutch Method is that in the latter the term  $(q_{b1} + q_{b2})/2$  is calculated using  $q_c$

values obtained from XD below the pile tip, X is varied between 0 to 3.75 and minimum  $(q_{b1} + q_{b2})/2$  is chosen in  $q_o$  calculations. It should be noted that the

Dutch method was developed for sandy soils where tip bearing contribution to the ultimate capacity is major and a such care must be taken in choosing a proper unit tip bearing capacity  $q_o$ . [14]

Delft laboratory method (Sanglerat,1972) stated that, the value of point resistance of the pile of diameter B may be calculated as,

$$q_p = 0.5 (q_1 + q_2) \quad (5.2)$$

where

$q_1$  : Average of the cone resistance over a depth of 8 diameters above base of the pile.

$q_2$  : Average of the cone resistance below the point of the pile tip for a depth of 3.5 diameter.

Meyerhof (1976) proposed the following method for calculating the point bearing of a pile. [14]

$$q_p = q_1 + \frac{q_{11} - q_1}{10B} z \quad (5.3)$$

where

$q_1$  = cone penetration resistance just above the bearing

stratum

$q_{11}$  = cone penetration resistance at a depth of 10 diameters

measured from the surface of the bearing stratum.

$z$  = pile embedded depth.

$B$  = pile diameter.

Nordlund (1963) recommends taking an average value of  $q_c$  over a depth range of 3 pile diameters above the pile base down to 2 diameters below the pile base. The end-bearing pressure is then taken as this average value of  $q_c$ . [11]

Fleming and Thorburn (1983) recommend more detailed schemes for averaging the cone readings, in order to put more weight on the minimum values. The range over which the average is taken is extended up to 8 pile diameters above the level of the pile base. Thus end-bearing pressure is estimated as:

$$q_b = (q_{c1} + q_{c2} + 2q_{c3}) / 4 \quad (5.4)$$

where

$q_{c1}$  = Average cone resistance over 2 diameters below the pile base

$q_{c2}$  = Minimum cone resistance over 2 diameters below pile base

$q_{c3}$  = Average of minimum values lower than  $q_{c2}$  over 8

diameters above pile base.[11]

Generally, CPT soundings are used to estimate insitu relative density of the granular soil strata. Angle of internal friction are not determined directly from CPT data. Friction angles can be estimated from intermediate parameter of relative density. Table 5.1 illustrates a typical correlation of cone resistance and relative density.

Cone resistance results of CPT 2 were used to predict the ultimate end bearing capacity of test pile G2, by using four different method. Results were summarized in Table 5.2.

### 5.3.2 Ultimate Shaft Resistance From Local Side Friction In Cohesive Soils

The method of estimating  $Q_s$  proposed by Nottingham (Nottingham, 1975; Schmertman, 1978) uses the expression

Table 5.1 Correlation of Cone Resistance and Relative Density

<u>DENSITY</u>	<u>CONE RESISTANCE, <math>q_c</math>, MN/m<sup>2</sup></u>	<u>RELATIVE DENSITY, %</u>
LOOSE	LESS THAN 4	0 TO 35
MEDIUM DENSE	4 TO 12	35 TO 65
DENSE	12 TO 20	65 TO 85
VERY DENSE	GREATER THAN 20	85 TO 100

**Table 5.2 Ultimate End Bearing of G2 Test Pile  
From Cone Resistance in Granular Soil.**

	SANGLERAT (1972)	MEYERHOF (1966)	NORDLUND (1963)	FLEMING THORNBURN (1983)
ULTIMATE TIP RESISTANCE (kN)	1840	2190	1030	1490

**Table 5.3 Ultimate Shaft Resistance of B30 Test  
Pile From Local Side Friction in Cohesive Soils**

	CONE-M METHOD	LAMBDA-CONE METHOD	NOTTINGHAM
ULTIMATE SHAFT RESISTANCE (kN)	1150	1540	670

$$Q_s = k_{c,s} \left[ \sum_{l=0}^{8d} \left( \frac{l}{8d} \right) f_s A_s + \sum_{l=8d}^L f_s A_s \right] \quad (5.5)$$

where

$Q_s$  = Total ultimate side friction

$k_{c,s}$  =  $f_s$  correction factors,  $k_c$  in clay layers,  $k_s$  in sand layers from

Figure 5.2

$l$  = Depth to  $f_s$  value considered

$f_s$  = Unit local friction sleeve resistance from CPT.

$A_s$  = Pile soil contact area per  $f_s$  depth interval.

$L$  = Total embedded length of pile.

$d$  = pile width

Two different procedures are also presented to calculate the ultimate shaft resistance.[11]

- (1) Cone - M method      (2) Lambda - Cone method.

In Cone-M method, the unit pile frictions,  $f$  of the piles are determined from their total frictional capacities. An attempt is made to relate  $f$  to the average local friction,  $f_s$ . The  $f_s$  values are calculated by the following relationship :

$$f_s = \frac{F_t}{L} \quad (5.6)$$

where

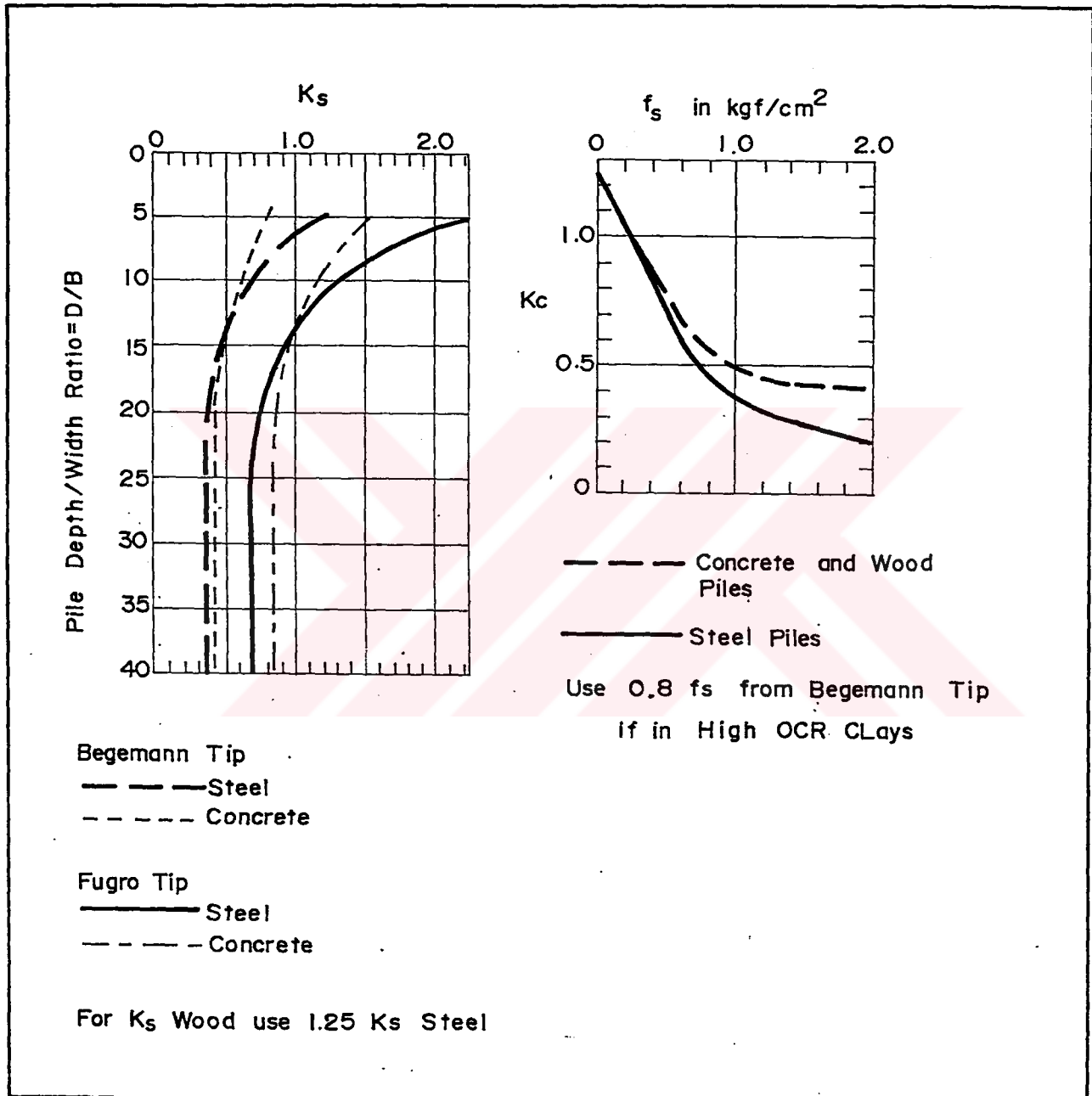


Figure 5.1 Correction Factor,  $k_c$  in Clay Layers,  $k_s$  in Sand Layers

L = length of pile penetration

$F_t$  = total friction at depth L

The ratio  $f/f_s$  is called m. And m curve may be expressed by the following equation:

$$m = 10.0 - 9.5(1 - e^{-0.09fs}) \quad (5.7)$$

The expression suggests that the adherence coefficient, m could vary between 10.0 and 0.50. The unit pile friction may then be given by:

$$f = m \times f_s < 0.75 \text{ kg/cm}^2 \quad (5.8)$$

In Lambda-cone method it was possible to calculate pile friction factors for various pile lengths was named Lambda-cone ( $\lambda_c$ ). The pile friction correction factor ( $\lambda_c$ ) may be expressed by the following. [11]

$$\lambda_c = 0.50 - 0.40 (1 - e^{-0.09L}) \quad (5.9)$$

Where L is the penetration length in meters. Total frictional capacity,  $Q_s$  of a pile may be determined by:

$$Q_s = f \times A_s \times L \quad (5.10)$$

where

$A_s$  = surface area of the shaft

f = Average unit friction =  $\lambda_c (\sigma_m + 2mf_s)$

$\sigma_m$  = the mean effective overburden pressure

Many investigators now believe that the cone resistance,  $f_s$  data provide a better indication of the undrained shear strength,  $C_u$  of cohesive soils, thereby explaining the unit pile friction,  $f$ . Experimental correlation of  $f_s$  and  $C_u$  presented by Wesley indicated  $f_s$  to be slightly higher than  $C_u$ . Nottingham assumed undrained cohesion,  $C_u$  to be equal to  $f_s$ . In cohesive soils,  $f$  may be estimated from the  $q_c$  data by assuming a proper  $q_c / C_u$  ratio,  $N_k$ , to estimate the undrained shear strength,  $C_u$ . [11]

In this study, it is intended to use the  $f_s$  data for directly estimating the unit pile friction, Begemann and Vesic suggested that  $f_s$  may be taken as equal to or half of the unit friction,  $f$  of piles respectively.

Nottingham applied Tomlinson's adhesion factor ( $\alpha$ ) to relate  $f$  to  $f_s$  values.

Shaft resistance sounding of CPT 3A was used for prediction of ultimate shaft resistance of test pile B30. Results were given in Table 5.3. Relation between ultimate bearing capacity and depth was also investigated in Figure 5.2, Figure 5.3, Figure 5.4, from CPT 2, CPT 3A, CPT 4 data. Results were summarized in Table 5.4.

#### 5.4 Limit Values for Ultimate End Bearing and Ultimate Shaft Resistance of a Pile

It appears that there is an upper and lower limit for the unit pile friction  $f$  of piles. One suggested by Tomlinson is about  $0.50 \text{ kg/cm}^2$  for all piles. Many investigators recommend on upper limit of  $0.75 \text{ kg/cm}^2$  for  $f$ .

	CPT
PILE NO	(KN)
E10	1800
E54	2800
B30	4200
B50	2500
K39	4050
G2	4000
#1	2600
#2	2900
#3	4200
#4	4300
#6	4000

**Table 5.4 Prediction of Ultimate Bearing Capacity of the Test Piles from CPT Data**

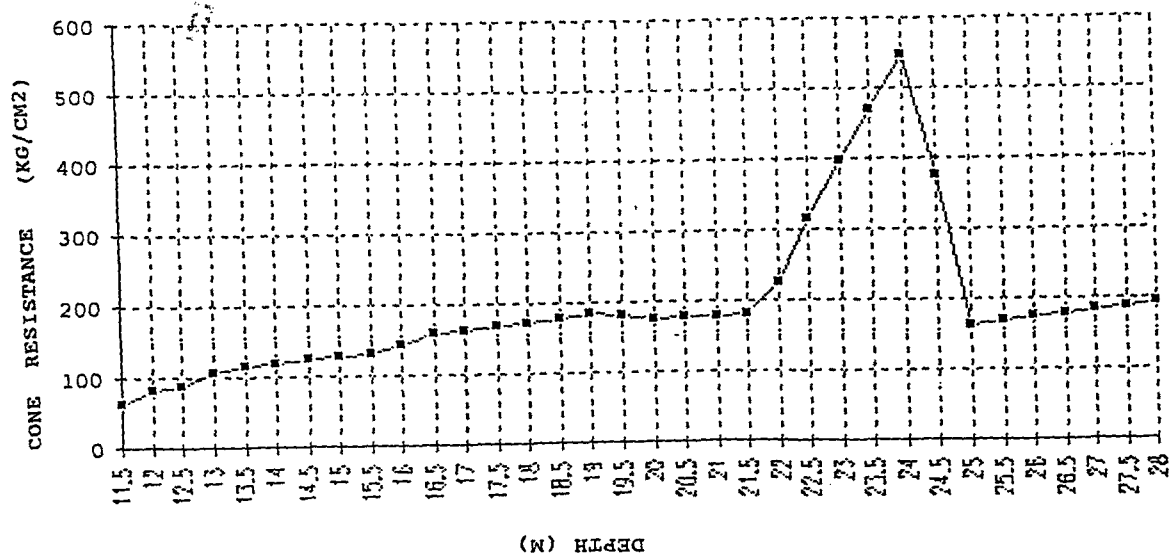
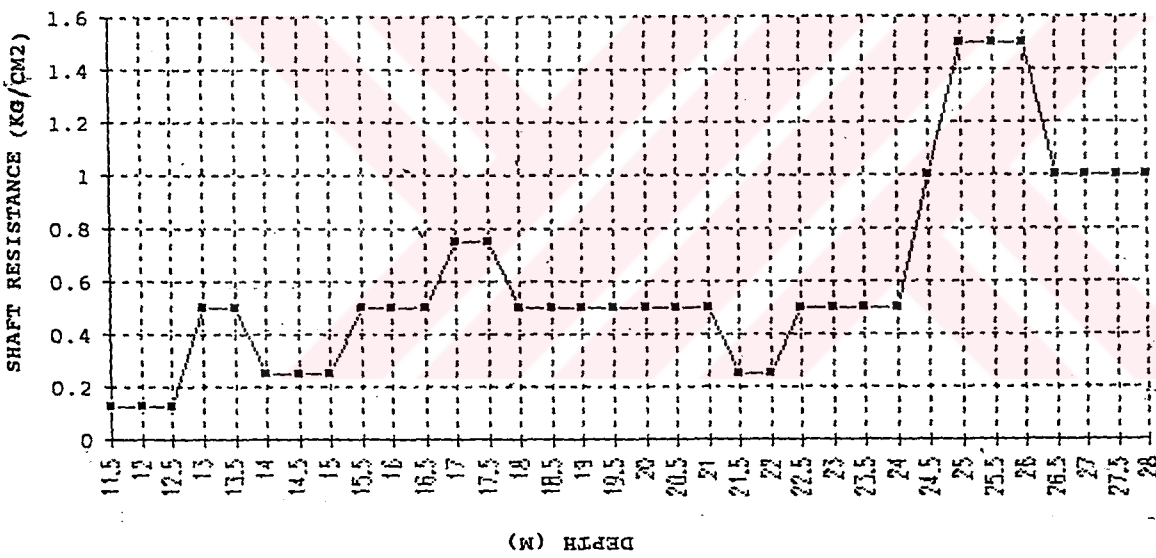
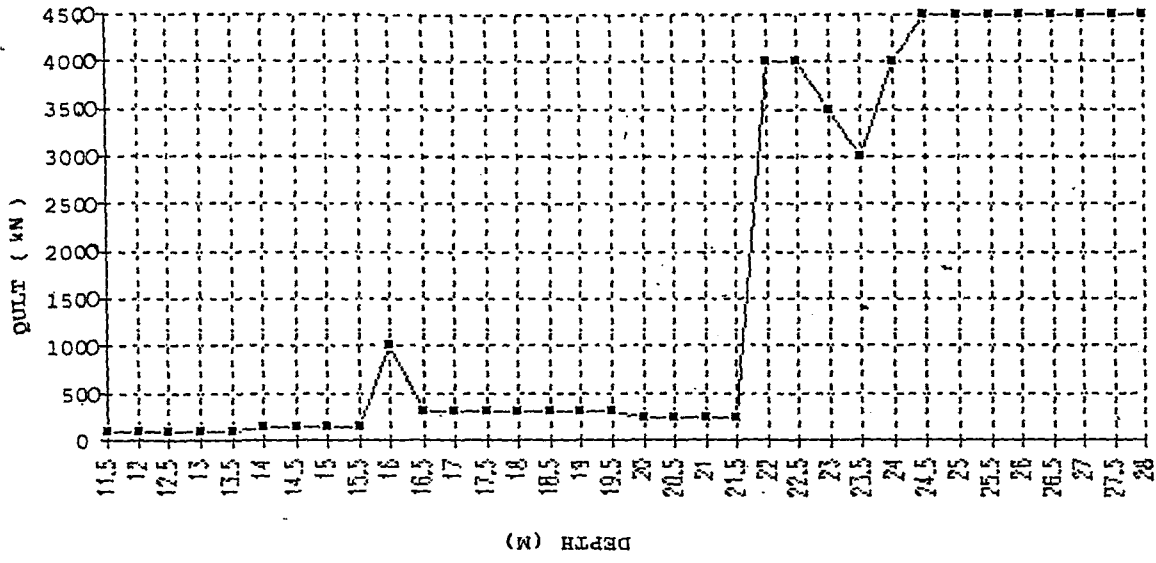


Figure 5.2 Prediction Of Ultimate Bearing Capacity Of a Pile From

CPT 2 Data

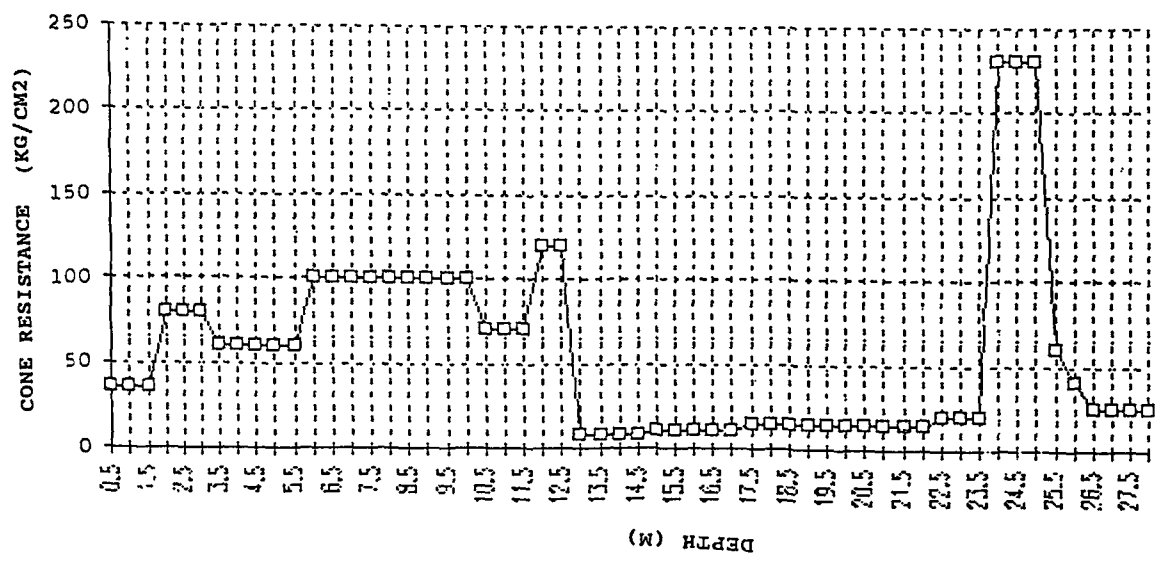
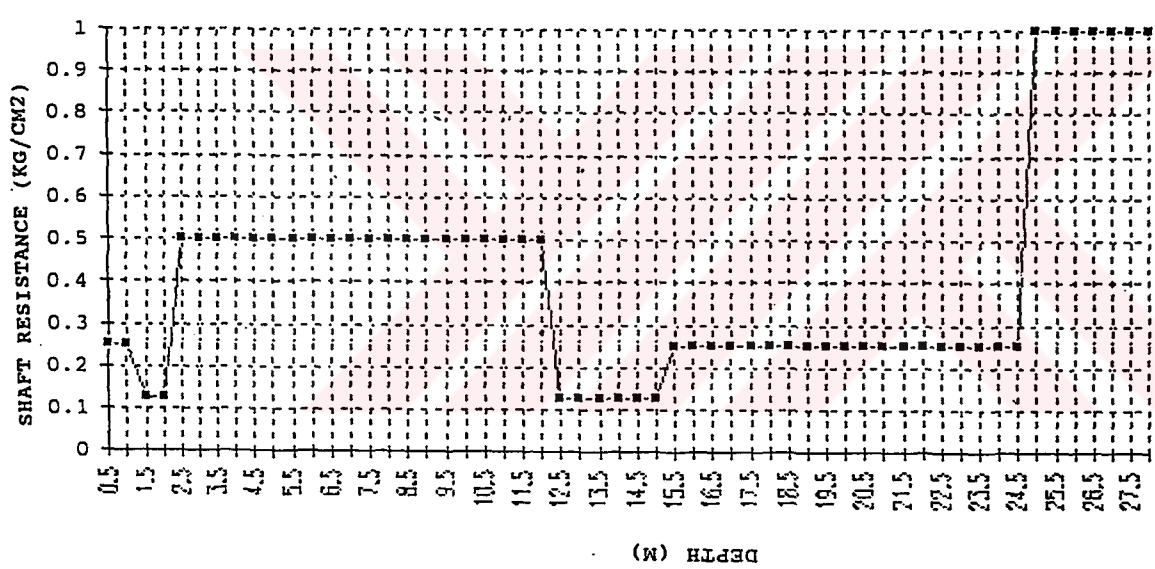
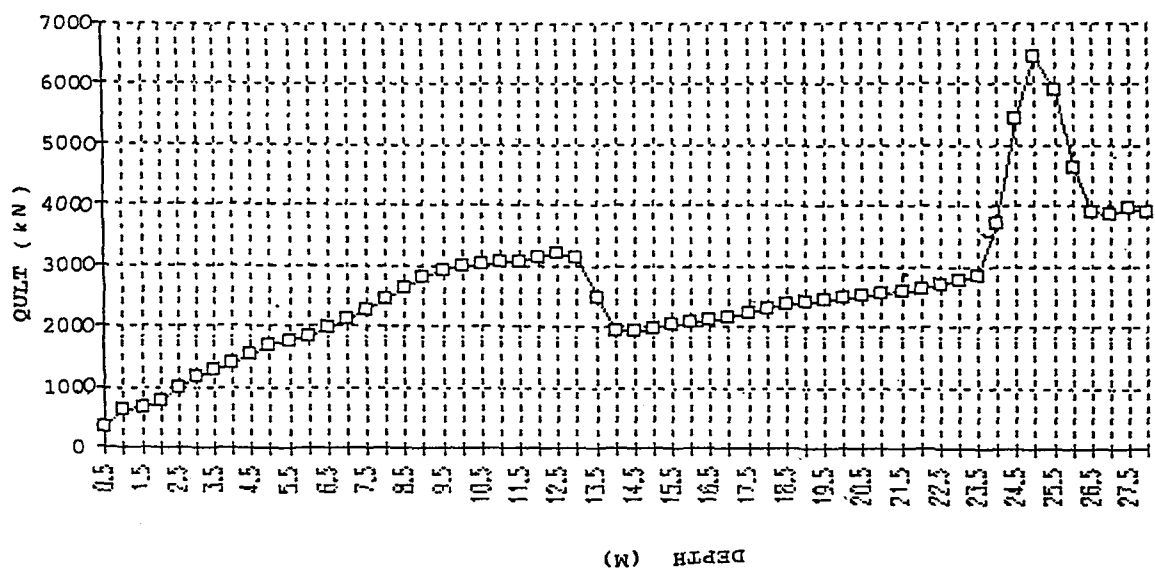


Figure 5.3 Prediction Of Ultimate Bearing Capacity Of a Pile From CPT 3A Data

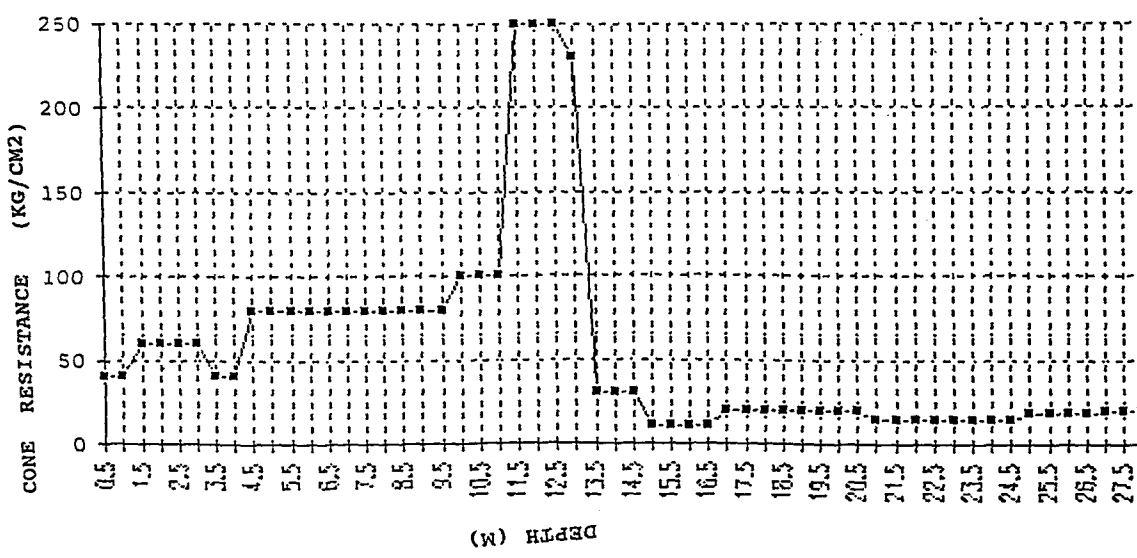
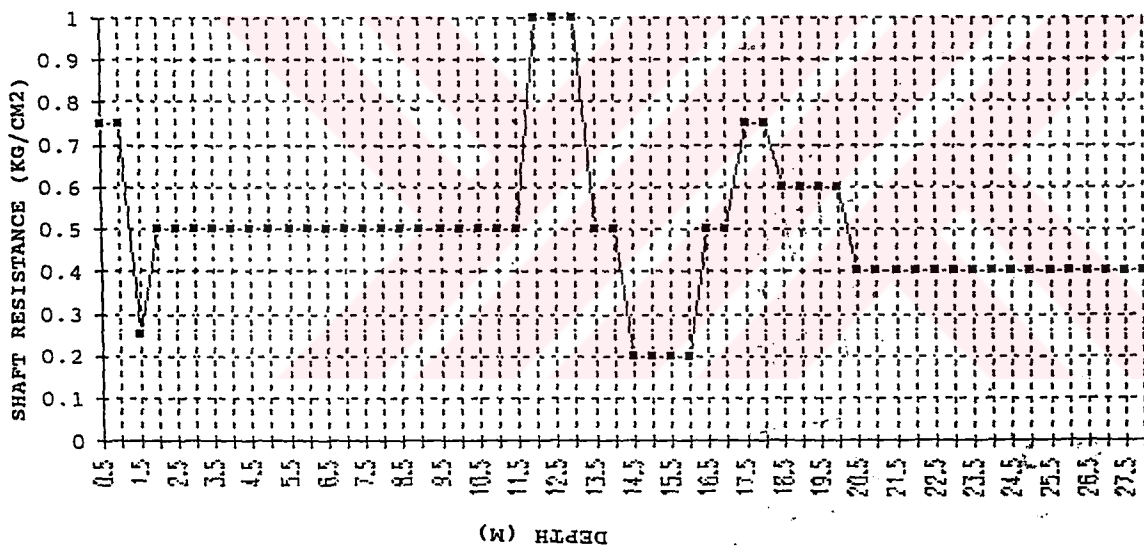
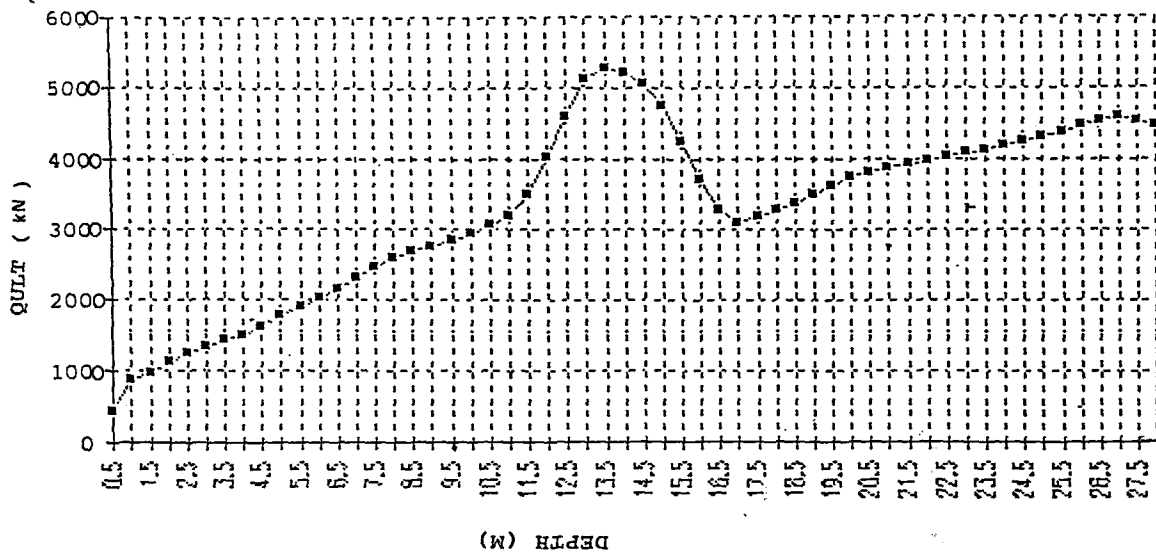


Figure 5.4 Prediction Of Ultimate Bearing Capacity Of a Pile From CPT 4 Data

Typical Dutch practise in assessing  $q_c$  is to limit the value of  $q_c$  used (normally  $30 \text{ MN/m}^2$ ) and to limit the ultimate end bearing capacity to a value not exceeding  $15 \text{ MN/m}^2$ , which depends on OCR.

Typical Dutch practise is to adopt a limit value of  $q_s = 0.12 \text{ MN/m}^2$ . [11]



## CHAPTER VI

### COMPRESSION LOAD TESTS ON DRIVEN PILES IN ALLUVIAL DEPOSIT

#### 6.1 Introduction

Load tests are made on piles mainly for the research purpose to improve the general knowledge of the pile behaviour or for the design and construction purposes. At the preliminary design stage, an analysis of the pile capacity is based on the interpretation of the subsurface investigation. Since there may be large difference between the predicted and actual pile capacities, the analysis can be verified by load tests.

These tests may be performed;

i) before the construction of the contract pile as a part of field investigation. These piles are tested to ultimate load to check the result of the analysis of the ultimate pile capacity and to serve as a guide for the final design. According to test results a suitable type and size of the pile or another type of deep foundation may be selected.

ii) at the beginning or during the construction of the contract pile to check their capacity. These tests provide an indication of settlement of contract pile under specified load and give an idea about the settlement behaviour of further piles. [8]

A series of pile load tests was accomplished during the design phase for the reinforced concrete port grain silo project. Six different locations were selected within the silo block area for working test pile and six different places are also chosen for trial piles outside the construction site, which are shown in Figure 6.1.

Each test pile was subjected to Maintained Load Test. Only the trial test piles were re-loaded, after unloading, until failure using the Constant Rate of Penetration Test procedure.

## 6.2 Method of Testing

There are many different pile loading test methods. Differences between them are mainly based on the increments of load, duration of load for each increment, maintaining the load or maintaining the settlement rate during the test.

Pile load testing, using the Maintained Load or the Constant Rate of Penetration Test procedures, is the most commonly adopted method of checking the performance of a pile.

The Maintained Load Test is convenient for testing end bearing piles and for determining the load/settlement characteristics in clay soil. It is not however suitable for determining ultimate pile loads.

The Constant Rate of Penetration Test procedure is best suited to determining the ultimate bearing capacity of a pile. In clay soil, rapid pile testing may approximate to undrained loading conditions, a constant load for several days may be necessary to allow full dissipation of pore pressure.

### 6.3 Pile Load Test Procedures

#### 6.3.1 Maintained Load Test (ML):

The ML test requires a careful specification of loading increments and periods for which these increments are hold constant. The ICE Piling model procedures and specification sets out a suitable minimum scheme in Table 6.1, and the ASTM Test Designation D-1143 specifies a similar procedure. The ICE Piling Model Procedures and specification limits the rate of movement to 0.25 mm/hr. Some engineers prefer a limit of 0.1 mm/hr and a frequent requirement is to hold the load constant for 24 hours at design load. The particular details of the loading path followed are not of great significance, however it is important that the holding time at each load increment is the same so as to lead to the same degree of consolidation. [16]

#### 6.3.2 Constant Rate of Penetration Test (CRP)

The constant rate of penetration form of testing is confined to special test piles and is usually carried out at the precontract stage (Whittaker and Cooke, 1961). As the name implies, the loading is strain-controlled and a set rate of penetration of the pile load is specified. Rates of penetration between 0.5 and 2 mm/min are commonly used, the lower rate being used in clay soils. Great care is required to maintain a steady rate of penetration, but this is difficult to achieve with

**Table 6.1 Suggested Load Increments and Holding Times (ICE piling Model Procedures And Specification.)**

Load, percentage of working load	Minimum time of holding load
25	1 h
50	1 h
75	1 h
100	1 h
75	10 min
50	10 min
25	10 min
0	1 h
100	6 h
125	1 h
150	6 h
125	10 min
100	10 min
75	10 min
50	10 min
25	10 min
0	1 h

manual pumping without some practice. For this type of testing it is much more satisfactory to use a hydraulic power pack and control the rate of penetration with a dial gauge fitted with a pacing ring. Control of the jack movements is achieved by manual operation of the rate of oil flow. Fully automatic systems have been devised but are more complex, and present difficulties in operation on site.

Loading of the CRP test should be continued to deflection which goes to or beyond failure of the pile. This may be typically, until a constant load has been recorded or until the penetration is at least 10% of the pile diameter.

#### 6.4 Pile Load Tests and Results

Presented here in are pile load capacity prediction for twelve test piles in grain silo project.

Before the construction of working piles, tests have been carried out on 4 No, 400x400 mm, and 2 No, 500x500 mm, trial piles. ML tests were carried out on 400x400 piles No, 1, 4, 6 and 500x500 piles No.2 and 3. These test piles were shown in Figure 6.2 through Figure 6.4. Pile no's 1 through 6 were driven to soil with depths varying from 23.1 m to 27 m. Unlike the working piles, these piles were driven through a casing for the upper 12 m to eliminate the effect of skin friction within the "fill" material. The piles terminates at depth corresponding to that of a sand/gravel layer as identified in the site investigation boreholes.

Trial pile No.7, shown in Figure 6.9 a 400x400 pile, was driven without casing to a depth of 12.2 m. This single pile test was only to identify a possible



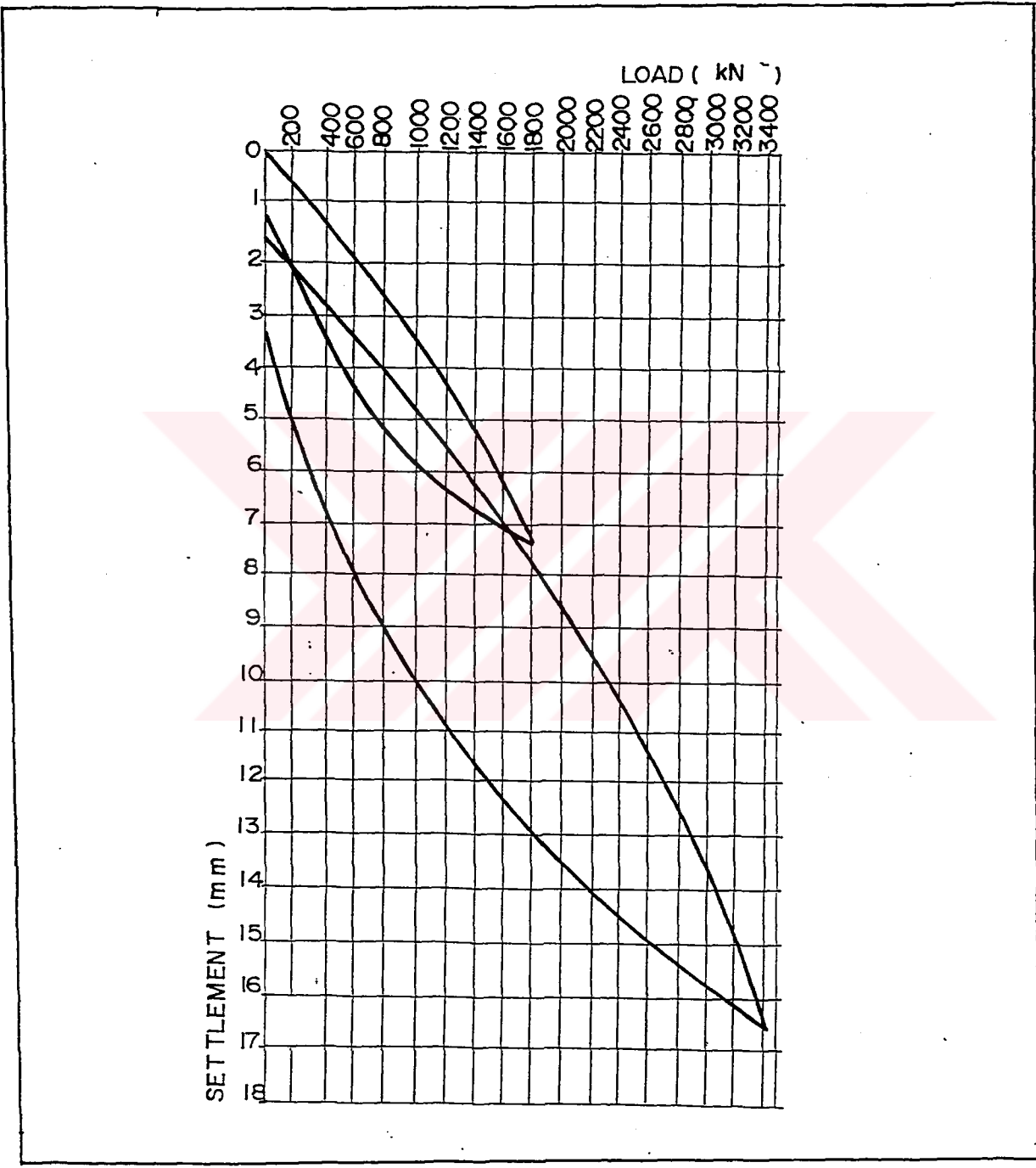


Figure 6.3 Maintained Load Test On Pile No 3.

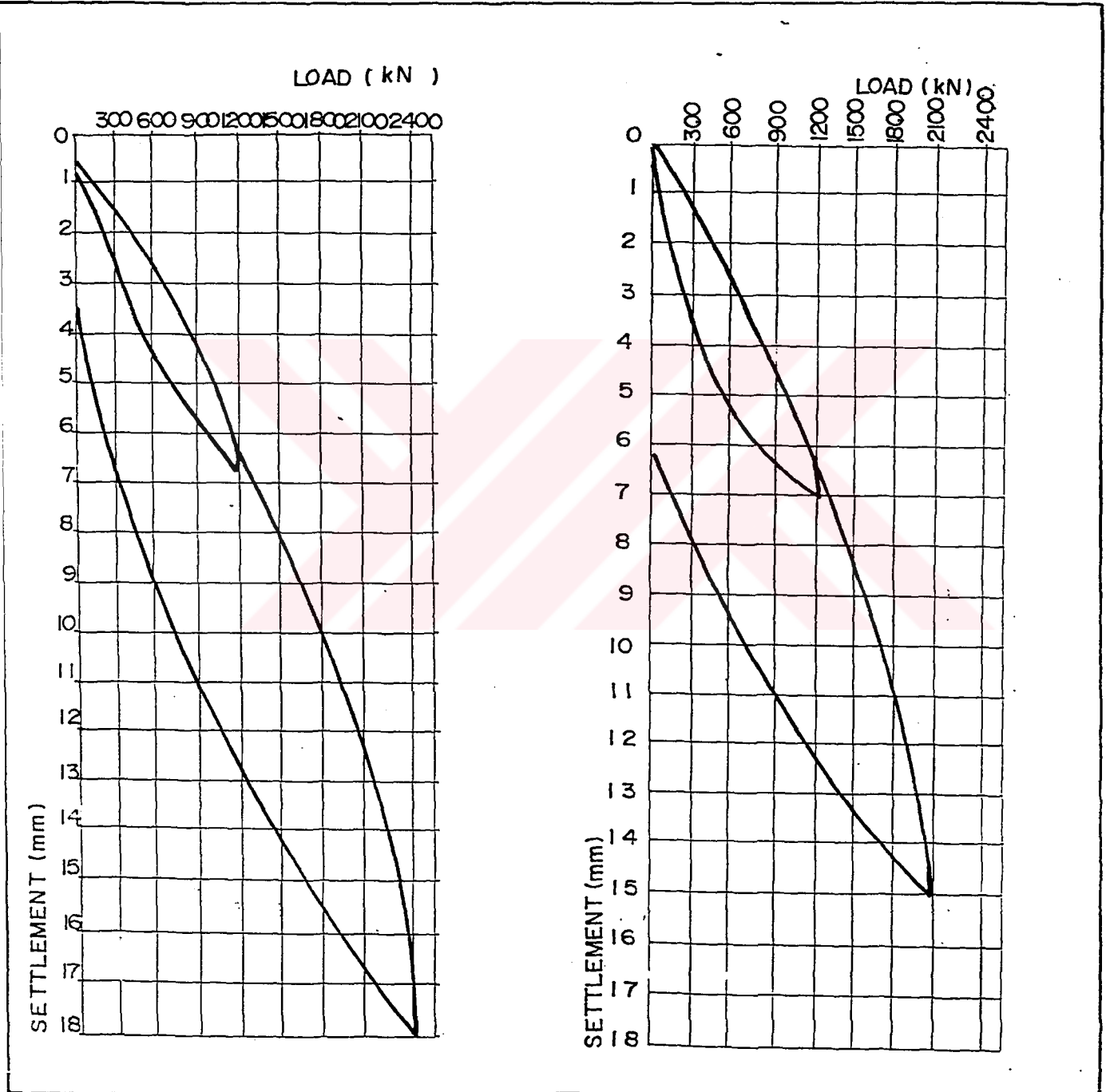


Figure 6.4 Maintaned Load Test On Pile No 4 and Pile No 6

minimum value of skin friction of the fill not to maximum value. Because pile driving in group of piles with a close spacing would densify the ground around the piles. This will increase the frictional force and lead to a greater skin friction. It will be useful to point out that the result of this test should not also used to establish the maximum negative skin friction.

The results of ML tests on trial piles are as follows:

Pile No.1 was loaded to maximum load of 1800 kN and recorded a maximum residual settlement of 2mm. The pile behaved linearly for loading range.

Pile No.2 was loaded to maximum load of 2400 kN and behaved linearly for the range tested. Residual settlement was 3mm.

Pile No 3 was loaded to maximum load of 3400 kN and behaved linearly for the range tested. The residual settlement was 3.5 mm.

Pile No 4 was loaded to maximum load of 2400 kN and appears to have behaved perfectly elastic up to load of 2400 kN. The residual settlement was 2.9 mm.

Pile No. 6 was loaded to a maximum load of 2400 kN. Up to 1100 kN the behaviour of the pile appears to be the perfectly elastic. The load/settlement curve only deviate slightly from straight line between 1100 kN and 2100 kN. Further deviation from straight line occurs between 2100 kN to 2400 kN and results in a residual settlement of 6 mm.

Result of CRP tests on trial pile are summarized in the following paragraphs and shown in Figure 6.5 and Figure 6.6

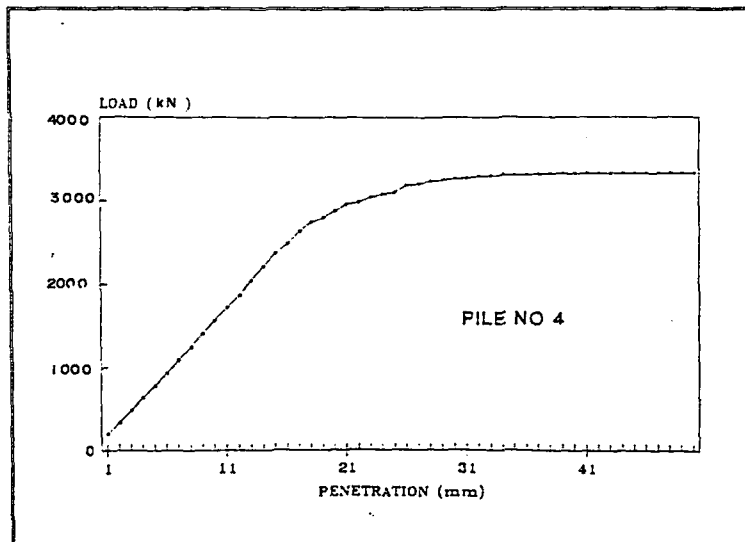
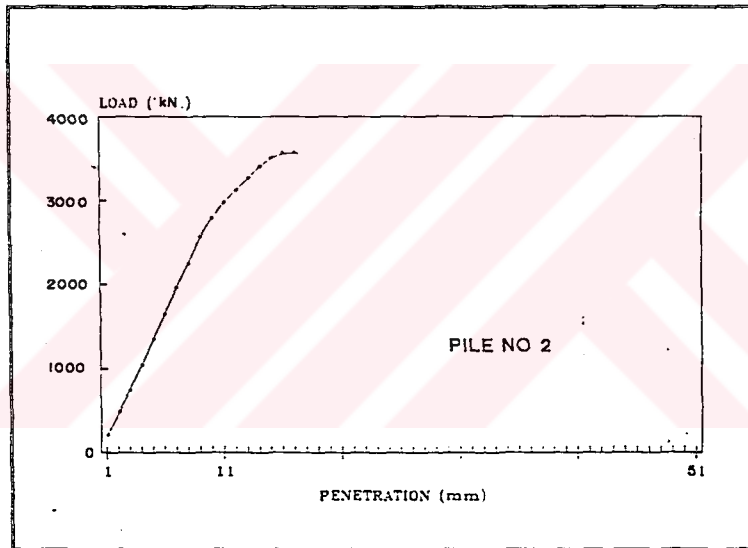
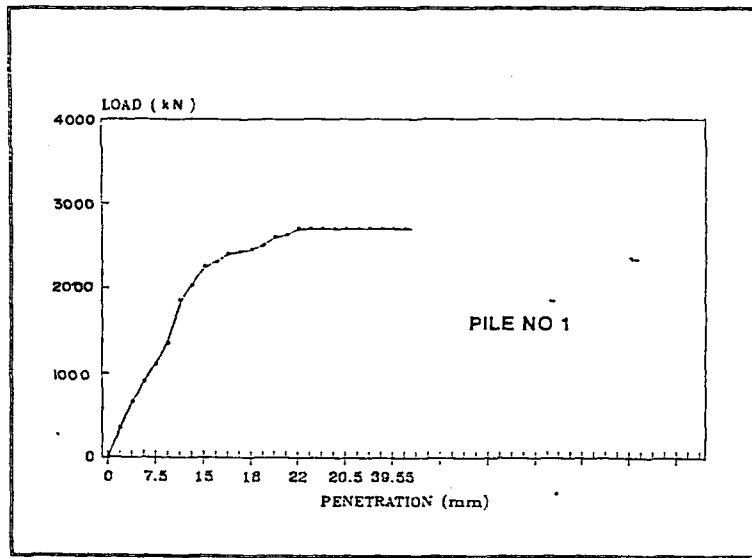


Figure 6.5 Constant Rate Of Penetration Test Results Of Single Test Piles.

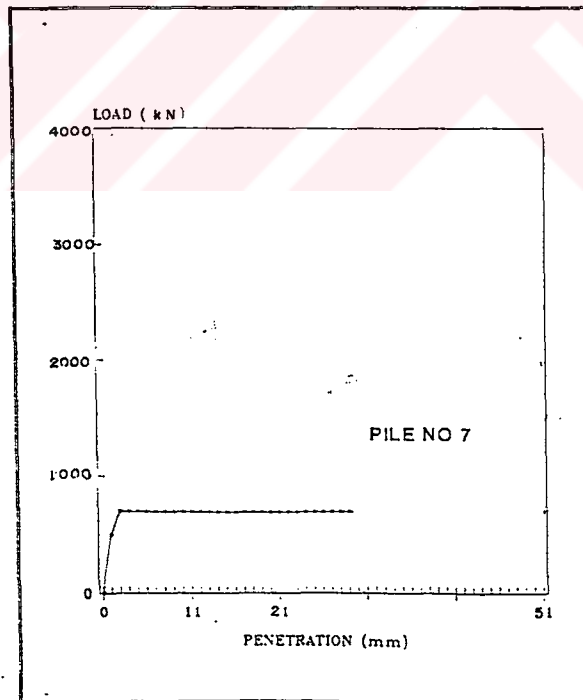
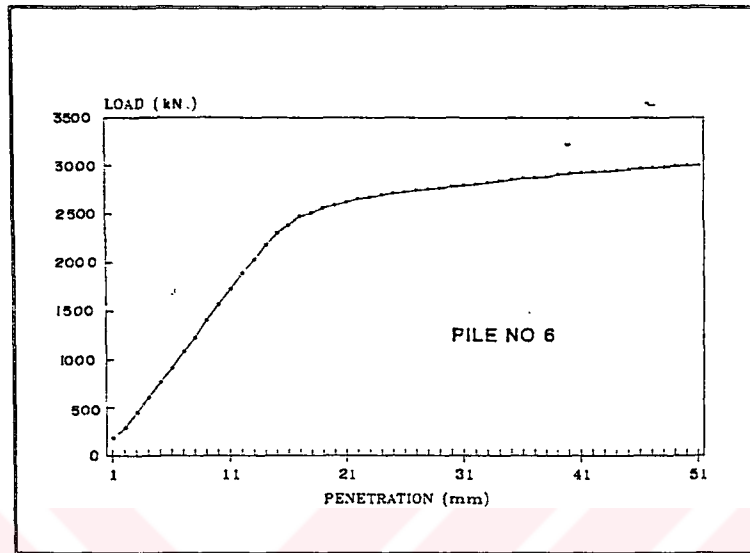


Figure 6.6 Constant Rate Of Penetration Test Results Of Single Test Piles

Pile No 1 was re-loaded to 2700 kN for CRP test. Up to 2250 kN the response was perfectly linear, but slightly deviated from linearity there after.

Pile No 2 was loaded to 3550 kN. Chin failure analysis suggested a failure load of around 5900 kN, but it is behaved that this is unrealistically high.

Pile No 4 was loaded to 3200 kN but departed from linearity at 2650 kN at which point failure began. The ultimate failure corresponds to the maximum loading of 3200 kN.

Pile No 6 was loaded to 2980 kN, but departed from linearity at approximately 2550 kN.

It can be concluded from these observations that, a 400x400 pile would behave approximately linear manner with respect to load/settlement up to typical value of 2400 kN. The ultimate failure load of the pile will be around 3000 kN. A 500x500 pile behave in a near linear manner to at least 3500 kN. The ultimate failure load of the pile is estimated as 4000 kN.

As in the case of trial test piles, at loads which are only a small proportion of the ultimate load, a pile/soil system behaves elastically, much of the settlements being recovered when the applied load is removed. As loads are increased, permanent displacement occurs, a smaller proportion of the deflection being recovered when the pile is unloaded. Small residual settlements are therefore associated with piles working well within their capacity, and large residual settlements are generally seen to indicate incipient 'failure'. Acceptance criteria may therefore be estimated by setting limits on the residual settlement. Unfortunately, tolerable residual settlements are frequently selected on an arbitrary basis. [21]

In mainly cohesive soils, residual settlements due to design loads would be expected to be small, but dependent to some extent on the length of time due to consolidation effects and end restraint of long piles by reversal in the direction of frictional forces. A pile in cohesive soil is expected to recover of the order of 30% of the total settlement.

Piles depending to a greater extent on end bearing and/or installed in less cohesive strata might recover less.

Movement at the pile head is caused by the elastic deformation of pile and soil and plastic deformation of soil. The latter causes undue settlement of structures and must be guarded against. This is the value which is the significant one to be obtained from load tests. [2 1]

As explained before, trial test piles behave in a near linear manner that their total settlement is mostly caused by elastic shortening of the trial test pile. Examples will be presented to calculate elastic shortening of test pile for different loading ranges in the following paragraph.

Elastic shortening of 400x400 mm end bearing pile for typical load values was calculated as:

- Elastic shortening ( $\Delta L$ ) =  $FL/AE$
- Pile length (L) = 25000 mm
- Area of pile (A) =  $400 \times 400 = 16 \times 10^4 \text{ mm}^2$
- Modulus of Elasticity (E) = 32 kN/ m<sup>2</sup>

For  $F = 1000 \text{ kN}$

$$\Delta L = \frac{1000 \times 25000}{32 \times 16 \times 10^4} = 4.9 \text{ mm.}$$

For  $F = 1400 \text{ kN}$

$$\Delta L = \frac{1400 \times 25000}{32 \times 16 \times 10^4} = 6.8 \text{ mm}$$

For  $F = 1800 \text{ kN}$

$$\Delta L = \frac{1800 \times 25000}{32 \times 16 \times 10^4} = 8.8 \text{ mm}$$

For  $F = 2700 \text{ kN}$

$$\Delta L = \frac{2700 \times 25000}{32 \times 16 \times 10^4} = 13.2 \text{ mm}$$

When it comes to working test piles, where groups of driven piles are employed, the effects on the test pile of the presence or absence of adjacent piles should be considered. The installation of adjacent piles may modify the performance of the test pile, by causing uplift in cohesive soils or additional compaction in granular soils.

For example, unlike B30 working test pile, K39 working test pile which is close to B30 indicates quite satisfactorily the general trend of increasing of load carrying capacity due to pile driving. These piles are shown in Figure 6.7.

The difference in load carrying capacity for the same settlement of working test piles is due to increase in relative density which is caused by volume displacement. The volume displacement for 40x40 cm piles at 1.928m. spacing is of the order of 5%.

Consider the area enclosed within the boundry formed from the center parts of the piles.

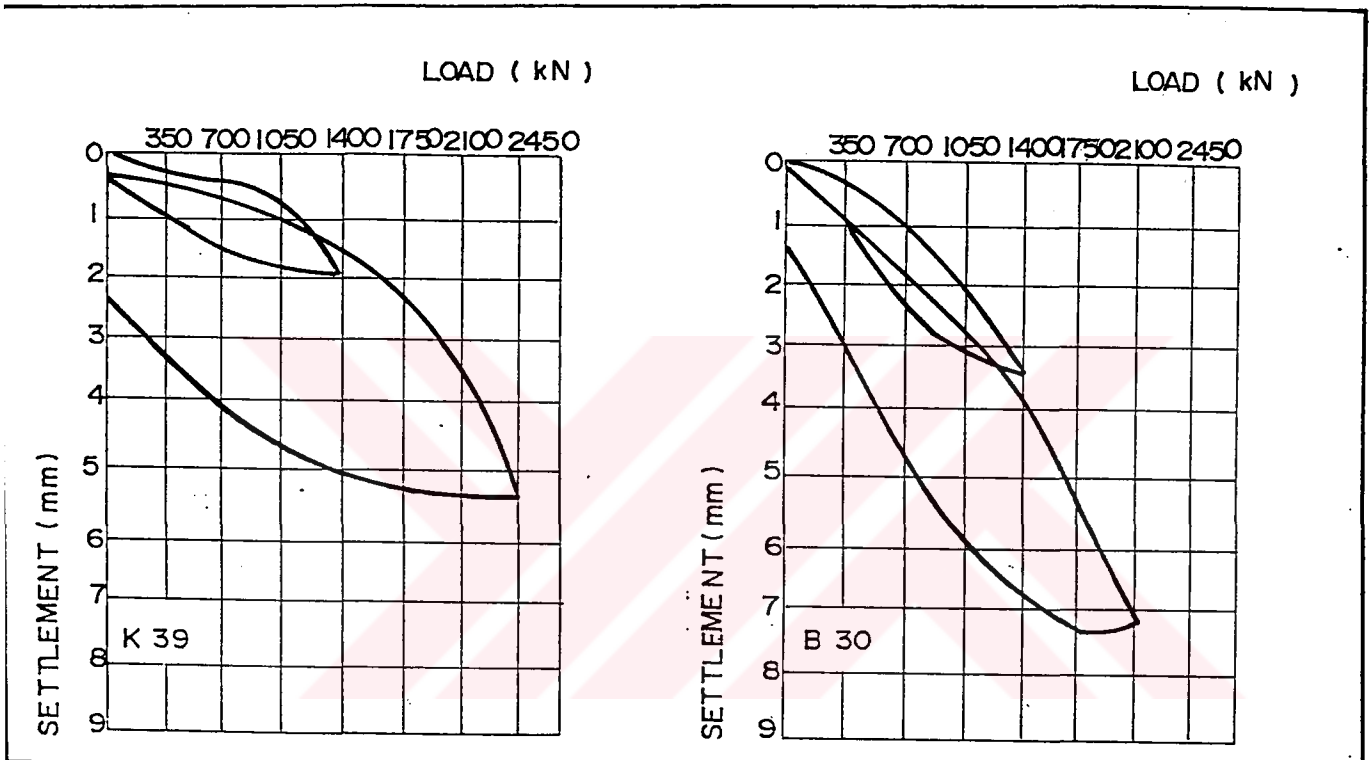
$$\text{Area} = 1.928 \times 1.928 = 3.72 \text{ m}^2$$

Area reduction caused by driving of piles:

$$\text{Area reduction} = 0.40 \times 0.40 = 0.16 \text{ m}^2$$

$$\text{Percentage change} = \frac{3.72 - 0.16}{3.72} \times 100 = 95.7\%$$

Working test pile were embedded to depths varying from 21.1 m to 24.80 m. ML test procedure was applied to all working test piles as shown in Figure 6.7 and Figure 6.8. The results of Maintained Load Tests on Working piles are as follows.



1 Figure 6.7 Maintaned Load Test On Working Piles:

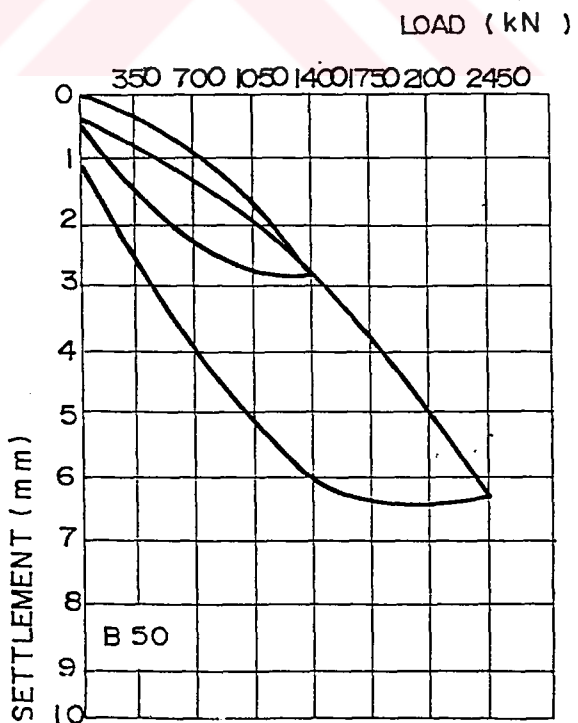
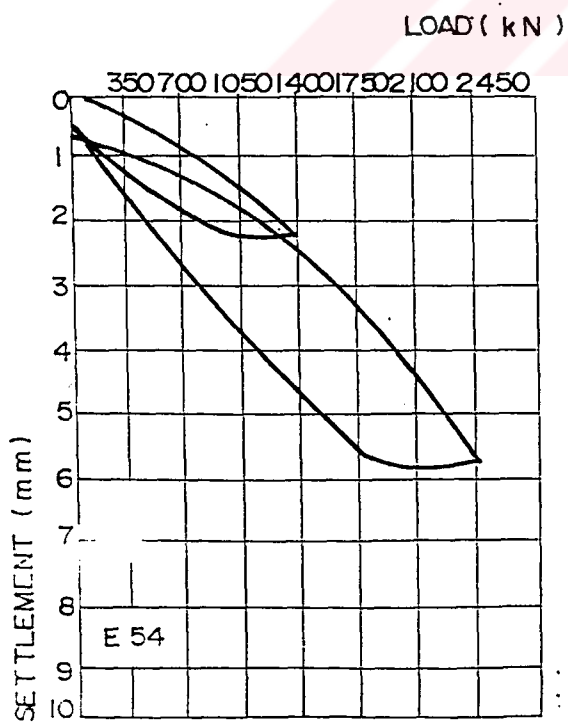
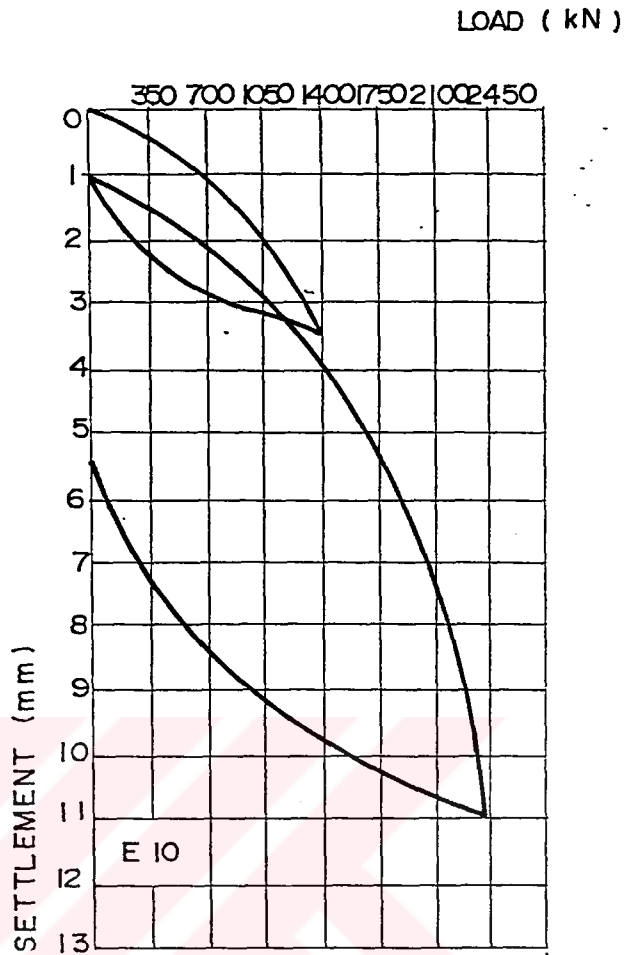


Figure 5.8 Maintained Load Test On Working Piles

Pile E54 was loaded to maximum load of 2450 kN. and recorded a maximum residual settlement of 0.5 mm. The pile behaved linearly for loading range.

Pile G2 was loaded to maximum load of 2450 kN. Up to 1200 kN the response was perfectly linear. The load/settlement curve deviated slightly from straight line between 1200 kN and 1800 kN. Further deviation from straight line occurred between 1800 kN and 2200 kN. and for the range 2200 kN-2450 kN. The residual settlement was 6.25 mm.

Pile E10 was loaded to maximum load of 2450 kN. Up to 1400 kN pile behaviour was elastic. The curve deviated very slightly from straight line between 1750 kN and 2100 kN. Further deviation from straight line occurred between 2100 kN and 2450 kN. Residual settlement was 5.4mm.

Pile K39 was loaded to 2450 kN. and behaved linearly for the range 0 to 1400 kN. The load/settlement curve deviated from line between 1400 kN and 1800 kN. Deviation again occurred between 1800 kN and 2100 kN. Between 2100 kN and 2450 kN the curve deviated once again and recorded maximum residual settlement of 3mm.

Pile E10 was loaded to 2450 kN. and behaved linearly up to 1400 kN. The curve deviated very slightly from straight line between 1750 kN and 2100 kN. Further deviation from straight line between 2100 kN and 2450 kN. The residual settlement was 5.4 mm.

Pile B50 was loaded to 2800 kN. Up to 1400 kN pile behaved elastically. The load/settlement curve deviated up to 2100 kN. Further deviation again occurred thereafter. Residual settlement was equal to 1.02mm.

It can be concluded from these observations that a 400x400 mm working pile behave linear manner with respect to load/settlement up to approximately 1300 kN.

### 6.5 Estimation of Ultimate Load

The ultimate load of a pile is usually not well defined. In practise an exact definition of the ultimate load is not all that important, provided an adequate factor of safety is clearly demonstrated. Two simple criteria for the definition of the ultimate load which cover most situations are

i) the load at which settlement continues to increase without further increase in load.

ii) the load causing a settlement of 10 % of the pile diameter

Other definitions of ultimate load are summarized by Tomlinson (1977) and Fellenius(1980) compares a number of methods of estimating the ultimate load.

Unfortunately many of the proposed techniques are empirical several of the methods are also sensitive to the shape of the load/deformation curve, therefore it is preferable to use a considerable number of load increments to define the shape clearly.

For example, two methods of estimating the ultimate pile load are proposed by Chin(1970) and Brinch Hansen (1963). Chin's method assumes the form of the load/deformation curve is hyperbolic and is an empirical method. Ultimate capacities of 6 No trial test piles, 6 No project test pile were estimated by using only Chin's method as shown in Figure 6.9 through Figure 6.12.

From these Figures, it can be concluded that Chin's failure load of 400x400 working pile and trial pile was approximately equal to 2500 kN and 4150 kN respectively.

#### 6.6 Empirical Methods for Working Load

A considerable number of arbitrary or empirical rules have been used or are contained in codes to serve as criteria for determining the allowable working load from load-test results. A number of these rules have been summarized by Chellis (1961). Davis and Poulos consider that two of them are the most reasonable. They are quoted below.

i) Observe the point at which the gross settlement begins to exceed 0.03 in. per ton of additional load and divide by a factor of safety of 2 for static loads or 3 for vibratory loads (W.H.Rabe).

ii) Observe the point at which the gross settlement begins to exceed 0.05 in. per ton of additional load, or at which the plastic settlement begins to exceed 0.03 in. per ton of additional load, and divide by a factor of safety of 2 for static loads, or 3 for vibratory loads (R.L. Nordlund). [2 1]

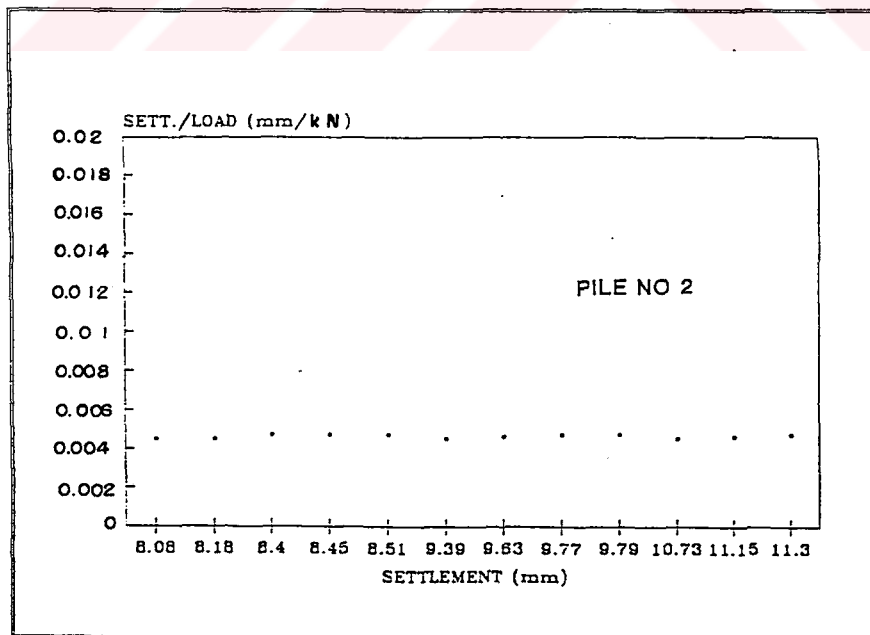
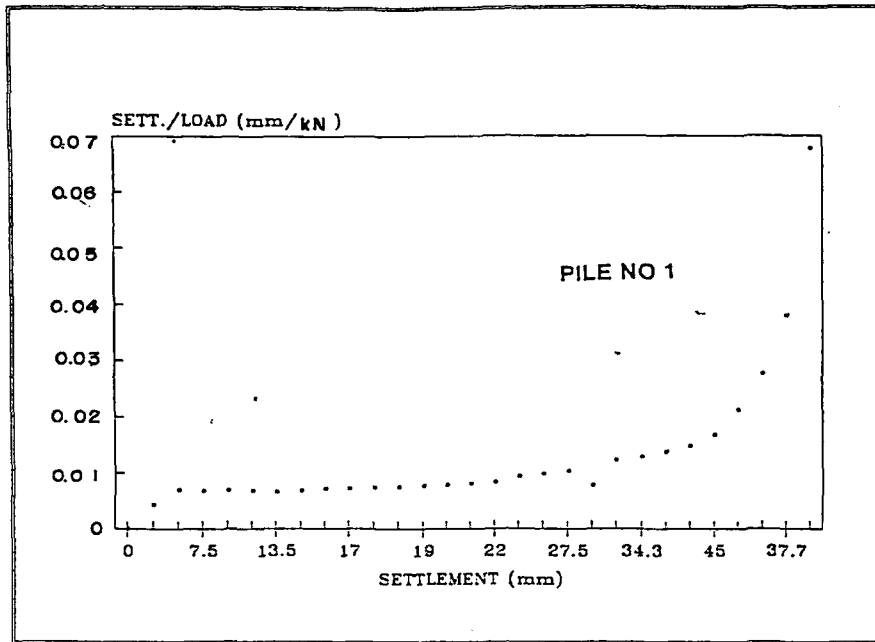


Figure 6.9 Chin Failure Method For Calculation Of Ultimate Bearing Capacities Of Trial Test Piles.

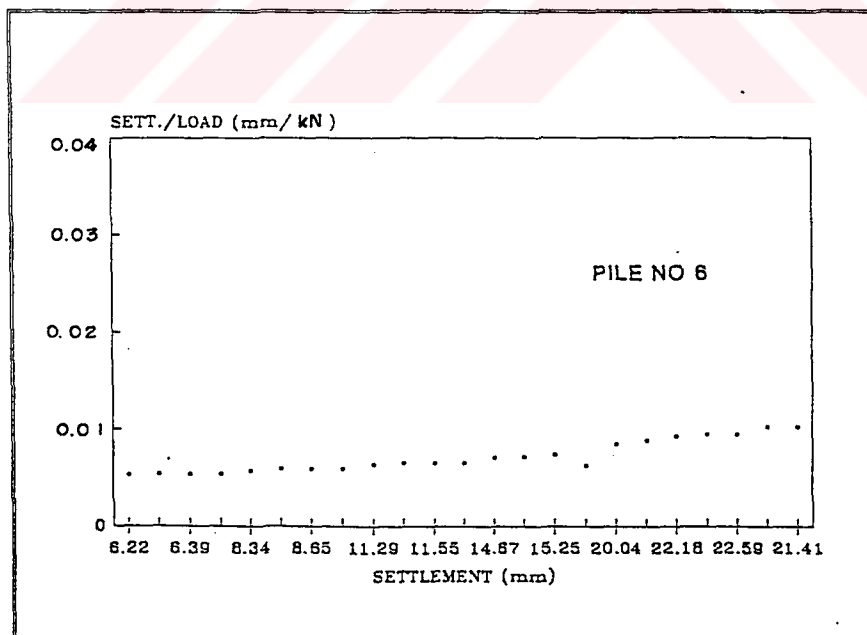
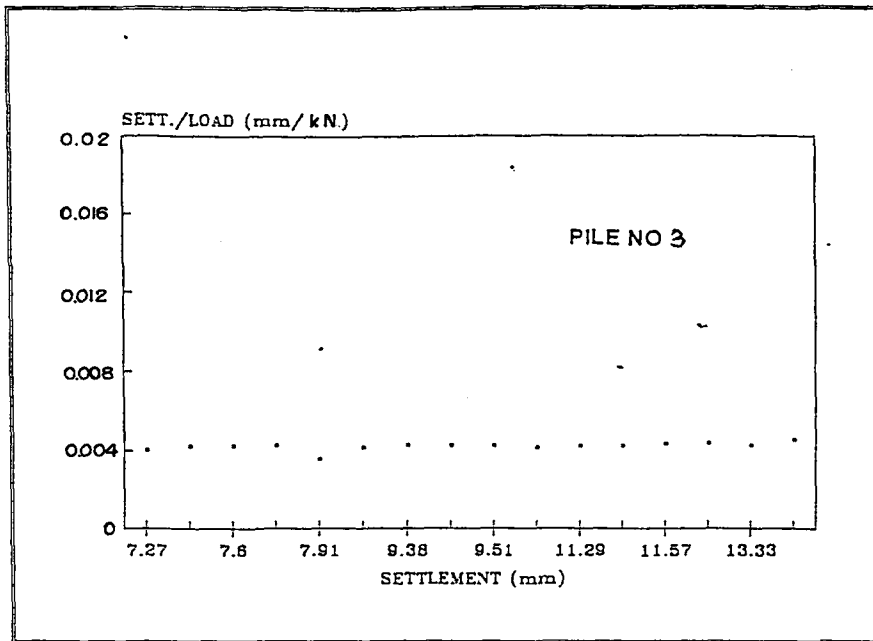


Figure 6.10 Chin Failure Method For Calculation Of Ultimate Bearing Capacities Of Trial Test Piles.

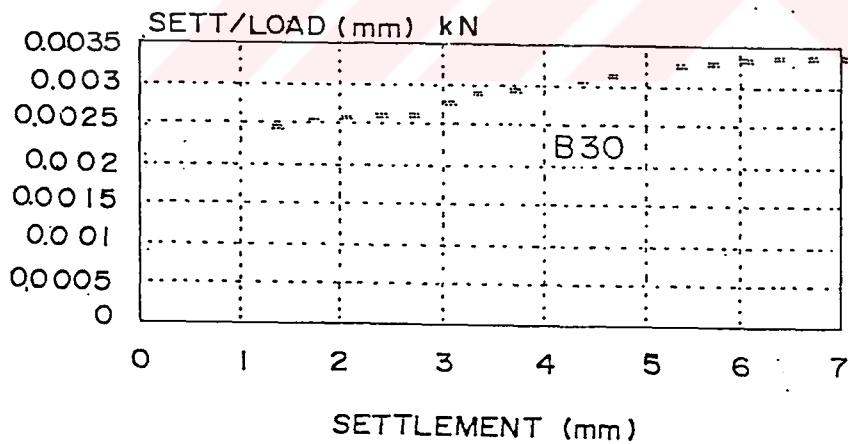
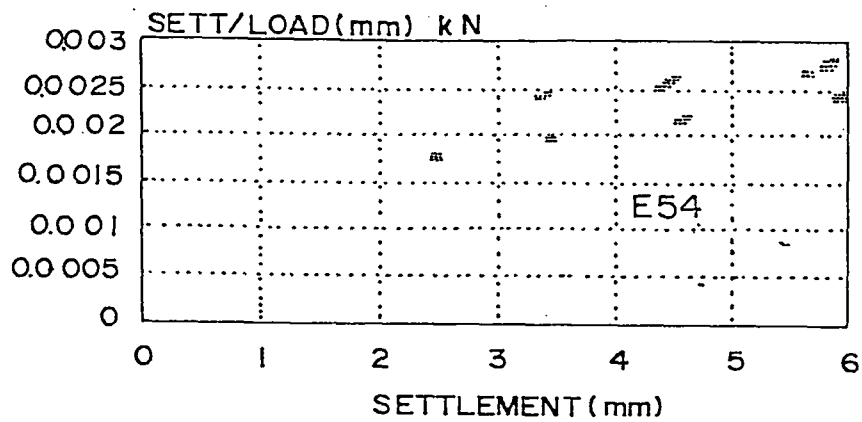


Figure 6.11 Chin Failure Method For Calculation Of Ultimate Bearing Capacities Of Working Test Piles.

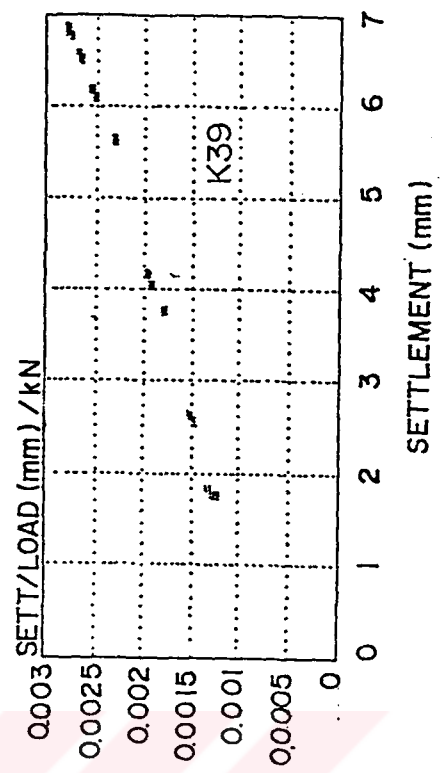
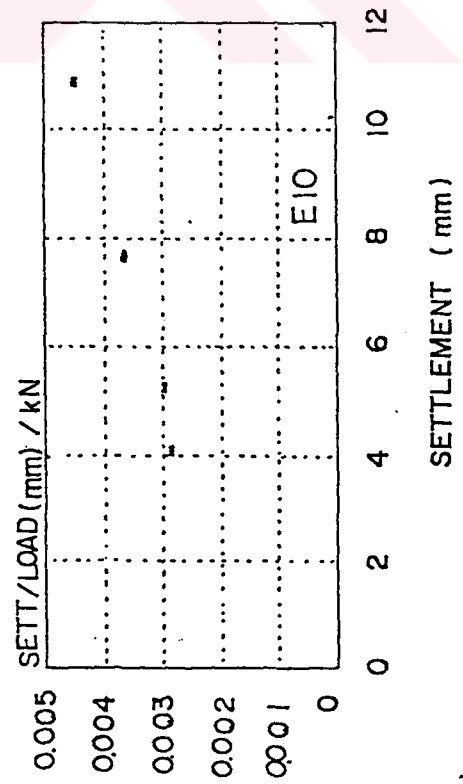
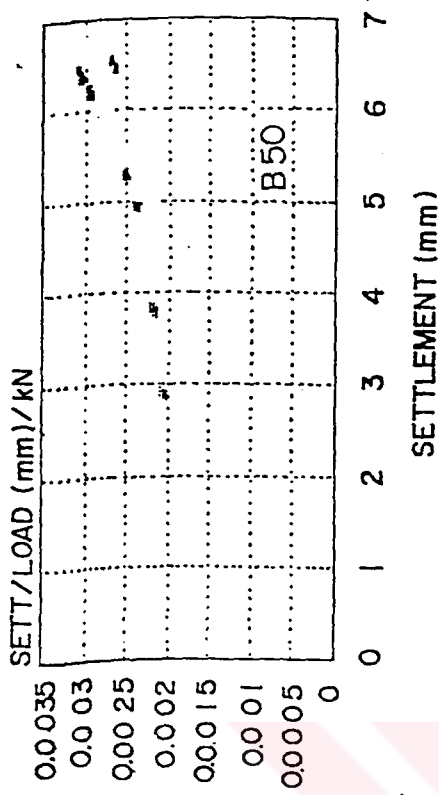
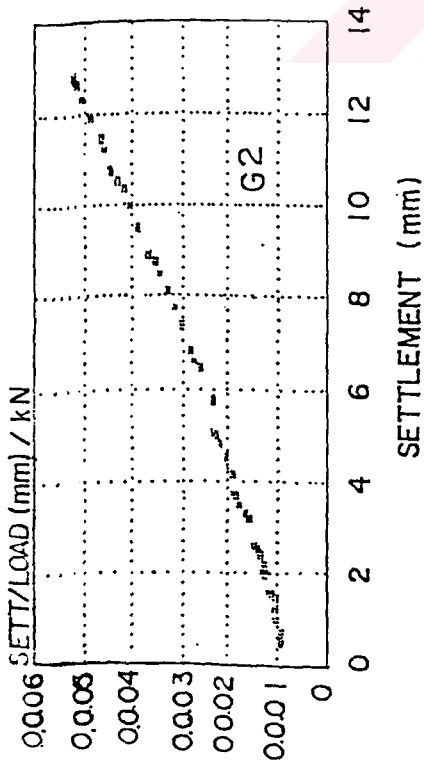


Figure 6.12 Chin Failure Method For Calculation Of Ultimate Bearing Capacities Of Working Test Piles

## CHAPTER VII

### SUMMARY AND CONCLUSION

Pile foundation behavior has been studied for the decades, but there are several gaps in the proper and quantitative understanding of the response of piles, both under static and dynamic loads. Field tests are the best methods of the study of their response, but these are expensive. Therefore, study of case history is important.

In this study a recorded case history was put in a report form and results were analysis and discussed by using various methods to provide reference document.

A large reinforced concrete grain silo has been recently constructed on reclaimed land from the sea at Izmir Bay. Soils are deep alluvial deposits and consist of bands of clay, sand and gravel. Three cone penetrometer testing were made in the construction area to investigate the soil profiling. In addition to CPT, soil profiles in nine boreholes and SPT were available made by the contractor. 400x400 precast concrete piles have been driven to carry the foundation loads. Approximately 800 piles were driven to 22-28 m. depth. Before the final design stage, 500x500 and 400x400 precast trial piles, six in number were driven outside the silo block and test loaded. Six more tests on project piles were performed before the raft was completed.

Static and dynamic pile capacities, results of pile load tests and capacities predicted based on CPT tests are all summarized in Table 7.1 and Figure 7.1. The following conclusions are derived from this study.

1. Prediction of ultimate bearing capacities of piles obtained from driving data by using Janbu driving formula was made in only Block No.4 . Because the existence of friction piles in Block No 4 is less. In this study , analysis suggest that not all piles of the construction site were end bearing on the sand and gravel layer, but are carrying a significant proportion of load by skin friction, 55% of piles are identified as end bearing piles , 22% of piles are accepted as friction piles , the remaining 23% are probably end bearing but results are inconclusive .

2. Average dynamic ultimate bearing capacity of the piles in block No 4 was found to be 2910 kN with standard deviation of 540 kN . Dynamic capacities of two test piles E10, G2 in Block No 4 were similar.

3. Pile driving can be accepted as a dynamic penetration test . It can detect the deviation in the geological profile. The information was used to estimate soil profiling of test piles for bearing capacity calculations in Chapter IV . In this manner an indirect correlation between the dynamic and static behavior of a pile was made .

4. A direct correlation between the pile driving resistance and the static bearing capacity does not exist ,but there is a purely empirical form valid for this specific situation This relation is as follow:

$$(Q_{ult})_{dynamic} / (Q_{ult})_{static} = 0.898$$

5. The only important difference between the many dynamic formulas is the classification and magnitude of the allowances made for energy losses . In Janbu driving formula , which is previously explained in Chapter 2 reduction factor,  $k_u$ , was found to be 6.38 .This means 15 % of reduction was made in ultimate dynamic capacity of Block No 4 . In calculation of average energy loss used for pile analysis , average pile length 21.3m ., average stop blow count 35 blow were taken .

6. In this study , SPT and CPT field measurements have not been carried at after driving of the groups of piles. Consequently, the amount of compaction, in other words increase in relative density could not be verified . In Chapter III, an analysis of the two different test piles (single v.s. group) indicated that the general trend of increase in load carrying capacities for the same settlement were due to compaction of fill only , since clay was fully saturated . The volume displacement for 400 x 400 piles at 1.93 m spacing is of the order of 5%. It was concluded that increase in relative density was approximately 28%, when the increasing shaft resistance approximately 700 kN and the difference in  $K_s$  value was maximum. This calculation may be useful , since design of driven piles, unlike the bored piles, without considering the amount of compaction is conservative in other words the pile will be overdesigned.

7. 400x400 pile would behave approximately linear manner with respect to load settlement up to typical value of 2400 kN . The ultimate failure load of the pile will be around 3000 kN . A 500x500 pile behaved in a linear like manner up to 3500 kN. The ultimate failure load of the pile was estimated as 4000 kN .

8. In mainly cohesive soils , residual settlements due to design loads would be expected to be small , but depended to some extend on the length of time due to consolidation effects . As explain in Chapter VI, trial test piles behave in a near linear

manner that their total settlement is mostly caused by elastic shortening of the test piles. For a typical pile 400 x 400, 25m long, loaded to 2700 kN, the elastic shortening value was equal to 13.2mm which was close to total settlement.

9. Pile capacities predicted by static cone penetration tests are somewhat overestimated.

10. Unfortunately many of the proposed techniques are empirical in estimation of ultimate load. Several empirical methods are also sensitive to the shape of the load deformation curve, therefore it is preferable to use a considerable number of load increments and load cycling to define the shape clearly.

**Table 7.1 Ultimate Bearing Capacity Test Piles**

PILE NO	ULTIMATE BEARING CAPACITY		PILE LOAD TEST		CRP RESULT	CPT
	STATIC (KN)	DYNAMIC (KN)	CHIN (KN)	MAZURKIEWIC (KN)	(KN)	(KN)
E10	2070	2330	3330	3000	-	1800
E54	2590	1900	2800	2630	-	2800
E30	3240	2240	3600	2280	-	4200
E50	2880	1980	3000	2800	-	2500
K35	2000	2760	3000	2150	-	4050
G2	2570	2590	2500	2260	-	4000
#1	2310	HAMMER ENERGY IS MISSING	5000	2650	3600	2600
#2	2530		5880	3800	3650	2900
#3	2270		4150	3830	3400	4200
#4	2390		4080	3300	3450	4300
#5	2300		3360	3000	3000	4000

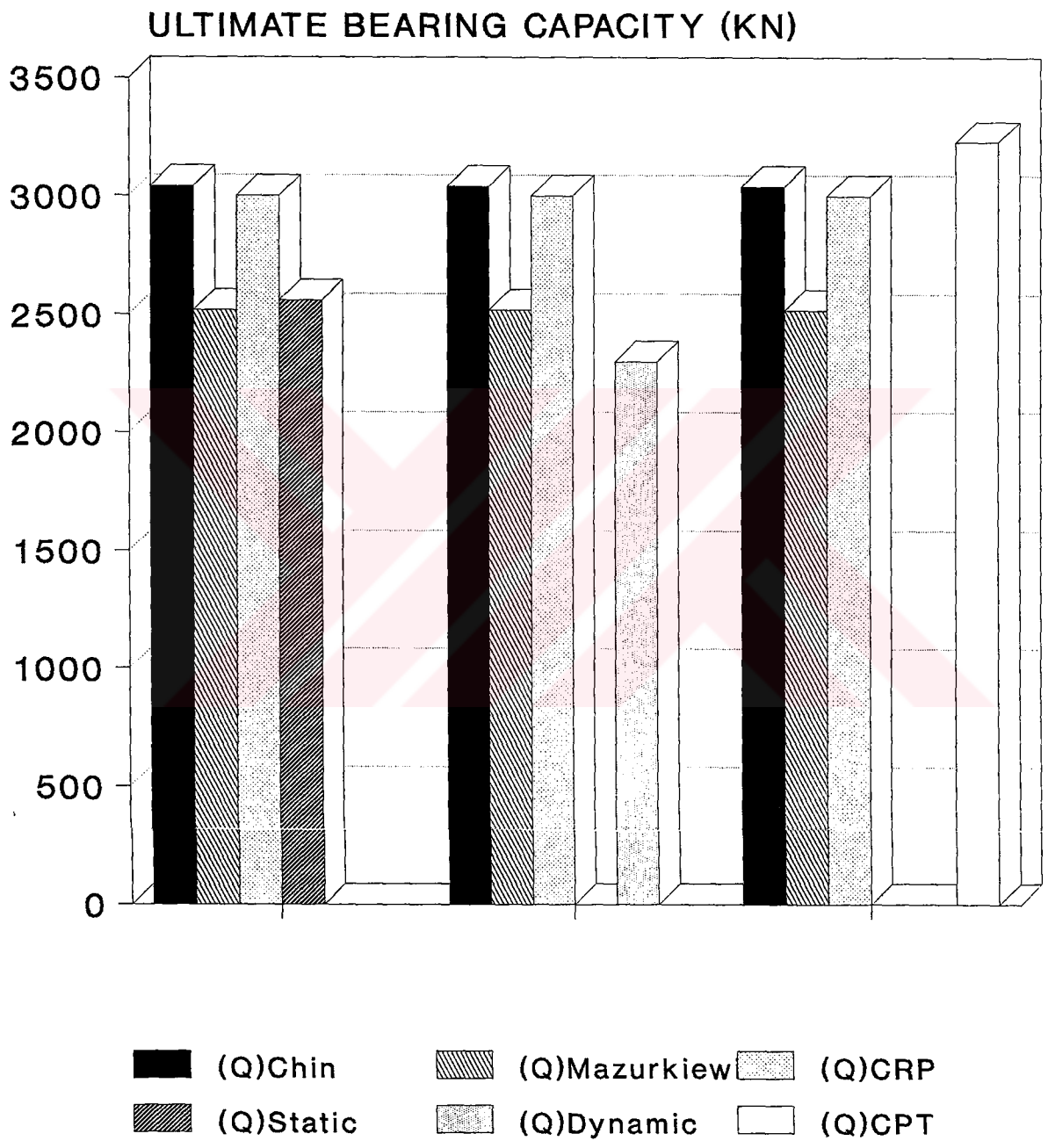


**Figure 7.1 Ultimate Bearing Capacity Test Piles.**

## REFERENCES

- [1] B.T Bircan,,I. "Evaluation of Pile Bearing Capacity and Settlement by Load Tests", MS Thesis, Dept.of Civil Engineering, Middle East Technical University,Ankara (1989)
- [2] J. Burland and J. Mitchell " Piling and Deep Foundations",Proceedings of the International Conference on Piling and Deep Foundation,London (1989).
- [3] R.D.Chellis "Pile Foundation",John Wiley and Sons ,London (1977)
- [4] E.H. Davis and H.G. Poulos "Pile Foundation Analysis and Design",John Wiley and Sons ,London (1980)
- [5] W.G.K Fleming and A.J. Weltman and M.F. Randolph and W.K. Elson " Piling Engineering", John Wiley and Sons ,London (1986)
- [6] \_\_\_\_\_ , "Report Concerning Static Cone Penetration Tests at Izmir TMO site",FUGRO ltd., Turkey (1987)
- [7] A.G.Holzmann and F.R Essen and H. Meseck " Production and Testing of 600 reinforced- concrete piles ",Proceedings of the International Conference on Piling and Deep Foundation,London (1989).

- [8] M .Koçak "Drilled Piers", MS Thesis, Dept .of Civil Engineering, Middle East Technical University ,Ankara(1984).
- [9] A.C.Meigh "Cone Penetration Testing Methods And Interpretation", Butterworths,London (1987).
- [10] J.R. Meyer "Analysis and Design Pile Foundation " American Society of Civil Engineers ,New York (1 984 )
- [11] G.M. Norris and R.D Holtzl " Cone Penetration Testing And Experience . Butterworths,London (1987)
- [12] I .Ordemir "Pile Foundations ", Dept. of Civil Engineering ,Middle East Technical University ,Ankara (1984)
- [13] \_\_\_\_\_, "Penetration Testing", Proceeding of the Second European Symposium on Penetration Testing , Amsterdam (1982).
- [14] \_\_\_\_\_, "Penetration Testing", Proceeding of the Second European Symposium on Penetration Testing , Rotterdam (1982).
- [15] S. Prakash and H.D. Sharma "Pile Foundation Analysis and Design", John Wiley and Sons ,London (1986)

- [16] \_\_\_\_\_, "Predicted and Observed Axial Behaviour of Piles "  
Proceedings Symposium sponsored by th ASCE in conjunction with the  
Foundation Engineering Congress, Northwestern University, Evanston ,  
Illinois ( 1989).
- [17] \_\_\_\_\_, " Recent Developments in Design and Construction of Piles"  
Proceeding of Conference ,Amsterdam ( 1979)
- [18] \_\_\_\_\_,"TMO Grain Storage Project, Soil Investigation Report of 40000  
Tons Silo of IZMIR", TEKAR Technical Research Ltd. Co. (1982) .
- [19] M.J. Tomlinson " Pile Design And Construction Practise ",AView Point  
Publication ,London (1977)
- [20] V.Uzun "A Critical Review of Bearing Pile Driving Formulae (Theory  
Versus Practice), M.S Thesis, Dept. of Civil Engineering ,Middle East  
Technical University ,Ankara (1971 )
- [21] A.J Weltman and J.A. Little " A Review of Bearing Pile Types ",Construction  
Industry Research Information Association ,London (1977).